RANDOM SUBCARRIER ALLOCATION IN OFDM-BASED COGNITIVE RADIO NETWORKS AND HYPER FADING CHANNELS

A Dissertation

by

SABIT EKIN

Submitted to the Office of Graduate Studies of
Texas A&M University
in partial fulfillment of the requirements for the degree of

DOCTOR OF PHILOSOPHY

Approved by:

Co-Chairs of Committee,	Erchin Serpedin
	Khalid A. Qaraqe
Committee Members,	Costas N. Georghiades
	Aydin I. Karsilayan
	Ibrahim Karaman
Department Head,	Chanan Singh

December 2012

Major Subject: Electrical Engineering

ABSTRACT

Advances in communications technologies entail demands for higher data rates. One of the popular solutions to fulfill this requirement was to allocate additional bandwidth, which unfortunately is not anymore viable due to spectrum scarcity. In addition, spectrum measurements around the globe have revealed the fact that the available spectrum is under-utilized. One of the most remarkable solutions to cope with the under-utilization of radio-frequency (RF) spectrum is the concept of cognitive radio (CR) with spectrum sharing features, also referred to as spectrum sharing systems. In CR systems, the main implementation issue is *spectrum sensing* because of the uncertainties in propagation channel, hidden primary user (PU) problem, sensing duration and security issues. Hence, the accuracy and reliability of the spectrum sensing information may inherently be suspicious and questionable.

Due to the imprecise spectrum sensing information, this dissertation investigates the performance of an orthogonal frequency-division multiplexing (OFDM)-based CR spectrum sharing communication system that assumes *random allocation* and absence of the PU's channel occupation information, i.e., *no spectrum sensing* is employed to acquire information about the availability of unused subcarriers or the PU's activity. In addition, no cooperation occurs between the transmitters of the PUs and secondary users (SUs). The main benefit of random subcarrier utilization is to uniformly distribute the amount of SUs' interference among the PUs' subcarriers, which can be termed as *interference spreading*. The analysis and performance of such a communication set-up provides useful insights and can be utilized as a valid benchmark for performance comparison studies in CR spectrum sharing systems that assume the availability of spectrum sensing information.

In the first part this dissertation, due to the lack of information about PUs' activities, the SU randomly allocates the subcarriers of the primary network and *collide* with the PUs' subcarriers with a certain probability. The average capacity of SU with subcarrier collisions is employed as performance measure to investigate the proposed random allocation scheme for both general and Rayleigh channel fading models. In the presence of multiple SUs, the multiuser diversity gain of SUs is also investigated. To avoid the subcarrier collisions at the SUs due to the random allocation scheme and to obtain the maximum sum rate for SUs based on the available subcarriers, an efficient centralized sequential algorithm based on the opportunistic scheduling and random allocation (utilization) methods is proposed to ensure the orthogonality of assigned subcarriers.

In the second part of this dissertation, in addition to the collisions between the SUs and PUs, the inter-cell collisions among the subcarriers of SUs (belonging to different cells) are assumed to occur due to the inherent nature of random access scheme. A stochastic analysis of the number of subcarrier collisions between the SUs' and PU's subcarriers assuming *fixed* and *random* number of subcarriers requirements for each user is conducted. The performance of the random scheme in terms of capacity and capacity (rate) loss caused by the subcarrier collisions is investigated by assuming an interference power constraint at PU to protect its operation.

Lastly, a theoretical channel fading model, termed hyper fading channel model, that is suitable to the dynamic nature of CR channel is proposed and analyzed. To perform a general analysis, the achievable average capacity of CR spectrum sharing systems over the proposed dynamic fading environments is studied.

DEDICATION

To my beloved wife Gülsüm,

my lovely daughter Rabia,

and my dear parents,

whom I love and admire...

ACKNOWLEDGEMENTS

The experience that I gained during my Ph.D. journey was not only wonderful and unforgettable but also overwhelming. This thesis would only have been a dream without the support and encouragement of many great people.

First and foremost, I wish to thank Dr. Erchin Serpedin and Dr. Khalid A. Qaraqe. I consider it an honor to work with them as my advisors. I value the freedom they gave me to pursue different research areas. Their influence in shaping my career and me will be everlasting. I also acknowledge the efforts of my Ph.D. committee members; Dr. Costas N. Georghiades, Dr. Aydin I. Karsilayan and Dr. Ibrahim Karaman. Their insightful suggestions and witty criticism during the preliminary exam and defending stages has proved valuable in improving this work. I would also like to thank Dr. Radu Stoleru for serving as a replacement during my Ph.D. defense. Throughout my Ph.D. study, I have also been privileged to know and collaborate with many great people; Dr. Mohamed-Slim Alouini, Dr. Mohamed M. Abdallah, Dr. Ferkan Yilmaz, Dr. Hasari Celebi and Dr. Serhan Yarkan. Their valuable guidance and collaboration during my PhD study was priceless. The work in this thesis was supported by our generous funding agencies; Qatar Telecom (Qtel) and Qatar National Research Fund (an initiative of Qatar Foundation).

In addition, it is my pleasure to acknowledge my colleagues in the Electrical and Computer Engineering Department of Texas A&M University, in particular, Ali Riza Ekti, Aitzaz Ahmad, Sang Woo Park, Nariman Rahimian, Abdallah Farraj, Tarun Agarwal, Arvind Yedla, Zied Bouida, Amina Noor, Yi Zhou, Fatemeh Sepehr, Engin Tunali and Celal Erbay. I am also grateful to Dr. Samel Celebi, Dr. Luca Blessent, Dr. Jianghong (Jane) Luo for hosting me at Qualcomm New Jersey Research Center

during Summer 2012 and serving as an excellent mentors. It is with immense gratitude that I acknowledge the support of all my dearest friends in College Station, especially, Selman Bastug, Serdar Ozturk, Yildirim Dogan, Sami Keskek and Talat Ozkan. I have had wonderful and unforgettable memories with them.

Finally, I will be forever indebted to my dear father Hamit and my dear mother Celile for all they have done. Their advice and encouragement always enlightened the grueling paths in my life. Furthermore, I owe my deepest gratitude to my brothers; Murtaza, Sadi and Suheyip, and my sisters; Halise, Garibe, Nesrin and Zeynep, and all other relatives for sharing their love all these years and being there when I needed them the most. I owe all my success to their blessings and prayers.

And the joy of my life, my lovely little daughter, sweetheart Rabia, has changed everything in my life from the very first day of her presence. Words cannot describe her importance in my life. I have realized that there had always been something missing without her.

The last but not the least, I cannot find words to express my sincere gratitude to my beloved wife Gülsüm, a very special person in my life. She has steadily and patiently been by my side and has always encouraged me during this tough and long journey. Pursuing a Ph.D. degree requires a tremendous dedication in all aspects, she certainly sacrificed more of her life. This thesis would not have been possible without her endless and unconditional support. For me, together with our little daughter, they have been and will always be the source of motivation and success, the reason for a smile and the hope for a promising future.

NOMENCLATURE

AWGN	Additive White Gaussian Noise
BS	Base Station
CDF	Cumulative Distribtuion Function
CF	Characteristic Function
CR	Cognitive Radio
CSI	Channel Side Information
CU	Cognitive User
IT	Interference Temperature
MGF	Moment Generating Function
OFDM	Orthogonal Frequency-Division Multiplexing
OFDMA	Orthogonal Frequency-Division Multiple Access
PBS	Primary Base Station
PDF	Probability Density Function
PMF	Probability Mass Function
PU	Primary User
QoS	Quality of Service
RF	Radio Frequency
RV	Random Variable
SBS	Secondary Base Station
SIR	Signal-to-Interference Ratio
SINR	Signal-to-Interference-plus-Noise Ratio
SNR	Signal-to-Noise Ratio
SU	Secondary User

TABLE OF CONTENTS

LIST OF FIGURES

FIGURE Page

LIST OF TABLES

1. INTRODUCTION

1.1 Cognitive Radio Networks

The radio frequency (RF) spectrum is one of the most precious and limited resources in wireless communication systems. Therefore, regulatory agencies exclusively allocate each band in spectrum to a specific user and guarantee that this licensed user will be protected from any interference. Under these conservative frequency allocation policies and the requirement of high data rates, the RF spectrum has become a very precious and very limited resource especially with the broad utilization of wireless technologies and the emergence of new wireless services.

On the other hand, recent spectrum measurement campaigns, performed by agencies such as Federal Communications Commission (FCC), reported that the RF spectrum is being used inefficiently [3, 19, 28, 43]. Hence, efficient utilization of the spectrum represents a crucial issue in the wireless communications field. For instance, the measurements for the spectrum occupancy in some of the spectrum bands in Chicago, IL, are shown in Table 1.1. The measurement results are for a very dense area, hence it shows how inefficiently the spectrum is being utilized.

The idea of cognitive radios (CRs) was advanced as a promising approach for the efficient utilization of spectrum. CRs assume that the RF spectrum can be utilized by secondary users (SUs) in addition to the legacy users also termed primary users (PUs) by complying with some predefined requirements imposed by PUs on SUs. In addition, CR is an emerging technology for intelligent next generation wireless communication systems. It is able to dynamically adapt to the radio environment to efficiently maximize the utilization of the limited and precious spectrum resources.

Generally, in CR networks the usage of spectrum by cognitive (secondary) users

Table 1.1: Measured spectrum occupancy in each band in Chicago [43].

Band	**MHz**	**Occupancy ratio (%)**
Fixed Mobile, Amateur, others	138-174	35
TV 14-20	470-512	60
Cell phone and SMR	806-902	55
Unlicensed	902-928	10
Aero Radar, Military	1300-1400	3
Mobile Satellite, GPS, Meteorologicial	1300-1400	3
Surveillance Radar	2686-2900	5

is maintained by three approaches:

- In *interweave* cognitive (opportunistic access) networks, primary and secondary users are not allowed to operate simultaneously, i.e., the SU accesses the spectrum while the PU is idle.

- In *underlay* cognitive (spectrum sharing) networks, PUs are allocated a higher priority to use the spectrum than SUs, and the coexistence of primary and secondary users is allowed under the PU's predefined interference constraint, also termed *interference temperature*. In other words, SU can concurrently use the same spectrum with a PU by regulating (adapting) its peak or average transmit power below a PU predefined interference temperature (power) constraint, so that the quality of service (QoS) requirement of PU is maintained.

- In *overlay* cognitive networks, SUs and PUs are allowed to transmit concurrently with the help of advanced coding techniques [29].

Combinations of the interweave (opportunistic access) and underlay (spectrum sharing) approaches are called hybrid CR networks [32]. In addition, note that the spectrum sharing is a more aggressive method than the opportunistic access method;

hence, recently, it has attracted considerable attention. It is well known that the spectrum sharing method is a more efficient method, and the opportunistic access method is a special case of it.

One of the most challenging issues in the implementation of CR networks is the acquisition of information about the spectrum occupancy of PU(s) [14, 63]. In other words, knowing whether at a certain physical location and moment of time the RF spectrum is occupied by PU(s), i.e., if there is a sensing mechanism in place for the available spectrum [12, 63]. Deploying an efficient spectrum sensing mechanism is difficult because of the uncertainties present in the propagation channels at device and network-level, the hidden PU problem induced by severe fading conditions, and the limited sensing duration. There have been a large number of studies to investigate solutions for the aforementioned challenges and issues. In [71] and references therein, a compact survey of the spectrum sensing algorithms and CR applications along with the design and implementation challenges are classified properly.

1.2 Overview of Orthogonal Frequency Division Multiplexing

In orthogonal frequency division multiplexing (OFDM)-based systems, the radio frequency spectrum is divided into non-overlapping bands, called subcarriers, and which are assigned to different cells and/or users. In OFDM, the main idea is to send the transmitted bitstream over many different orthogonal subchannels also called subcarriers [24]. Since the bandwidth of each subcarrier is less than the channel coherence bandwidth, the channel fading model in each subcarrier assumes a flat fading model. Therefore, the inter-symbol-interference (ISI) on each subcarrier is considerably negligible, and it can be completely eliminated through the use of cyclic prefix [24]. Cyclic prefix does not only eliminate ISI but also restores the eigenfunction property of sinusoids of linear time-invariant (LTI) systems [64], a result which

is often expressed alternatively as a transformation of a frequency-selective channel into a multitude of flat-fading channels.

Starting with the early deployment of cellular mobile communication networks, efficient sharing of the available radio spectrum among the users has represented an important design problem. In conventional OFDM-based systems, the universal frequency reuse is assumed, i.e., the same set of subcarriers can be used in different cells while assuring that the subcarriers assigned to users in each cell are orthogonal to each other. Therefore, one of the main challenges is subcarrier collisions for cell-edge users. In [7, 8, 18], stochastic subcarrier collision models have been proposed to investigate the performance of various scheduling and deployment methods, and to assess the inter-cell-interference for cell-edge users.

1.3 Related Work

Since Mitola's originating work [44], CRs have attracted huge attention and become a promising technology to solve and improve the problem of spectrum utilization. There have been reported an enormous number of works to cope with the challenges caused by the sharing of RF spectrum, and to investigate various aspects of CR networks, such as performance evaluation, implementation issues etc. Next we provide a brief overview on the most important contributions reported in the literature and that present relevance to the work conducted for this dissertation.

To understand the performance limits of a spectrum sharing system, SU capacity is a very useful performance measure. Hence, the SU capacity is mostly used as a performance metric. The ergodic and outage capacities of CR spectrum sharing systems in Rayleigh fading environments are studied in [46], and a comprehensive analysis considering various combinations of power constraints under different types of channel fading models is performed in [36]. In [23], considering a point-to-point

communication scenario, the expressions for the average capacity of a single SU assuming the existence of a single PU and no PU's interference are derived for different channel fading models such as Rayleigh, Nakagami-m and Log-normal. As an extension of [23], in [62], the SU capacity assuming PU's interference with imperfect channel knowledge, and the average bit error rate over Rayleigh channel fading were derived. The ergodic sum capacity of CRs (SUs) with multiple access and broadcast fading channels with long-term average and short-term power constraints was established using optimal power allocation schemes in [73].

Opportunistic SUs scheduling yields multiuser diversity gain due to the channel fading randomness. The effects of multi-user diversity on the capacity of a spectrum sharing system where multiple SUs utilize the licensed spectrum are investigated in [6, 74], and for interweave CR networks in [29] and the references cited therein. In the multi-user diversity (gain) technique, the aim is to have the best channel quality for the communication system. This method shows that the system presents maximum throughput [67] in non-spectrum sharing systems. There have been numerous studies on the effects of multi-user diversity on non-spectrum-sharing systems [30, 34, 38, 56, 64, 67]. In spectrum sharing systems, this effect has been actively studied in [20, 21, 23].

In addition, assuming imperfect channel side information (CSI), the authors in [47, 53, 62] conducted capacity and power allocation studies. The multiple-input multiple-output (MIMO) opportunistic spectrum access set-up was studied in [26]. Besides the SU average and peak transmit power constraints, in [40], the PU's outage loss is assumed as a constraint to maintain PU's QoS requirement. However, most of the studies require either knowledge of spectrum occupation by PU via the mechanism of *spectrum sensing* [29, 32] or knowledge of CSI between the PU-transmitter and PU-receiver to implement the interference level constraint for protecting the

operation of PU [40].

The capacity of SU in a spectrum sharing system is derived in [20] over non-fading AWGN channels under received power constraint. The limits on the channel capacity for a CR system has been recently studied in [31, 35]. In addition, the capacity of a spectrum sharing system is analyzed in [23] considering *symmetric* fading models (Rayleigh and Nakagami) in the presence of multiple PUs. The work in [23] is extended in [60] by studying the channel capacity limits of spectrum sharing systems in *asymmetric* fading environments. This is the set-up where the SU transmitter-PU receiver path and SU transmitter-SU receiver path could experience different fading types and link powers due to path length or shadowing.

1.4 Contributions of This Dissertation

Recall that due to the challenges and implementation issues in CR networks, the spectrum sensing information is an imprecise and unreliable resource. Therefore, the current challenges in terms of spectrum sensing and subcarriers scheduling, and the existing studies motivated us to investigate the performance of a primitive (basic) OFDM-based CR system in which the SUs randomly (blindly) utilize the available subcarriers assuming that some of the subcarriers are utilized by the PUs with the assumption of no spectrum sensing information available at the secondary (cognitive) network. The analysis and performance of such a communication set-up provides useful insights and can be utilized as a valid benchmark for performance comparison studies in CR spectrum sharing systems that assume the availability of spectrum sensing information.

This dissertation focuses on a communication scenario that assumes *random allocation* and *no spectrum sensing*. An immediate challenge to be addressed is the fact that the SU's subcarriers collide with PUs' subcarriers. However, there are no

studies available to assess the effect of subcarrier collisions in such CR spectrum sharing systems. Therefore, the requirement for a more comprehensive system analysis including the development of a stochastic model to capture the subcarrier collisions and the protection of the PUs operation in an OFDM-based CR spectrum sharing system turns out to be indispensable. In addition, the results obtained in this dissertation can be utilized as a performance benchmark for the spectrum sharing systems that assume spectrum sensing information available at the SUs. Nonetheless, the main benefit of random subcarrier utilization is to uniformly distribute the amount of SUs' interference among the PUs' subcarriers, which can be termed as *interference spreading*.

In the case of a single secondary user (SU) in the secondary network, due to the lack of information about the PUs' activities, the SU randomly allocates the subcarriers of the primary network and *collides* with the PUs' subcarriers with a certain probability. The subcarrier collisions model is shown to assume a hypergeometric distribution. To maintain the QoS requirements of PUs, the interference that SU causes onto PUs is controlled by adjusting SU's transmit power below a predefined threshold, referred to as interference temperature. The average capacity of SU with subcarrier collisions is employed as a performance measure to investigate the proposed random allocation scheme for both general and Rayleigh channel fading models. Bounds and scaling laws of average capacity with respect to the number of SU's, PUs' and available subcarriers are derived [13].

In the presence of *multiple* SUs, due to the random subcarrier allocation scheme, collisions will occur among the subcarriers used by the SUs in addition to the collisions with the subcarriers used by the PUs. The collisions among the SUs' subcarriers will decrease the system performance drastically. To overcome this issue, this work presents also an efficient centralized algorithm that sequentially assigns the randomly

selected subcarrier sets to the SUs while maintaining the orthogonality among these sets, to avoid collisions between their subcarriers. In the proposed centralized algorithm, the opportunistic scheduling of users, which yields multiuser diversity gain, is employed and the performance limits of the system in terms of multiuser diversity gain and sum capacity of multiple SUs are studied [14].

In addition, in this dissertation it is assumed that a set-up in which no spectrum sensing is performed, and the CSI between the PU transmitter and receiver pair is not known. Therefore, the complexity of the proposed random access method with respect to the methods based on spectrum sensing is much lower.

Nonetheless, considering practical systems (multiple secondary networks or cells), there may exist inter-cell subcarrier collisions not only between SUs and PUs but also among the SUs themselves due to the random access scheme[1]. Therefore, two different SU transmitter and receiver pairs belonging to different cells are considered, and the performances in terms of capacity and rate loss due to collisions (interference) between SUs in addition to that of PU are studied. The average capacity expressions of target SU's (SU-1) at the ith subcarrier are derived for no interference case, and when there is interference from only SU-2, only PU, and both SU-2 and PU [15].

The number of subcarriers required by PU or SUs can also vary based on either PU's or SUs' rate requirements. The long term average performance of the system is investigated by using a stochastic model for the required number of subcarriers of PU and SUs. The statistical analysis of the number of subcarrier collisions between the users is also conducted. The probability mass functions and the average number of subcarrier collisions are derived when there are *fixed* and *random* number of subcarriers required by users. Finally, upper bounds for instantaneous and average

[1]Under the assumption that no centralized subcarrier scheduling algorithm is employed.

maximum capacity (rate) loss of SU-1 due to collisions are derived [15].

Last but not least, the previous works motivated us to develop a theoretical fading model that can be used to perform a unified analysis for CR spectrum sharing systems. Due to the highly dynamic nature of propagation environment, several single-fading models were employed in the literature for the analysis of CR spectrum sharing systems. However, considering practical scenarios, it would be more efficient and convenient to use a generic fading model, which can be degenerated onto widely used single-fading models with an appropriate selection of parameters. Furthermore, if the environment conditions and primary network constraints allow, SUs can opportunistically allocate spectrum regions corresponding to different frequencies and bandwidths. Since the small-scale fading is frequency dependent, the resulting channel fading model can be dynamic.

In the last part of this dissertation, we proposed a generic fading model, which is termed hyper Nakagami-m fading (hyper-fading), and that incorporates several widely encountered propagation scenarios such as line-of-sight (LOS)/non-line-of-sight (NLOS) environments and fixed/mobile transmissions. Additionally, instantaneous and average power/capacity calculations can also be carried out with the proposed generic model properly. In the light of the analysis presented for the proposed method, the capacity of SU in a spectrum sharing system is studied under interference temperature constraints [16, 17, 52].

2. RANDOM SUBCARRIER ALLOCATION*

2.1 Introduction

In this chapter, the OFDM-based CR spectrum sharing communication system is considered assuming random subcarrier allocation and absence of the PU's channel occupation information, i.e., no spectrum sensing information is available at the secondary (cognitive) network. An immediate challenge to be addressed is the fact that the SU's subcarriers collide with PUs' subcarriers. Furthermore, the main idea of random subcarrier allocation (also termed random access) is provided considering the single-cell scenario. Firstly, the single SU and multiple PUs scenario is considered. Then, utilizing the byproducts of the first part, the analysis is carried out for multiple SUs, where the multiuser diversity gain of SUs and a centralized random subcarrier scheduling algorithm are proposed and studied.

The average and instantaneous capacity of SU, which are chosen as the performance criterion throughout this dissertation, with subcarrier collisions is employed to investigate the proposed random allocation scheme for both general and Rayleigh channel fading models.

Due to high volume of this chapter, the main results and contributions of this chapter are summarized as follows.

- A random subcarrier allocation method, where an arbitrary mth SU randomly utilizes F_m^S subcarriers from an available set of F subcarriers in the primary network, in an OFDM-based system is proposed. In the proposed scheme,

*Reprinted with permission from "Random subcarrier allocation in ofdm-based cognitive radio networks," by Sabit Ekin, Mohamed M. Abdallah, Khalid A. Qaraqe, and Erchin Serpedin, IEEE Transactions on Signal Processing, Volume 60, Issue 9, Page(s): 4758–4774, Sept. 2012, Copyright 2012 by IEEE.

the SUs do not have knowledge about the PUs' subcarriers utilization, i.e., no spectrum sensing is performed. Therefore, with some probability, collisions between the subcarrier sets of PUs and SU occur. It is shown that the subcarrier collision model follows a multivariate hypergeometric distribution.

- Considering the average capacity as performance measure, the SU average capacity expressions under the interference constraint of PUs in the case of single or multiple PU(s) are derived. Upper and lower bounds on average capacity are derived. It is found that the average capacity of the mth SU scales with respect to the number of subcarriers in the sets F, F_n^P and F_m^S as[1] $\Theta\left(1+1/F\right)$, $\Theta\left(1-F_n^P\right)$ and $\Theta\left(F_m^S\right)$, respectively. Furthermore, the convergence rate of average capacity as F goes to infinity is found to be logarithmic.

- To find the probability density function (PDF) and outage probability (cumulative distribution function (CDF)) of the SU capacity, which is the sum capacities of subcarriers with "interference" and "no-interference" from PU(s), the characteristic function (CF) and moment generation function (MGF) approaches are in general used to obtain the PDF and CDF of sum of variates [5]. However, the obtained PDF and CDF for the capacity of the ith subcarrier for "interference" and "no-interference" cases are too complicated and intractable using the aforementioned approaches. Therefore, by using the moment matching method, the PDF and CDF of the ith subcarrier capacity are approximated by a more tractable distribution, namely the Gamma distribution. There are various reasons for using the Gamma approximation such as being a Type-III

[1]Where F stands for the total number of available subcarriers in the primary network, and F_n^P and F_m^S are the number of subcarriers of the nth PU and the mth SU, respectively. The notation $\Theta(\cdot)$ is introduced in *Definition* 3.

Pearson distribution, widely used in fitting positive random variables (RVs), and its skewness and tail are determined by its mean and variance [4, 59, 68]. Even though the Gamma distribution approximation makes the analysis much easier to track the sum of capacities of all collided and collision-free subcarriers, we end up with a sum of Gamma variates with some of the shape and scale parameters equal or non-equal, and not necessarily integer-valued. This constraint stems from the fact that individual PUs can have distinct or the same transmit power for their subcarriers. In such a case, there are no closed-form expressions for the PDF and CDF of SU capacity. Fortunately, Moschopoulos [45] in 1985, proposed a single Gamma series representation for a sum of Gamma RVs with the scale and shape parameters having the properties mentioned above. Utilizing this nice feature of Moschopoulos PDF, the PDF and CDF of SU capacity are obtained.

- Using extreme value theory, the asymptotic analysis of multiuser diversity is investigated. The analysis conducted at this stage reveals a novel result: the limiting CDF distribution of the maximum of $\mathcal{R}$ RVs following a common Moschopoulos PDF and CDF converges to a Gumbel-type extreme value distribution as $\mathcal{R}$ converges to infinity.

- A centralized sequential algorithm based on random allocation (utilization) and assuming an opportunistic scheduling method is proposed for scheduling the subcarriers of multiple SUs while maintaining their orthogonality. The probability mass function (PMF) of the number of subcarrier collisions for the mth scheduled SU in the algorithm is derived. In addition, the proposed algorithm is compared with the case, where the SUs are selected arbitrarily, i.e., no multiuser diversity gain is exploited. Last but not least, to present the

impact of collisions among the SUs' subcarriers on the sum capacity of SUs, simulation results are provided and compared with the centralized algorithm performance with and without opportunistic scheduling.

2.1.1 Organization

The rest of the chapter is structured as follows. In Section 2.2, some essential mathematical preliminaries and definitions are provided. The system model is presented in Section 2.3. The SU capacity analysis over arbitrary and Rayleigh fading channels is investigated in Section 2.4. The multiuser diversity gain in the opportunistic scheduling of SUs is studied in Section 2.5. Section 2.6 presents a centralized algorithm for orthogonal subcarrier scheduling of SUs. The numerical and simulation results are given in Section 2.7. Finally, concluding remarks are drawn in Section 2.8.

2.2 Mathematical Preliminaries and Definitions

In this section, the hypergeometric distribution and some important definitions that are frequently used throughout this chapter and dissertation are provided.

Definition 1 (Hypergeometric Distribution [54]). *Suppose that an urn contains n balls, of which r are red and $n-r$ are white. Let K denote the number of red balls drawn when taking m balls without replacement. Then, K is a hypergeometric random variable (RV) with parameters r, n and m, and its PMF is given by:*

$$Pr(K=k) = p(k) = \binom{r}{k}\binom{n-r}{m-k}\Big/\binom{n}{m},$$

where the notation $\binom{\cdot}{\cdot}$ stands for the binomial coefficient.

Proposition 1 (PMF of Number of Subcarrier Collisions). *When the mth SU randomly utilizes (allocates) F_m^S subcarriers from a set of F available subcarriers without replacement, and F_n^P subcarriers are being used by the nth PU, then the PMF*

of the number of subcarrier collisions, k_{nm}, follows the hypergeometric distribution, $k_{nm} \sim \texttt{HYPG}(F_m^S,\ F_n^P,\ F)$, and is expressed as:

$$Pr(K_{nm} = k_{nm}) = p(k_{nm}) = \binom{F_n^P}{k_{nm}} \binom{F - F_n^P}{F_m^S - k_{nm}} \Big/ \binom{F}{F_m^S},$$

where the notation $\binom{\cdot}{\cdot}$ stands for the binomial coefficient.

The average number of subcarrier collisions is

$$\mathbb{E}\left[k_{nm}\right] = \frac{F_m^S F_n^P}{F},$$

where $\mathbb{E}\left[\cdot\right]$ denotes the expectation operator.

Proof. The proof can be readily shown by interpreting the process of allocating the subcarriers as selecting balls from an urn without replacement. Furthermore, the expected value of the number of subcarriers is obtained from $\mathbb{E}\left[k_{nm}\right] = \sum_{k_{nm}} k_{nm} p(k_{nm})$. □

In the case of multiple PUs, the mth SU might have subcarrier collisions with up to N PUs. Let $\mathbf{k}_m = [k_{1m}, k_{2m}, \ldots, k_{Nm}, k_{fm}]^T \in \mathbb{Z}_{0+}^{N+1}$ represent the number of collisions of the mth SU with N PUs and with the collision-free subcarriers, k_{fm}. Then, the (joint) PMF of $\mathbf{k}_m$ is given by

$$\begin{aligned} \Pr(\mathbf{K}_m = \mathbf{k}_m) = p(\mathbf{k}_m) &= \binom{F_1^P}{k_{1m}} \binom{F_2^P}{k_{2m}} \cdots \binom{F_N^P}{k_{Nm}} \binom{F - \sum_{n=1}^N F_n^P}{k_{fm}} \Big/ \binom{F}{F_m^S} \\ &= \left[\binom{F_f}{k_{fm}} \prod_{n=1}^N \binom{F_n^P}{k_{nm}} \right] \Big/ \binom{F}{F_m^S}, \end{aligned} \tag{2.1}$$

where $F_f = F - \sum_{n=1}^N F_n^P$ stands for the number of free subcarriers in the primary net-

work. One can observe that $\mathbf{k}_m$ follows a modified multivariate hypergeometric distribution $\mathbf{k}_m \sim \texttt{M-HYPG}\left(F_m^S,\ \mathbf{F^P},\ F\right)$, where $\mathbf{F^P} = \left[F_1^P, F_2^P, \ldots, F_N^P, F_f\right]^T \in \mathbb{Z}_{0+}^{N+1}$, and the *support* of $\mathbf{k}_m$ is given by:

$$\left\{\mathbf{k}_m : \sum_{n=1}^{N} k_{nm} + k_{fm} = F_m^S \text{ and } k_{nm} \in \left[\left(F_m^S + F_n^P - F\right)^+, \ldots, \min\left\{F_m^S, F_n^P\right\}\right]\right\},$$

where $(x)^+ = \max\{0, x\}$.

Definition 2 (Rate of Convergence [66])**.** *An infinite sequence $\{A_n\}$ converging to the limit A is said to be logarithmically convergent if*

$$\lim_{n\to\infty} \frac{|\Delta A_{n+1}|}{|\Delta A_n|},$$

and

$$\lim_{n\to\infty} \frac{|A_{n+1} - A|}{|A_n - A|},$$

both exist and are equal to unity, where $\Delta A_n = A_{n+1} - A_n$.

If only $\lim_{n\to\infty} |\Delta A_{n+1}| / |\Delta A_n| = 1$ holds, then the sequence $\{A_n\}$ converges sublinearly to A.

Definition 3 (Knuth's notations [39])**.** *Let $f(n)$ and $g(n)$ be nonnegative functions. The notation:*

- *$f(n) = O(g(n))$ means that there exist positive constants c and n_0 such that $f(n) \leq cg(n)$ for all $n \geq n_0$.*
- *$f(n) = \Omega(g(n))$ means that there exist positive constants c and n_0 such that $f(n) \geq cg(n)$ for all $n \geq n_0$, i.e., $g(n) = O(f(n))$.*
- *$f(n) = \Theta(g(n))$ means that there exist positive constants c, c' and n_0 such*

that $cg(n) \leq f(n) \leq c'g(n)$ *for all* $n \geq n_0$*, i.e., both* $f(n) = O(g(n))$ *and* $f(n) = \Omega(g(n))$ *hold.*

Definition 4. *The capacity of* m*th SU with* F_m^S *subcarriers is defined as the summation of capacities for each subcarrier. Let* $S_{m,i}$ *be the signal-to-interference plus noise ratio (SINR) for the* i*th subcarrier of the* m*th user, then the SU capacity is given by:*[2]

$$C_m = \sum_{i=1}^{F_m} \log\left(1 + S_{m,i}\right).$$

Definition 5 (Capacity with Collisions)**.** *Let* $S_{m,i}^{I,n}$ *and* $S_{m,i}^{NI}$ *be the SINR for the* i*th subcarrier of the* m*th SU with "interference" and "no-interference" from the* n*th PU, respectively.*[3] *If* k_{nm} *subcarriers of the* m*th SU collide with the* n*th PU's subcarriers, then the capacity of SU in Definition 4 with subcarrier collisions can be redefined as*

$$C_m^1 = \sum_{i=1}^{k_{nm}} \log\left(1 + S_{m,i}^{I,n}\right) + \sum_{i=1}^{k_{fm}} \log\left(1 + S_{m,i}^{NI}\right),$$

where k_{nm} *and* $k_{fm} = F_m^S - k_{nm}$ *are hypergeometric RVs that denote the number of collided (i.e., interference) and collision-free (i.e., no-interference) subcarriers between the* n*th PU and the* m*th SU, respectively. The superscript "1" indicates that collisions occur with only single PU's subcarriers (any arbitrary* n*th PU) in the primary network. The SU capacity expression in case of multiple* N *PUs is given in* (2.12).

---

[2] All logarithms in the following are with respect to the base e unless otherwise stated.

[3] $S_{m,i}^{NI}$ is indeed the signal-to-noise ratio (SNR) for the ith subcarrier. However, to emphasize the subcarrier collision and collision-free cases, it is called SINR with "no-interference" from PU throughout the dissertation.

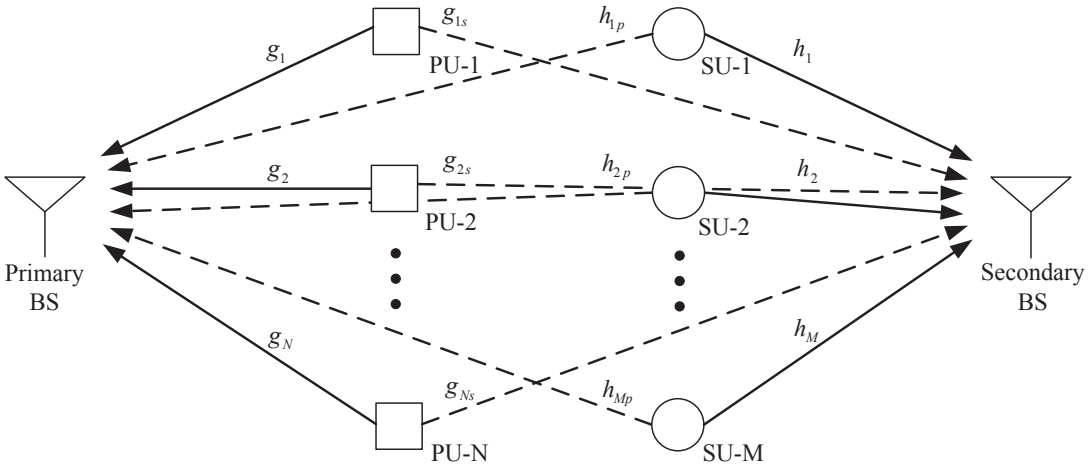

Figure 2.1: System model; M SUs transmit to the secondary base station (SBS) using the subcarriers in the primary network with subcarrier collisions following the hypergeometric distribution for accessing PUs' subcarriers, [(- -): Interference-link (channel), (–): Desired-link (channel)].

2.3 System Model

The system model is illustrated in Figure 2.1, where the primary and cognitive (secondary) networks consist of N PUs with a primary base station (PBS) and M SUs with a secondary base station (SBS), respectively. To preserve the quality of service (QoS) requirements of PUs in a spectrum sharing communication network, the interference power levels caused by the SU-transmitters at the primary receiver (PBS) must not be larger than a predefined value ($\Psi_i,\ i = 1, \ldots, F$) for each subcarrier, referred to as the *interference temperature* (IT). It is assumed that there is no correlation among the subcarriers. Nonetheless, due to the inherent nature of random allocation (utilization) method and the high number of available subcarriers in practice, the probability of a SU to select consecutive subcarriers, which are practically correlated, would be considerably negligible.

The *channel power gains* from the mth SU to SBS and PBS are denoted by h_m and h_{mp}, respectively. Similarly, g_n and g_{ns} represent the channel power gains from

the nth PU to PBS and SBS, respectively. All the channel gains are assumed to be unit mean independent and identically distributed (i.i.d.) flat Rayleigh fading channels. The channel power gains are hence exponentially distributed with unit mean. Further, to have a tractable theoretical analysis, it is assumed that perfect information about the interference channel power gains, h_{mp}, is available at SUs. The SUs can obtain this information, referred to as channel side information (CSI), through various ways, e.g., from the channel reciprocity condition[4] [72, 74], or from an entity called mediate band or CR network manager between the PBS and SU [6]. The thermal additive white Gaussian noise (AWGN) at both PUs and SUs is assumed to have circularly symmetric complex Gaussian distribution with zero mean and variance η, i.e., $\mathcal{CN}(0, \eta)$. Throughout the chapter, the parameters $h_{m,i}$, $h_{mp,i}$, $g_{n,i}$ and $g_{ns,i}$ denote the channel power gains associated with the ith subcarrier. Furthermore, for the sake of analysis simplicity, the value of IT is assumed to be the same for all subcarriers in the system and available at the SUs, and the transmit power of each user (either PU or SU) is the same for all its subcarriers, i.e., $P_{n,i} = P_n$ and $P_{m,i} = P_m$.

The total number of available subcarriers in the primary network is denoted by F. The subcarrier set of each PU is assumed to be assigned by preserving the orthogonality among the sets of subcarriers for all PUs, F_n^P for $n = 1, \ldots, N$. SU randomly allocates the subcarriers from the available subcarriers set F without having access to the information about the channel occupied by PUs. Therefore, SU will collide with the subcarriers of the PUs with a certain probability. Subcarrier collisions occur when SUs employ subcarriers which are in use by PUs, and the probabilistic

[4]With the assumptions of channel reciprocity and pre-knowledge of the PBS transmit power level, SU can estimate the received signal power from PBS when it transmits [72].

model for the number of subcarrier collisions follows a multivariate hypergeometric distribution.

During the evaluation of SU capacity in Section 2.4, it is assumed that there is only *a single SU* (any arbitrary mth SU) in the cognitive network, and the collisions occur between the subcarriers of the SU and PUs due to the random allocation scheme. This set-up can also be easily extended to multiple SUs with the assumption of no mutual interference among SUs. However, such a framework would not be practical, since due to the random allocation method, the likelihood of the same subcarriers being allocated to multiple SUs will be quite high. To avoid such a scenario, an efficient allocation of SUs' subcarriers is needed to preserve the orthogonality among SUs subcarriers. Therefore, an centralized algorithm, which sequentially allocates the subcarriers to multiple SUs based on the random allocation method, while maintaining orthogonality among SUs' subcarriers, is proposed and analyzed in Section 2.6.

2.4 Capacity of Secondary User

In this section, the average capacity of a single SU including the bounds and scaling laws with respect to the number of subcarriers for the case of an arbitrary channel fading model is investigated. Then, the Rayleigh channel fading model is used to study the impacts of the system parameters and to evaluate the expressions for the PDF and CDF of SU capacity.

2.4.1 Analysis of SU Average Capacity for General Fading

Theorem 1. *The average capacity of the mth SU in the presence of a single (nth) PU is given by*

$$\mathbb{E}\left[C_m^1\right] = \frac{F_m^S}{F}\left[F_n^P\left(\mathbb{E}\left[C_{m,i}^{I,n}\right] - \mathbb{E}\left[C_{m,i}^{NI}\right]\right) + F\mathbb{E}\left[C_{m,i}^{NI}\right]\right],$$

where variables $C_{m,i}^{I,n}$ and $C_{m,i}^{NI}$ represent the ith subcarrier capacity of the mth SU with "interference" and "no-interference" from the nth PU, respectively. In the case of Rayleigh channel fading, $\mathbb{E}\left[C_{m,i}^{I,n}\right]$ and $\mathbb{E}\left[C_{m,i}^{NI}\right]$ are given in (2.13) *and* (2.14)*, respectively.*

Proof. The proof is given in Appendix A. □

Corollary 1. *The average capacity of mth SU in the presence of N PUs is given by*

$$\mathbb{E}\left[C_m\right] = \frac{F_m^S}{F}\left[\sum_{n=1}^{N} F_n^P \mathbb{E}\left[C_{m,i}^{I,n}\right] + F_f \mathbb{E}\left[C_{m,i}^{NI}\right]\right].$$

Proof. The proof is given in Appendix B. □

2.4.1.1 Bounds on the Average Capacity

In this section, certain bounds on the average capacity of SU will be established. Intuitively, representing the relation of order between the average capacity of the ith subcarrier with PU's "interference" and "no-interference" as $\mathbb{E}\left[C_{m,i}^{I,n}\right] \leq \mathbb{E}\left[C_{m,i}^{NI}\right]$, the naive upper and lower bounds on the SU average capacity can be expressed as

$$F_m^S \mathbb{E}\left[C_{m,i}^{I,n}\right] \leq \mathbb{E}\left[C_m^1\right] \leq F_m^S \mathbb{E}\left[C_{m,i}^{NI}\right] \ , \tag{2.2}$$

which states that the upper bound, in the best case, is when all SU's subcarriers are collision-free, i.e., all subcarriers are interference-free, $k_{fm} = F_m^S$. Similarly for the lower bound, all SU's subcarriers are colliding with the PU's subcarriers, i.e., $k_{nm} = F_m^S$.

However, the maximum and minimum number of subcarrier collisions might not be necessarily F_m^S and 0, respectively. The following general result holds.

Corollary 2. *Tight upper and lower bounds on the average capacity of SU in the presence of a single PU are given by:*

$$k_{nm}^{\max}\mathbb{E}\left[C_{m,i}^{I,n}\right]+k_{fm}^{\min}\mathbb{E}\left[C_{m,i}^{NI}\right]\leq\mathbb{E}\left[C_{m}^{1}\right]\leq k_{nm}^{\min}\mathbb{E}\left[C_{m,i}^{I,n}\right]+k_{fm}^{\max}\mathbb{E}\left[C_{m,i}^{NI}\right],$$

where $k_{nm}^{\max}$ *and* $k_{nm}^{\min}$ *represents the maximum and minimum number of subcarrier collisions, respectively, and are defined as* $k_{nm}^{\min}=\left(F_{m}^{S}+F_{n}^{P}-F\right)^{+}$ *and* $k_{nm}^{\max}=\min\left\{F_{m}^{S},F_{n}^{P}\right\}$. *Also,* $k_{fm}^{\max}=F_{m}^{S}-k_{nm}^{\min}$ *and* $k_{fm}^{\min}=F_{m}^{S}-k_{nm}^{\max}$.

Proof. The number of subcarrier collisions does not depend only on SU's subcarriers but also on PU's subcarriers. Therefore, the support region of k_{nm}, considering the PU's subcarriers, is given by $\left\{\left(F_{m}^{S}+F_{n}^{P}-F\right)^{+},\ldots,\min\left\{F_{m}^{S},F_{n}^{P}\right\}\right\}$. Using this support region, the bounds are established. □

It is worth to note that the naive upper bound, given in (2.2), on the average capacity is the limit point of capacity as the number of available subcarriers F goes to infinity. Formally,

$$\lim_{F\to\infty}\mathbb{E}\left[C_{m}^{1}\right]=F_{m}^{S}\mathbb{E}\left[C_{m,i}^{NI}\right],$$

which states that for a fixed number of PU's subcarriers as the number of available subcarriers increases, the average capacity converges to the case where no SU's subcarrier collides.

2.4.1.2 Scaling Laws for the Average Capacity

Corollary 3. *The average capacity of the mth SU in the presence of a single PU scales with respect to the number of subcarriers* F, F_{m}^{S} *and* F_{n}^{P} *as* $\Theta\left(1+1/F\right)$, $\Theta\left(F_{m}^{S}\right)$ *and* $\Theta\left(1-F_{n}^{P}\right)$, *respectively.*

Proof. Using the Knuth's notation from *Definition* 3, one can infer that

$$\lim_{F\to\infty} \frac{\mathbb{E}\left[C_m^1\right]}{1+\frac{1}{F}} = \lim_{F\to\infty} \frac{\frac{F_m^S F_n^P}{F}\left(\mathbb{E}\left[C_{m,i}^{I,n}\right] - \mathbb{E}\left[C_{m,i}^{NI}\right]\right) + F_m^S \mathbb{E}\left[C_{m,i}^{NI}\right]}{1+\frac{1}{F}}$$
$$= F_m^S \mathbb{E}\left[C_{m,i}^{NI}\right] > 0.$$

Following the same approach, one can establish the scaling laws of SU average capacity with respect to F_m^S and F_n^P. □

Further, it can be also shown that for the multiple PUs case, the average capacity of the mth SU is converging to the lower bound on average capacity for the single PU case as $N, F \to \infty$. Assume without loss of generality that an infinite number of subcarriers F is available. Because the orthogonality of PUs' subcarriers is maintained, then $\sum_{n=1}^{N} F_n^P \approx F$ as $F, N \to \infty$. Hence,

$$\lim_{N,F\to\infty} \mathbb{E}\left[C_m^1\right] = \lim_{N,F\to\infty} \frac{F_m^S}{F}\left[\sum_{n=1}^{N} F_n^P \mathbb{E}\left[C_{m,i}^{I,n}\right] + F_f \mathbb{E}\left[C_{m,i}^{NI}\right]\right]$$
$$= F_m^S \mathbb{E}\left[C_{m,i}^{I,n}\right],$$

where it is assumed that all the PUs have the same transmit power. Thus, $\mathbb{E}\left[C_{m,i}^{I,n}\right]$ is the same for all N PUs.

Corollary 4. *The average capacity of the mth secondary user in the presence of a single PU converges logarithmically to* $F_m^S \mathbb{E}\left[C_{m,i}^{NI}\right]$ *as* F *increases towards infinity:*

$$\mathbb{E}\left[C_m^1\right] \xrightarrow[\text{with } \log(F)]{F\to\infty} F_m^S \ \mathbb{E}\left[C_{m,i}^{NI}\right]. \tag{2.3}$$

Proof. The proof is given in Appendix C. □

Using similar steps, one can readily obtain the bounds and the scaling laws of the

SU average capacity in the presence of multiple (N) PUs in the primary network.

2.4.2 SU Capacity Analysis over Rayleigh Channel Fading

In this section, the SU capacity over a Rayleigh channel fading model is investigated. Thus far, the CR capacity studies in the literature have mostly assumed two types of PUs' interference constraints on the SU transmit power: the *peak power interference constraint* and the *average interference constraint* [62,72]. The peak power interference constraint is adapted in this work, and an adaptive scheme is used to adjust the transmit power of SU to maintain the QoS of PUs. Hence, the transmit power of the mth SU corresponding to the ith subcarrier is given by[5]

$$P_{m,i}^{T} = \begin{cases} P_{m,i} \ , & \Psi_i \geq P_{m,i} h_{mp,i} \\ \frac{\Psi_i}{h_{mp,i}}, & \Psi_i < P_{m,i} h_{mp,i} \end{cases} = \min \left\{ P_{m,i}, \frac{\Psi_i}{h_{mp,i}} \right\},$$

for $i = 1, \ldots, F$.

Let $\lambda_{m,i} = h_{m,i} P_{m,i}^{T}$, then the received SINR of the mth SU's ith subcarrier is

$$S_{m,i}^{I,n} = \frac{\lambda_{m,i}}{I_{n,i}^{P} + \eta}, \quad \text{for } n = 1, \ldots, N, \tag{2.4}$$

where $I_{n,i}^{P} = P_{n,i} g_{ns,i}$ stands for the mutual interference caused by nth PU on the ith subcarrier. In (2.4), $S_{m,i}^{I,n}$ represents the SINR in case when subcarrier collision occurs. Therefore, when there is no collision, i.e., the subcarrier is not being used by two users, there is no interference caused by PUs. Hence, $S_{m,i}^{NI} = \lambda_{m,i}/\eta$.

[5]Notice that due to the random allocation, the SU transmit power is adapted (regulated) considering the worst case scenario, as if all the subcarriers in the primary network are utilized by PUs. This condition assures the QoS requirements of PUs.

The CDF of $\lambda_{m,i}$ can be obtained as follows [33]:

$$F_{\lambda_{m,i}}(x) = F_{h_{mp,i}}\left(\frac{\Psi_i}{P_{m,i}}\right) F_{\vartheta_1}(x) + F_{\vartheta_2|h_{mp,i}>\frac{\Psi_i}{P_{m,i}}}\left(x \;\middle|\; h_{mp,i} > \frac{\Psi_i}{P_{m,i}}\right),$$

where $\vartheta_1 = h_{m,i}P_{m,i}$ and $\vartheta_2 = \Psi_i h_{m,i}/h_{mp,i}$, with their corresponding PDFs given by $f_{\vartheta_1}(x) = e^{-x/\Psi_i}/\Psi_i$, and $f_{\vartheta_2}(x) = \Psi_i/(x+\Psi_i)^2$, respectively. Hence the CDF and the PDF can be expressed, respectively, as

$$\begin{aligned} F_{\lambda_{m,i}}(x) &= \left(1 - e^{-\frac{\Psi_i}{P_{m,i}}}\right)\left(1 - e^{-\frac{x}{P_{m,i}}}\right) + e^{-\frac{\Psi_i}{P_{m,i}}} - \frac{\Psi_i}{P_{m,i}+x} e^{-\frac{x+\Psi_i}{P_{m,i}}} \\ &= 1 - e^{-\frac{x}{P_{m,i}}} + \frac{x}{\Psi_i + x} e^{-\frac{x+\Psi_i}{P_{m,i}}}, \end{aligned} \tag{2.5}$$

$$\begin{aligned} f_{\lambda_{m,i}}(x) &= \frac{dF_{\lambda_{m,i}}(x)}{dx} \\ &= \frac{e^{-\frac{x}{P_{m,i}}}}{P_{m,i}}\left[1 - e^{-\frac{\Psi_i}{P_{m,i}}}\left(\frac{x^2 + \Psi_i x - \Psi_i P_{m,i}}{(\Psi_i + x)^2}\right)\right]. \end{aligned} \tag{2.6}$$

Similarly, by using a transformation of RVs, the PDF of $S_{m,i}^{I,n}$ with $f_{I_{n,i}^P}(y) = e^{-y/P_{n,i}}/P_{n,i}$ can be expressed as [62]

$$\begin{aligned} F_{S_{m,i}^{I,n}}(x) &= \Pr\left(\lambda_{m,i} < x\left(I_{n,i}^P + \eta\right)\right) \\ &= \int_0^\infty F_{\lambda_{m,i}}\left(x\left(y+\eta\right)\right) f_{I_{n,i}^P}(y)\mathrm{d}y. \end{aligned} \tag{2.7}$$

Plugging (2.5) into (2.7), it follows that

$$\begin{aligned} F_{S_{m,i}^{I,n}}(x) =& 1 - \frac{\left(1 - e^{-\frac{\Psi_i}{P_{m,i}}}\right) e^{-\frac{x\eta}{P_{m,i}}}}{1 + \frac{xP_{n,i}}{P_{m,i}}} - \frac{\Psi_i}{xP_{n,i}} e^{\frac{\Psi_i}{xP_{n,i}} + \frac{\eta}{P_{n,i}}} \\ &\times \Gamma\left(0, \left(\eta + \frac{\Psi_i}{x}\right)\left(\frac{1}{P_{n,i}} + \frac{x}{P_{m,i}}\right)\right), \end{aligned}$$

where the upper incomplete Gamma function is defined as
$\Gamma(x,y) = \int_y^\infty t^{x-1}e^{-t}\mathrm{d}t$, and the derivation of CDF yields the PDF

$$\begin{aligned} f_{S_{m,i}^{I,n}}(x) =& \frac{x\eta P_{n,i} + P_{m,i}(\eta + P_{n,i})}{(xP_{n,i} + P_{m,i})^2}\left(e^{\frac{\Psi_i}{P_{m,i}}} - 1\right)e^{-\frac{x\eta+\Psi_i}{P_{m,i}}} + \frac{\Psi_i}{x^3P_{n,i}^2}e^{\frac{x\eta+\Psi_i}{xP_{n,i}}} \\ &\times \left[(\Psi_i + xP_{n,i})\Gamma\left(0, \left(\eta + \frac{\Psi_i}{x}\right)\left(\frac{1}{P_{n,i}} + \frac{x}{P_{m,i}}\right)\right)\right. \\ &\left. + \frac{xP_{n,i}(x^2\eta P_{n,i} - \Psi_i P_{m,i})}{(x\eta + \Psi_i)(xP_{n,i} + P_{m,i})}e^{-\left(\eta + \frac{\Psi_i}{x}\right)\left(\frac{1}{P_{n,i}} + \frac{x}{P_{m,i}}\right)}\right]. \end{aligned} \tag{2.8}$$

Similarly, when there is no primary interference using (2.6) and the transformation $f_{S_{m,i}^{NI}}(x) = \eta f_{\lambda_{m,i}}(\eta x)$, it follows that

$$f_{S_{m,i}^{NI}}(x) = \frac{\eta e^{-\frac{\eta x}{P_{m,i}}}}{P_{m,i}}\left[1 - e^{-\frac{\Psi_i}{P_{m,i}}}\left(\frac{(\eta x)^2 + \Psi_i\eta x - \Psi_i P_{m,i}}{(\Psi_i + \eta x)^2}\right)\right], \tag{2.9}$$

and the CDF is given by

$$F_{S_{m,i}^{NI}}(x) = 1 - e^{-\frac{\eta x}{P_{m,i}}} + \frac{\eta x}{\Psi_i + \eta x}e^{-\frac{\eta x + \Psi_i}{P_{m,i}}}. \tag{2.10}$$

Finally, the desired expressions for the PDFs of $C_{m,i}^{I,n}$ and $C_{m,i}^{NI}$ can be obtained by transforming the RVs as follows:

$$\begin{aligned} f_{C_{m,i}^{I,n}}(x) &= \left|\frac{dy}{dx}\right| f_{S_{m,i}^{I,n}}(y)\Big|_{y=e^x-1} \\ &= e^x f_{S_{m,i}^{I,n}}(e^x - 1), \\ f_{C_{m,i}^{NI}}(x) &= e^x f_{S_{m,i}^{NI}}(e^x - 1). \end{aligned} \tag{2.11}$$

Using *Definition* 5, for any arbitrary mth SU and multiple (N) interfering PUs,

the instantaneous SU capacity with subcarrier collisions is given by

$$\begin{aligned} C_m &= \sum_{i=1}^{k_{1m}} \underbrace{\log\left(1+S_{m,i}^{I,1}\right)}_{C_{m,i}^{I,1}} + \cdots + \sum_{i=1}^{k_{Nm}} \underbrace{\log\left(1+S_{m,i}^{I,N}\right)}_{C_{m,i}^{I,N}} + \sum_{i=1}^{k_{fm}} \underbrace{\log\left(1+S_{m,i}^{NI}\right)}_{C_{m,i}^{NI}} \\ &= \underbrace{\sum_{n=1}^{N} \overbrace{\sum_{i=1}^{k_{nm}} C_{m,i}^{I,n}}^{C_m^{I,n}}}_{C_m^I} + \underbrace{\sum_{i=1}^{k_{fm}} C_{m,i}^{NI}}_{C_m^{NI}}. \end{aligned} \tag{2.12}$$

There are two types of well known methods available to evaluate the distribution for sum of variates, namely, the characteristic function (CF) and the moment generating function (MGF) based methods [5]. Unfortunately, by employing these methods, it is often hard and intractable to obtain explicit closed form expressions for the PDF and CDF of SU capacity in (2.12) from (2.8)-(2.11). Even if we obtain, it will hardly provide any insights because of the complicated expressions. Therefore, in order to sum up the rates for the cases of interference and no-interference, we will approximate the PDFs of $C_{m,i}^{I,n}$ and $C_{m,i}^{NI}$ using a Gamma distribution. There are important properties of the Gamma distribution that are suitable for approximating the PDFs of the variables $C_{m,i}^{I,n}$ and $C_{m,i}^{NI}$. First, the sum of Gamma distributed RVs with the same scale parameters is another Gamma distributed RVs. Second, the skewness and tail of distribution are similar for the whole range of interest and are determined by mean and variance [68]. Last but not least, Gamma distribution is a Type-III Pearson distribution which is widely used in fitting *positive* RVs [4, 59, 68]. In addition, since Gamma distribution is uniquely determined by its mean and variance, we employed the moment matching method to the first two moments: mean and variance.

Definition 6. *X follows a Gamma distribution, $X \sim \mathcal{G}(\alpha, \beta)$, if the corresponding*

PDF of X with scale and shape parameters, $\beta > 0$ and $\alpha > 0$, respectively, is given by

$$f_X(x) = \frac{x^{\alpha-1}\exp\left(-\frac{x}{\beta}\right)}{\beta^{\alpha}\Gamma(\alpha)}U(x),$$

where $U(\cdot)$ denotes the unit step function, and the Gamma function is defined as $\Gamma(x) = \int_0^{\infty} t^{x-1}e^{-t}\mathrm{d}t$.

Since the mean and variance of Gamma distribution are $\alpha\beta$ and $\alpha\beta^2$, respectively, mapping the first two moments with the PDFs of $C_{m,i}^{I,n}$ and $C_{m,i}^{NI}$ yields

$$\alpha_n^I = \frac{\left(\mathbb{E}\left[C_{m,i}^{I,n}\right]\right)^2}{\mathbf{var}\left[C_{m,i}^{I,n}\right]}, \quad \beta_n^I = \frac{\mathbf{var}\left[C_{m,i}^{I,n}\right]}{\mathbb{E}\left[C_{m,i}^{I,n}\right]},$$
$$\alpha^{NI} = \frac{\left(\mathbb{E}\left[C_{m,i}^{NI}\right]\right)^2}{\mathbf{var}\left[C_{m,i}^{NI}\right]}, \quad \beta^{NI} = \frac{\mathbf{var}\left[C_{m,i}^{NI}\right]}{\mathbb{E}\left[C_{m,i}^{NI}\right]},$$

for $n = 1, 2, \ldots, N$, and $\mathbf{var}(x)$ denotes the variance of x.

From [62], using (2.8)-(2.11), the average capacity of $C_{m,i}^{I,n}$ and $C_{m,i}^{NI}$ can be expressed, respectively, as

$$\begin{aligned}
\mathbb{E}\left[C_{m,i}^{I,n}\right] &= \int_0^{\infty} x f_{C_{m,i}^{I,n}}(x)\mathrm{d}x \\
&= \int_0^{\infty} \log(1+x) f_{S_{m,i}^{I,n}}(x)\mathrm{d}x \\
&= \frac{1-e^{-\frac{\Psi_i}{P_{m,i}}}}{1-\frac{P_{n,i}}{P_{m,i}}}\left(\Gamma\left(0, \frac{\eta}{P_{m,i}}\right)e^{\frac{\eta}{P_{m,i}}} - \Gamma\left(0, \frac{\eta}{P_{n,i}}\right)e^{\frac{\eta}{P_{n,i}}}\right) \\
&\quad + \frac{\Psi_i}{P_{n,i}}e^{\frac{\eta}{P_{n,i}}}\int_0^{\infty}\Gamma\left(0, \left(\eta + \frac{\Psi_i}{x}\right)\left(\frac{1}{P_{n,i}} + \frac{x}{P_{m,i}}\right)\right)\frac{e^{\frac{\Psi_i}{xP_{n,i}}}}{x(1+x)}\mathrm{d}x,
\end{aligned} \tag{2.13}$$

and

$$\begin{aligned}\mathbb{E}\left[C_{m,i}^{NI}\right] &= \int_0^\infty x f_{C_{m,i}^{NI}}(x)\mathrm{d}x \\ &= \int_0^\infty \log(1+x) f_{S_{m,i}^{NI}}(x)\mathrm{d}x \\ &= \Gamma\left(0, \frac{\eta}{P_{m,i}}\right) e^{\frac{\eta}{P_{m,i}}} \left(1 + \frac{e^{-\frac{\Psi_i}{P_{m,i}}}\eta}{\Psi_i - \eta}\right) + \frac{\Psi_i}{\eta - \Psi_i}\Gamma\left(0, \frac{\Psi_i}{P_{m,i}}\right).\end{aligned} \tag{2.14}$$

The variance of $C_{m,i}^{I,n}$ is given by

$$\mathbf{var}\left[C_{m,i}^{I,n}\right] = \mathbb{E}\left[\left(C_{m,i}^{I,n}\right)^2\right] - \left(\mathbb{E}\left[C_{m,i}^{I,n}\right]\right)^2,$$

where the second moment of $C_{m,i}^{I,n}$ is expressed as

$$\begin{aligned}\mathbb{E}\left[\left(C_{m,i}^{I,n}\right)^2\right] &= \int_0^\infty \left[\log(1+x)\right]^2 f_{S_{m,i}^{I,n}}(x)\mathrm{d}x \\ &= \int_0^\infty \frac{2\log(1+x)}{1+x}\left[1 - F_{S_{m,i}^{I,n}}(x)\right]\mathrm{d}x \\ &\simeq \sum_{j=1}^{N_p} w_j \frac{2\log(1+s_j)}{1+s_j}\left[1 - F_{S_{m,i}^{I,n}}(s_j)\right],\end{aligned}$$

where the second equality is obtained by using integration by parts [62]. The resulting integral is readily estimated by employing Gauss-Chebyshev quadrature (GCQ) formula, where the weights (w_j) and abscissas (s_j) are defined in [70, Eqs. (22) and (23)], respectively. The truncation index N_p could be chosen to make the approximation error negligibly small such as $N_p = 50$ for a sufficiently accurate result.

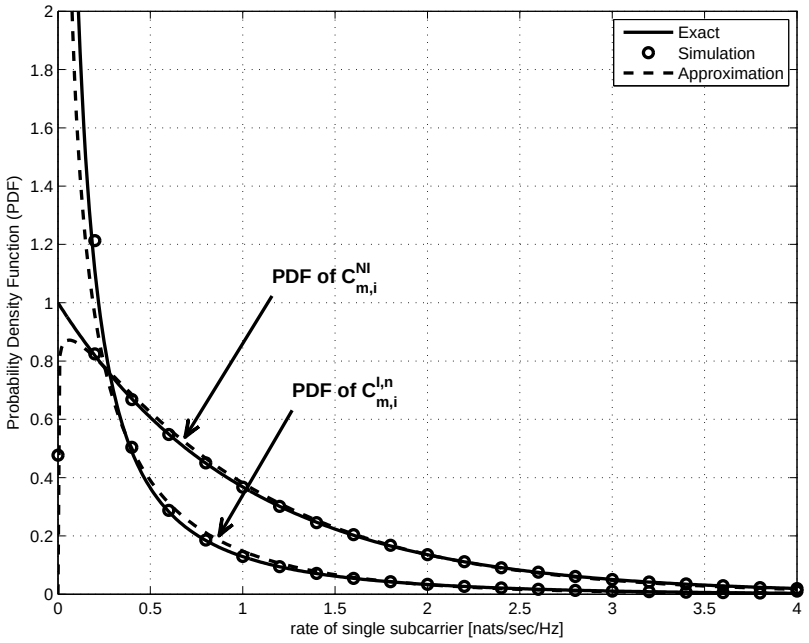

Figure 2.2: Comparison between the exact and approximation of $f_{C_{m,i}^{I,n}}(x)$ and $f_{C_{m,i}^{NI}}(x)$ using the PDF of Gamma distribution for $P_{m,i} = 20$ dB, $P_{n,i} = 10$ dB, $\Psi_i = 0$ dB and $\eta = 1$.

Similarly, the variance of $C_{m,i}^{NI}$ is expressed as

$$\mathbf{var}\left[C_{m,i}^{NI}\right] = \mathbb{E}\left[\left(C_{m,i}^{NI}\right)^2\right] - \left(\mathbb{E}\left[C_{m,i}^{NI}\right]\right)^2,$$

where the second moment of $C_{m,i}^{NI}$ is calculated as follows

$$\mathbb{E}\left[\left(C_{m,i}^{NI}\right)^2\right] \simeq \sum_{j=1}^{N_p} w_j \frac{2\log(1+s_j)}{1+s_j}\left[1 - F_{S_{m,i}^{NI}}(s_j)\right].$$

Therefore, using the Gamma approximation, the capacities are approximated as $C_{m,i}^{I,n} \sim \mathcal{G}\left(\alpha_n^I, \beta_n^I\right)$ and $C_{m,i}^{NI} \sim \mathcal{G}\left(\alpha^{NI}, \beta^{NI}\right)$.

In Figures 2.2 and 2.3, the exact and approximative expressions of $f_{C_{m,i}^{I,n}}(x)$ and $f_{C_{m,i}^{NI}}(x)$, including the simulations results, for different system parameters are shown. It can be observed that the approximation is very close to the exact results.

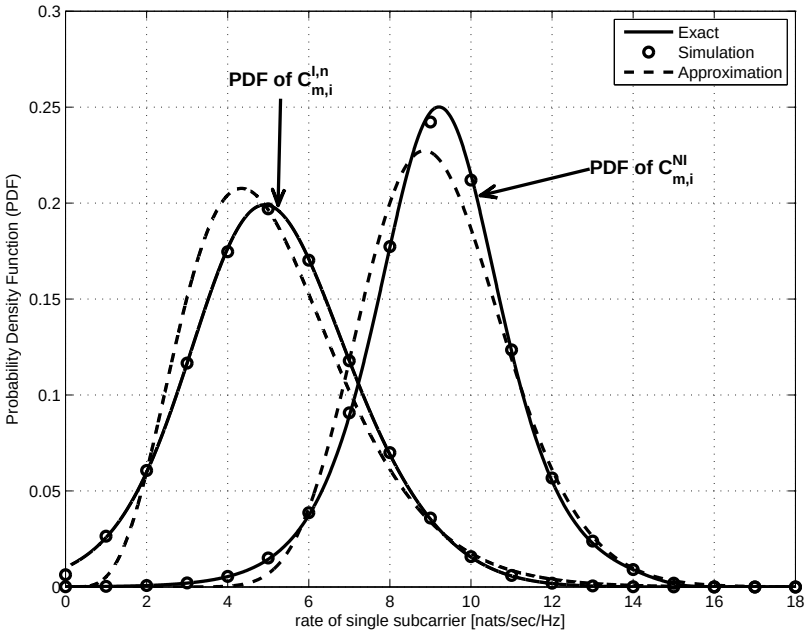

Figure 2.3: Comparison between the exact and approximation of $f_{C^{I,n}_{m,i}}(x)$ and $f_{C^{NI}_{m,i}}(x)$ using the PDF of Gamma distribution for $P_{m,i} = 40$ dB, $P_{n,i} = 0$ dB, $\Psi_i = 20$ dB and $\eta = 0.01$.

Since both $C^{I,n}_{m,i}$ and $C^{NI}_{m,i}$ are i.i.d. for given k_{nm}, the conditional characteristic functions for the rate sums $\sum_{i=1}^{k_{nm}} C^{I}_{m,i}$ and $\sum_{i=1}^{k_{fm}} C^{NI}_{m,i}$ can be expressed as follows

$$\begin{aligned}
\Phi_{C^{I,n}_{m}}(\omega|k_{nm}) &= \left(\Phi_{C^{I,n}_{m,i}}(\omega)\right)^{k_{nm}} \\
&= \left(1 - j\omega\beta^{I}_{n}\right)^{-\alpha^{I}_{n}k_{nm}}, \\
\Phi_{C^{NI}_{m}}(\omega|k_{nm}) &= \left(\Phi_{C^{NI}_{m,i}}(\omega)\right)^{k_{fm}} \\
&= \left(1 - j\omega\beta^{NI}\right)^{-\alpha^{NI}k_{fm}},
\end{aligned}$$

where $\Phi_{C^{I,n}_{m,i}}(\omega|k_{nm})$ and $\Phi_{C^{NI}_{m,i}}(\omega|k_{nm})$ are the characteristic functions of $f_{C^{I,n}_{m,i}}(x|k_{nm})$ and $f_{C^{NI}_{m,i}}(x|k_{nm})$, respectively. Using the nice feature of the Gamma distribution that the sum of i.i.d. Gamma distributed RVs, with the same scale parameters (β)

is another Gamma distributed RV, the conditional PDFs are expressed as follows

$$\begin{aligned} f_{C_m^{I,n}|k_{nm}}(x|k_{nm}) &= \mathcal{G}\left(\alpha_n^I k_{nm}, \beta_n^I\right), \\ f_{C_m^{NI}|k_{nm}}(x|k_{nm}) &= \mathcal{G}\left(\alpha^{NI} k_{fm}, \beta^{NI}\right). \end{aligned} \tag{2.15}$$

In (2.12), even though the conditional PDFs of $C_m^{I,n}$ and C_m^{NI} are obtained, to find the PDF expression for C_m, we first need to evaluate the PDF of C_m^I, and then the PDF of its sum with C_m^{NI}. At this point, one needs to be aware that there are $N+1$ terms in (2.12), and each follows a Gamma distribution where the shape (α) and scale (β) parameters can be arbitrary. Therefore, the aforementioned feature of Gamma distribution for a sum of Gamma variates cannot be employed here.

Expressions for the PDF of sum of Gamma RVs are derived by Moschopoulos [45], Mathai [42], and Sim [57]. In addition, constraining the shape parameters to take integer values[6] and be all distinct, by using the convolution of PDFs Coelho [9] and Karagiannidis *et al.* [37], or partial-fractions methods Mathai [42], derived an expression for the PDF of a sum of Gamma RVs. Nevertheless, Moschopoulos PDF provides a mathematically tractable solution that it does not restrict the scale and shape parameters to be necessarily integer-valued or all distinct [42]. Therefore, the following theorem will help us in this regard.

Theorem 2 (Moschopoulos, 1985 [45])**.** *Let $\{X_s\}_{s=1}^{\mathcal{S}}$ be independent but not necessarily identically distributed Gamma variates with parameters α_s and β_s, respectively, then the PDF of $Y = \sum_{s=1}^{\mathcal{S}} X_s$ can be expressed as*

[6] If the shape parameter is an integer, Gamma distribution is referred to as Erlang distribution.

$$f_Y(y) = \prod_{s=1}^{\mathcal{S}} \left(\frac{\beta_1}{\beta_s}\right)^{\alpha_s} \sum_{k=0}^{\infty} \frac{\delta_k y^{\sum_{s=1}^{\mathcal{S}} \alpha_s + k - 1} \exp\left(-\frac{y}{\beta_1}\right)}{\beta_1^{\sum_{s=1}^{\mathcal{S}} \alpha_s + k} \Gamma\left(\sum_{s=1}^{\mathcal{S}} \alpha_s + k\right)} U(y), \tag{2.16}$$

where $\beta_1 = \min_s\{\beta_s\}$*, and the coefficients* δ_k *can be obtained recursively by the formula*

$$\begin{aligned} \delta_0 &= 1 \\ \delta_k &= \frac{1}{k+1} \sum_{i=1}^{k+1} \left[\sum_{j=1}^{\mathcal{S}} \alpha_j \left(1 - \frac{\beta_1}{\beta_j}\right)^i\right] \delta_{k+1-i} \quad \textit{for } k = 0, 1, 2, \ldots \end{aligned}$$

Proof. See [45]. □

The Moschopoulos PDF provides a nice and tractable representation of sum of Gamma variates in terms of a single Gamma series with a simple recursive formula to calculate the coefficients. This representation is applicable for any arbitrary shape parameters $\{\alpha_s\}_{s=1}^{\mathcal{S}}$ and scale parameters $\{\beta_s\}_{s=1}^{\mathcal{S}}$ including the possibility of having some of the parameters identical.

The CDF of Y can be obtained from the PDF as $F_Y(y) = \int_{-\infty}^{y} f_Y(x)\mathrm{d}x$. Therefore,

$$F_Y(y) = \prod_{s=1}^{\mathcal{S}} \left(\frac{\beta_1}{\beta_s}\right)^{\alpha_s} \sum_{k=0}^{\infty} \frac{\delta_k}{\beta_1^{\sum_{s=1}^{\mathcal{S}} \alpha_s + k} \Gamma\left(\sum_{s=1}^{\mathcal{S}} \alpha_s + k\right)} \int_0^y x^{\sum_{s=1}^{\mathcal{S}} \alpha_s + k - 1} \exp\left(-\frac{x}{\beta_1}\right) \mathrm{d}x. \tag{2.17}$$

The interchange of summation and integration above is justified using the uniform convergence of (2.16) (see e.g., [45] for a rigorous proof). From [61], we can simplify (2.17) by using $\int_0^u x^{\nu-1} e^{-\mu x}\mathrm{d}x = \mu^{-\nu}\gamma(\nu, \mu u)$ for $\Re[\nu > 0]$ [25, pg. 346, Sec.

3.381, Eq. 1], where $\gamma(\cdot,\cdot)$ is the lower incomplete Gamma function and is defined as $\gamma(x,y) = \int_0^y t^{x-1}e^{-t}dt$. Hence,

$$\begin{aligned} F_Y(y) =& \prod_{s=1}^{\mathcal{S}} \left(\frac{\beta_1}{\beta_s}\right)^{\alpha_s} \sum_{k=0}^{\infty} \delta_k \frac{\gamma\left(\sum_{s=1}^{\mathcal{S}} \alpha_s + k, \frac{y}{\beta_1}\right)}{\Gamma\left(\sum_{s=1}^{\mathcal{S}} \alpha_s + k\right)} \\ =& \prod_{s=1}^{\mathcal{S}} \left(\frac{\beta_1}{\beta_s}\right)^{\alpha_s} \sum_{k=0}^{\infty} \delta_k \mathcal{P}\left(\sum_{s=1}^{\mathcal{S}} \alpha_s + k, \frac{y}{\beta_1}\right), \end{aligned} \tag{2.18}$$

where $\mathcal{P}(\cdot,\cdot)$ is the regularized (also termed normalized) incomplete Gamma function and defined as[7] $\mathcal{P}(a,z) = \frac{\gamma(a,z)}{\Gamma(a)} = 1 - \frac{\Gamma(a,z)}{\Gamma(a)}$. For practical purposes, based on the required accuracy of application one may use the first h, i.e., $k = h-1$, terms in the sum series (2.16). The expression for truncation error is given in [45]. In Figures 2.4 and 2.5, the Moschopoulos PDF and CDF are shown for $\mathcal{S} = 4$ and $\mathcal{S} = 2$ where only the first 25 terms in the infinite sum series, i.e., $h = 25$, are considered. One can observe that the Moschopoulos PDF and CDF perfectly agree with the simulation results for same values of α and β. Since in our system model, with some probability the transmit power of PUs $P_{n,i}$ for $n = 1,\ldots,N$, can be the same, which means that the corresponding α_n^I and β_n^I are the same. Such a scenario can arise when the PUs are at the same distance from their corresponding common PBS.

Recall that from (2.12) and (2.15), we have to evaluate the PDF of the sum $C_m^{I,1} + C_m^{I,2} + \cdots + C_m^{I,N} + C_m^{NI}$, for a given number of set of subcarrier collisions $\mathbf{k}_m = [k_{1m}, k_{2m}, \ldots, k_{Nm}, k_{fm}]$. Recall also that C_m^I and C_m^{NI} are Gamma distributed and independent but not necessarily identical. Therefore, the conditional PDF of

[7]For integer values of $\sum_{s=1}^{\mathcal{S}} \alpha_s + k$, using [25, Eq. 8.353.6] the regularized incomplete Gamma function can be further simplified to $\mathcal{P}\left(\sum_{s=1}^{\mathcal{S}} \alpha_s + k, \frac{y}{\beta_1}\right) = 1 - \exp(-y/\beta_1) \sum_{j=1}^{\sum_{s=1}^{\mathcal{S}} \alpha_s + k - 1} \frac{1}{j!} \left(\frac{y}{\beta_1}\right)^j$.

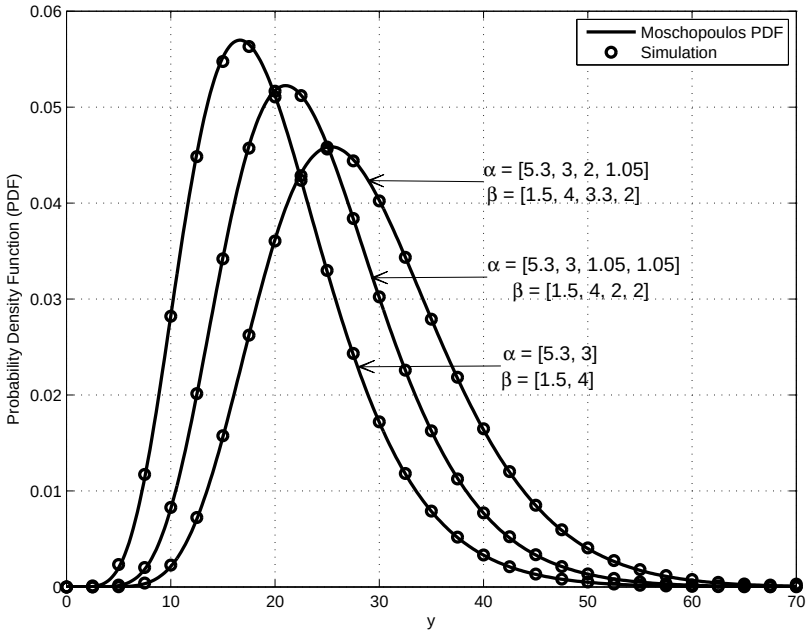

Figure 2.4: Moschopoulos PDF (2.16) for $h = 25$, and the total number of Gamma distributed RVs in sum as $\mathcal{S} = 4$ and $\mathcal{S} = 2$.

their sum can be expressed by means of *Theorem* 2 as follows:

$$f_{C_m|\mathbf{K}_m}(x|\mathbf{k}_m) = \left(\frac{\beta_{\min}}{\beta^{NI}}\right)^{\alpha^{NI}k_{fm}} \prod_{n=1}^{N} \left(\frac{\beta_{\min}}{\beta_n^I}\right)^{\alpha_n^I k_{nm}} \times \sum_{k=0}^{\infty} \frac{\delta_k x^{\sum_{n=1}^{N} \alpha_n^I k_{nm} + \alpha^{NI}k_{fm} + k - 1} \exp\left(-\frac{x}{\beta_{\min}}\right)}{\beta_{\min}^{\sum_{n=1}^{N} \alpha_n^I k_{nm} + \alpha^{NI}k_{fm} + k} \Gamma\left(\sum_{n=1}^{N} \alpha_n^I k_{nm} + \alpha^{NI}k_{fm} + k\right)} U(x), \tag{2.19}$$

where $\beta_{\min} = \min\{\beta_1^I, \beta_2^I, \ldots, \beta_N^I, \beta^{NI}\}$, and the coefficients δ_k are obtained recursively as follows:

$$\delta_k = \frac{1}{k+1} \sum_{i=1}^{k+1} \left[\sum_{j=1}^{N} \alpha_i^I k_{jm} \left(1 - \frac{\beta_{\min}}{\beta_j^I}\right)^i + \alpha^{NI} k_{fm} \left(1 - \frac{\beta_{\min}}{\beta^{NI}}\right)^i \right] \delta_{k+1-i}$$

where $\delta_0 = 1$, $k = 0, 1, 2, \ldots$

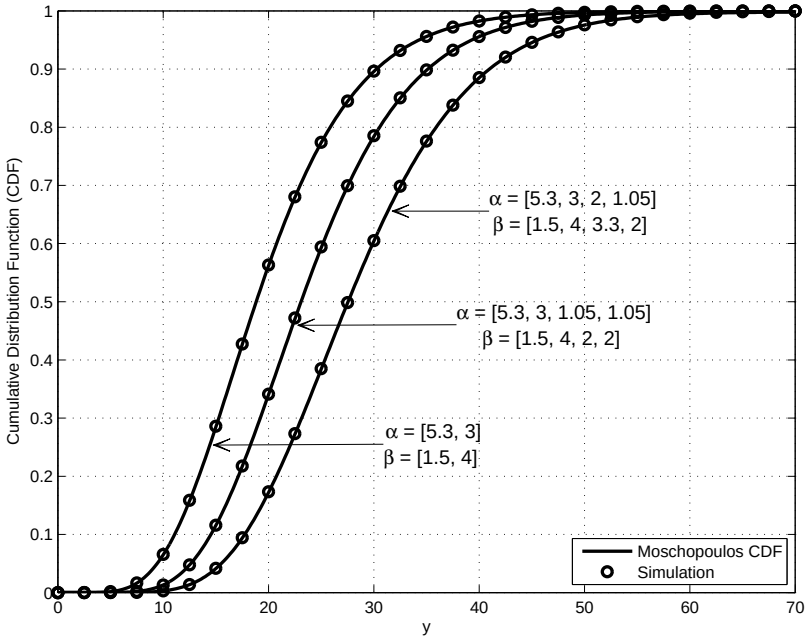

Figure 2.5: Moschopoulos CDF (2.18) for $h = 25$, and the total number of Gamma distributed RVs in sum as $\mathcal{S} = 4$ and $\mathcal{S} = 2$.

Now, the PDF of C_m can be found by averaging over the PMF of subcarrier collisions as follows:

$$f_{C_m}(x) = \sum_{\mathbf{k}_m} f_{C_m,\mathbf{K}_m}(x, \mathbf{k}_m) = \sum_{\mathbf{k}_m} f_{C_m|\mathbf{K}_m}(x|\mathbf{k}_m) p(\mathbf{k}_m). \tag{2.20}$$

Plugging (2.1) and (2.19) into (2.20), the PDF is expressed as

$$\begin{aligned} f_{C_m}(x) = & \sum_{k_{1m}} \sum_{k_{2m}} \cdots \sum_{k_{Nm}} \sum_{k_{fm}} \left\{ \left[\binom{F_f}{k_{fm}} \Big/ \binom{F}{F_m^S} \right] \right. \\ & \times \prod_{n=1}^{N} \binom{F_n^P}{k_{nm}} \left(\frac{\beta_{\min}}{\beta^{NI}} \right)^{\alpha^{NI} k_{fm}} \prod_{n=1}^{N} \left(\frac{\beta_{\min}}{\beta_n^I} \right)^{\alpha_n^I k_{nm}} \\ & \left. \times \sum_{k=0}^{\infty} \frac{\delta_k x^{\sum_{n=1}^{N} \alpha_n^I k_{nm} + \alpha^{NI} k_{fm} + k - 1} \exp\left(-\frac{x}{\beta_{\min}} \right)}{\beta_{\min}^{\sum_{n=1}^{N} \alpha_n^I k_{nm} + \alpha^{NI} k_{fm} + k} \, \Gamma\left(\sum_{n=1}^{N} \alpha_n^I k_{nm} + \alpha^{NI} k_{fm} + k \right)} U(x) \right\}. \end{aligned} \tag{2.21}$$

The outage probability is a common performance metric in fading environments. Hence, here we consider the outage probability of SU capacity in terms of the following measure:

$$\begin{aligned} P_{C_m}^{\text{out}}(\varphi_{\text{th}}) &= Pr\left(C_m < \varphi_{\text{th}}\right) \\ &= \int_0^{\varphi_{\text{th}}} f_{C_m}(x)\mathrm{d}x, \end{aligned}$$

which is the CDF of the SU capacity over the outage threshold φ_{th} [dB]. Using (2.18) and (2.21), the CDF of C_m can be expressed as

$$\begin{aligned} F_{C_m}(x) = &\sum_{k_{1m}}\sum_{k_{2m}}\cdots\sum_{k_{Nm}}\sum_{k_{fm}}\left\{\left[\binom{F_f}{k_{fm}}\Big/\binom{F}{F_m^S}\right]\prod_{n=1}^{N}\binom{F_n^P}{k_{nm}}\left(\frac{\beta_{\min}}{\beta^{NI}}\right)^{\alpha^{NI}k_{fm}}\right. \\ &\left.\times\prod_{n=1}^{N}\left(\frac{\beta_{\min}}{\beta_n^I}\right)^{\alpha_n^I k_{nm}}\sum_{k=0}^{\infty}\delta_k\mathcal{P}\left(\sum_{n=1}^{N}\alpha_n^I k_{nm}+\alpha^{NI}k_{fm}+k,\frac{x}{\beta_{\min}}\right)\right\}. \end{aligned} \tag{2.22}$$

2.5 Asymptotic Analysis of Multiuser Diversity

In this section, the gain of multiuser diversity by employing opportunistic scheduling is investigated. In conventional systems, the multiuser diversity gain is attributed to *channel gains* only. However, in the proposed scheme, we additionally benefit from the randomness of *the number of subcarrier collisions*. Assuming all M SUs are accessing the F available subcarriers to randomly allocate their subcarriers,[8] the SU, which provides the best instantaneous capacity, is selected as:

$$C_{\max} = \max_{m\in[1,M]} C_m.$$

[8]It is assumed that no collisions occur among the subcarriers of SUs.

For fairness in the selection phase of the best SU, assume that each SU's data rate is the same, i.e., each SU requests for the same number of subcarriers, $F_m^S = F^S,\ m = 1, \ldots, M$. Then, by using order statistics, the PDF of $C_{\max}$ is expressed as

$$f_{C_{\max}}(x) = M f_{C_m}(x) F_{C_m}(x)^{M-1}. \tag{2.23}$$

Plugging (2.21) and (2.22) into (2.23), the PDF of $C_{\max}$ can be obtained. Nonetheless, using $\int_{-\infty}^{\infty} x f_{C_{\max}}(x) \mathrm{d}x$ is intractable to find the mean of $C_{\max}$. Even if we can carry out such a calculation, it will hardly provide any insights to fully understand the impacts of the main parameters on the capacity using the resulted expression. Therefore, we asymptotically analyze the capacity to understand the effects of system parameters and multiuser diversity gain in CR systems with spectrum sharing feature.

Theorem 3. *As the number of SUs M goes to infinity, the average capacity of $C_{\max}$ converges to*

$$\mathbb{E}\left[C_{\max}\right] = b_M + E_1 a_M,$$

where $E_1 = 0.5772\ldots$ is Euler's constant [10], and $a_M = \left[M f_{C_m}(b_M)\right]^{-1}$ and $b_M = F_{C_m}^{-1}(1 - 1/M)$.

Without loss of generality assuming a single PU case, i.e., $n \in [1, N]$, then b_M is given by

$$\begin{aligned} b_M &= F_{C_m^1}^{-1}\left(1 - \frac{1}{M}\right) \\ &= \mathcal{Q} \sum_{k=0}^{\infty} \delta_k \mathcal{P}^{-1}\left(\Delta + k, \frac{1 - \frac{1}{M}}{\hat{\beta}_{\min}}\right), \end{aligned}$$

where $\mathcal{P}^{-1}(\cdot, \cdot)$ stands for the inverse regularized incomplete Gamma function. Un-

fortunately, there is no closed form expression for this special function. Therefore, it can be evaluated numerically by using build-in functions in some well-known computational softwares such as MATLAB® and MATHEMATICA®.[9] *Additionally,* $\hat{\beta}_{\min} = \min\{\beta_n^I, \beta^{NI}\}$, $\Delta = \alpha_n^I k_{nm} + \alpha^{NI} k_{fm}$ *and* $\mathcal{Q}$ *takes the form:*

$$\mathcal{Q} = \left[\sum_{k_{nm}=0}^{F_m^S} \binom{F_n^P}{k_{nm}} \binom{F - F_n^P}{k_{fm}} \left(\frac{\hat{\beta}_{\min}^{\Delta}}{(\beta_n^I)^{\alpha_n^I k_{nm}} (\beta^{NI})^{\alpha^{NI} k_{fm}}} \right) \right] \Big/ \binom{F}{F_m^S},$$

where in considering a practical scenario, it is assumed that $F_m^S + F_n^P \leq F$ *and* $F_m^S \leq F_n^P$. *Hence, the support region for the number of subcarrier collisions is* $k_{nm} = 0, 1, \ldots, F_m^S$.

Proof. We start with the following *Lemma.*

Lemma 1 (Distribution of Extremes [10])**.** *Let* $z_1, \ldots, z_M$ *be i.i.d. RVs with absolutely continuous common CDF,* $F(z)$*, and PDF,* $f(z)$*, satisfying these conditions:* $F(z)$ *is less than 1 for all* z*,* $f(z) > 0$ *and is differentiable. If the growth function* $g(z) = (1 - F(z))/f(z)$ *satisfies the von Mises' sufficient condition:*

$$\lim_{z \to \infty} g(z) = c > 0, \tag{2.24}$$

then $F(z)$ *belongs to the domain of attraction of the Gumbel distribution. In other words,* $[\max_{1 \leq k \leq M} z_m - b_M]/a_M$ *converges in distribution to the Gumbel-type limiting distribution:*

$$G(x) = \exp\left(-e^{-z}\right) \quad , \quad -\infty < z < \infty \ .$$

---

[9] It is worth to note that by using [2, 6.5.12 & 13.5.5], the regularized incomplete Gamma function can be approximated as $\mathcal{P}(u, v) = \frac{v^u}{u\Gamma(v)} \ {}_1F_1(u; 1+u; -v) = \frac{v^u}{u\Gamma(u)}$ as $v \to 0$, where ${}_1F_1(\cdot;\cdot;\cdot)$ is confluent hypergeometric function [11]. Hence, its inverse can be obtained.

Thus, the maximum of M such i.i.d. RVs grows like b_M, also termed position parameter. The parameter b_M is given by $b_M = F^{-1}(1 - 1/M)$, and the scaling factor a_M is given by $a_M = g(b_M) = [Mf(b_M)]^{-1}$.

The PDF and CDF of C_m for a *single* PU are given, respectively, by

$$f_{C_m^1}(x) = \mathcal{Q} \sum_{k=0}^{\infty} \frac{\delta_k x^{\Delta+k-1} e^{-x/\hat{\beta}_{\min}}}{\hat{\beta}_{\min}^{\Delta+k} \, \Gamma(\Delta + k)} U(x), \tag{2.25}$$

$$F_{C_m^1}(x) = \mathcal{Q} \sum_{k=0}^{\infty} \delta_k \mathcal{P}\left(\Delta + k, \frac{x}{\hat{\beta}_{\min}}\right), \tag{2.26}$$

with the coefficients calculated iteratively as

$$\delta_0 = 1$$

$$\delta_k = \frac{1}{k+1} \sum_{i=1}^{k+1} \left[\alpha_n^I k_{nm} \left(1 - \frac{\hat{\beta}_{\min}}{\beta_n^I}\right)^i + \alpha^{NI} k_{fm} \left(1 - \frac{\hat{\beta}_{\min}}{\beta^{NI}}\right)^i \right] \delta_{k+1-i}$$

for $k = 0, 1, 2, \ldots$.

From *Lemma* 1, plugging (2.25) and (2.26) into (2.24) yields

$$\lim_{x \to \infty} \frac{1 - F_{C_m^1}(x)}{f_{C_m^1}(x)} = \hat{\beta}_{\min} > 0. \tag{2.27}$$

The respective intermediate steps in the evaluation of (2.27) are depicted in Appendix D. Hence, it belongs to an attraction domain of Gumbel-type with limiting CDF:

$$\hat{F}_{C_{\max}}(x) = \exp\left(-\exp\left(-\frac{x - b_M}{a_M}\right)\right).$$

Then, the limiting PDF of $C_{\max}$ is

$$\hat{f}_{C_{\max}}(x) = \frac{1}{a_M} \exp\left(-\frac{x - b_M}{a_M}\right) \exp\left(-\exp\left(-\frac{x - b_M}{a_M}\right)\right).$$

Therefore, using $\mathbb{E}[C_{\max}] = \int_{-\infty}^{\infty} x \hat{f}_{C_{\max}}(x) \mathrm{d}x$, the desired result can be readily obtained. □

In the proof stage, it came to our attention that, to the best of the authors' knowledge, there is no result reported in the literature for the limiting distribution of RVs that follows Moschopoulos PDF. Therefore, the following novel result can be stated.

Corollary 5. *Let $\{X_r\}_{r=1}^{\mathcal{R}}$ be the set of $\mathcal{R}$ i.i.d. RVs that follow Moschopoulos PDF and CDF [45], and $Y = \max\{X_1, X_2, \ldots, X_{\mathcal{R}}\}$, then the limiting distribution of the CDF of Y belongs to the domain of attraction of Gumbel distribution as $\mathcal{R}$ converges to infinity.*

Proof. It is immediate to see this result from the results presented in the proof of *Theorem* 3. □

The results obtained so far will help us to asymptotically analyze the scheduling of SUs' subcarriers in the following section.

2.6 Centralized Sequential and Random Subcarrier Allocation

2.6.1 Sum Capacity of SUs with Multiuser Diversity

In this section, a cognitive communication set-up involving multiple SUs that assume a random allocation method is studied. Recall that due to random allocation scheme, there can be the collisions among the subcarriers of SUs in addition

to those that are used by PUs. These collisions will decrease the system performance severely. To overcome this challenge, we propose an efficient algorithm that *sequentially* and *randomly* allocates SUs' subcarrier sets in a centralized manner by maintaining the orthogonality among the allocated subcarrier sets. Such an assignment can be thought of as the downlink scenario where the SBS performs the random assignment of subcarriers. Furthermore, to benefit from the multiuser diversity gain, the opportunistic scheduling method is employed in the algorithm [See Table 2.1], where it is assumed only a single PU. The multiple PUs case is a straightforward extension. In the selection step of the best SU, to preserve the fairness among the users, it is assumed that the data rate requirements of all SUs are the same, i.e., the individual numbers of subcarrier requirements are equal.

The algorithm can be summarized as follows. A randomly chosen set of subcarriers F_t^R from the set F is assigned to the available SUs. The first SU, which provides the best capacity, is selected among M SUs, then the selected subcarriers F_t^R (total of collided and collision-free subcarriers) are removed from the set F. In the next stage, another randomly chosen set of subcarriers F_t^S from the *updated* set F is allocated to the rest of SUs. The second best SU is selected among the $M-1$ SUs, and similarly the subcarrier set F is updated by removing the new set F_t^R. This sequential selection continues until it reaches the total number of the best $\hat{M}$ SUs, with $\hat{M} \leq M$. It is evident to observe that the multiuser diversity is attributed only to the randomness of the channel gains. Furthermore, some of the essential points in the algorithm can be highlighted as follows:

- In *step* 2: The PMF of the number of subcarrier collisions follows a *hypergeometric distribution* due to the random selection of subcarriers set F_t^R from the available set of subcarriers F.

- In *step* 4: The selection of the best SU is performed based on the capacity feedbacks obtained from the SUs.

- In *step* 5: Removing the randomly sampled subcarriers F_t^R from the available set of subcarriers F means that both collided and collision-free subcarriers are subtracted from set F (since $F_t^R = k_{nm} + k_{fm}$), i.e., $F \leftarrow F - F_t^R \Leftrightarrow F \leftarrow F - k_{nm} - k_{fm}$ and $F_n^P \leftarrow F_n^P - k_{nm}$. In other words, since $F = F_n^P + F_f$, where F_f stands for the number of free subcarriers, the subcarriers that are occupied by the PU F_n^P in the set F are automatically updated when the randomly sampled set of subcarriers F_t^R is removed from the set F. Hence, the orthogonality among the subcarriers of SUs is maintained.

Theorem 4. *The sum capacity of $\hat{M}$ selected SUs in the centralized sequential and random scheduling algorithm for $M \gg \hat{M}$ is approximated*[10] *by*

$$\mathbb{E}\left[C_{\text{sum}}\right] \approx \hat{M}\mathbb{E}\left[C_{m_1^*}\right],$$

and as $M \to \infty$, it converges to

$$\mathbb{E}\left[C_{\text{sum}}\right] = \hat{M}\left[b'_M + E_1 a'_M\right],$$

where m_1^* is the index of the first selected best SU and defined as $m_1^* = \underset{m\in[1,M]}{\arg\max}\, C_m$. Further, a'_M and b'_M can be readily obtained by following the same approach as in Theorem 3 considering the fact that the multiuser diversity is only ascribed to channel randomness not the random subcarrier assignment. It is noteworthy to state that the

[10]Since $\mathbb{E}\left[C_{m_1^*}\right] \geq \mathbb{E}\left[C_{m_j^*}\right], \forall j \in \left[1, \hat{M}\right]$, it can also be considered as a tight upper bound for $M \gg \hat{M}$ as $\mathbb{E}\left[C_{\text{sum}}\right] \leq \hat{M}\mathbb{E}\left[C_{m_1^*}\right]$.

Table 2.1: Algorithm: Centralized Sequential and Random Subcarrier Allocation

1. *Initialization*
   - Assume $F_m^S = F^S \ \forall m \in [1, M]$ and a single PU is available, $n = 1$.
   - Set the number of available subcarriers to F and index $t = 1$.
2. *Subcarrier assignment step*
   - Randomly sample a set of subcarriers, F_t^R, with cardinality of F^S from set F: $k_{nm} \sim \texttt{HYPG}(F^S,\ F_n^P,\ F)$.
   - Assign the set F_t^R to all $M - t + 1$ SUs.
3. *Capacity calculation step*
   - For $m = 1, \ldots, M - t + 1$, SUs evaluate their capacities with the given random set of subcarriers: $C_m \big| F_t^R$.
   - SUs send *feedback* for the calculated capacities to the *central control entity* (SBS or CR Network Manager).
4. *Selection step*
   - Choose the SU that provides the best capacity:
     If $t = 1$ then $m_t^* = \underset{m \in [1,M]}{\arg\max} \left(C_m \big| F_t^R \right)$
     else $m_t^* = \underset{m \in [1,M] \setminus \left[m_1^*, m_{t-1}^* \right]}{\arg\max} \left(C_m \big| F_t^R \right)$ for $t = 2, \ldots, \hat{M}$.
5. *Updating the subcarrier sets step*
   - Remove the sampled (total of collided and collision-free) subcarriers from the available set of subcarriers:
     $F \leftarrow F - F_t^R$.
   - Set $t \leftarrow t + 1$ and go to Step 2 until $t = \hat{M}$.
6. *Sum capacity evaluation step*
   - Compute sum capacity of SUs: $C_{\text{sum}} = \sum_{t=1}^{\hat{M}} C_{m_t^*}$.

sum capacity scales linearly with the number of selected SUs.

Proof. The scheduler selects the SUs according to the following rule:

$$m_j^* = \underset{m \in [1,M] \setminus \left[m_1^*, m_{j-1}^*\right]}{\arg\max} C_m \quad \text{for } j = 2, \ldots, \hat{M} \ ,$$

which means that the selected SU(s) are ignored in the selection step of remaining users. Then, the sum capacity of selected SUs is defined as

$$C_{\text{sum}} = \sum_{j=1}^{\hat{M}} C_{m_j^*}. \tag{2.28}$$

For large M such that $M \gg \hat{M}$, it is immediate to observe that

$$\mathbb{E}\left[C_{m_j^*}\right] \approx \mathbb{E}\left[C_{m_1^*}\right] \quad \forall j \in \left[1, \hat{M}\right]. \tag{2.29}$$

This approximation is valid since removing the selected SUs does not considerably impact the mean of the rest of the selected SUs for $M \gg \hat{M}$, i.e., the maxima of M RVs and $M - \hat{M}$ RVs are approximately the same for $M \gg \hat{M}$, so their averages are approximately the same. Hence, plugging (2.29) into (2.28) yields the desired result. □

2.6.2 Sum Capacity of SUs without Opportunistic Scheduling

In order to investigate the performance of our proposed algorithm due to multiuser diversity gain, the performance of the centralized sequential subcarrier scheduling without employing the opportunistic scheduling method is analyzed in this section, i.e., the multiuser diversity of SUs is not maintained. Therefore, the sum

capacity of any *arbitrarily* $\hat{M}$ selected SUs (among M SUs) can be expressed as

$$C_{\text{sum}}^{\text{a}} = \sum_{m=1}^{\hat{M}} C_m.$$

Recalling the upper and lower bounds on the average capacity of a single SU C_m, one can conclude that the average sum rate of the SUs scales linearly with the number of selected SUs ($\hat{M}$). Mathematically speaking, $\mathbb{E}\left[C_{\text{sum}}^{\text{a}}\right] = \hat{M}\mathbb{E}\left[C_m\right]$.

During the sequential scheduling of SUs' subcarriers, the PMF of the number of subcarrier collisions can be obtained as a special case of the following result.

Proposition 2. *The PMF of the number of subcarrier collisions for the mth SU in the presence of N PUs, when assigning the subcarriers sequentially to preserve the orthogonality between SUs' subcarriers, is given by*

$$p(\mathbf{k}_m) = \sum_{\mathbf{k}_1} \sum_{\mathbf{k}_2} \cdots \sum_{\mathbf{k}_{m-1}} p(\mathbf{k}_1, \mathbf{k}_2, \ldots, \mathbf{k}_m),$$

where the joint PMF is

$$p\left(\mathbf{k}_1, \mathbf{k}_2, \ldots, \mathbf{k}_m\right) = \left\{ \left[\binom{F_f}{k_{f1}} \Big/ \binom{F}{F_1^S} \right] \prod_{n=1}^{N} \binom{F_n^P}{k_{n1}} \right\} \prod_{r=2}^{m} \left\{ \left[\binom{F_f - \sum_{j=1}^{r-1} k_{fj}}{k_{fr}} \Big/ \binom{F - \mathbf{1}^{\mathrm{T}} \left(\sum_{j=1}^{r-1} \mathbf{k}_j \right)}{F_r^S} \right] \prod_{n=1}^{N} \binom{F_n^P - \sum_{j=1}^{r-1} k_{nj}}{k_{nr}} \right\}.$$

The mean and support of k_{nm} are given, respectively, by

$$\mathbb{E}\left[k_{nm}\right] = \frac{F_m^S \left(F_n^P - \sum_{j=1}^{m-1} \mathbb{E}\left[k_{nj}\right] \right)}{F - \sum_{j=1}^{m-1} F_j^S},$$

$$\left\{ \mathbf{k}_m : \sum_{n=1}^{N} k_{nm} + k_{fm} = F_m^S \text{ and } k_{nm} \in \left(F_m^S + F_n^P - \sum_{j=1}^{m-1} k_{nj} - F \right)^+, \ldots, \min \left\{ F_j^S, F_n^P - \sum_{j=1}^{m-1} k_{nj} \right\} \right\}.$$

Proof. The proof is given in Appendix E. □

2.7 Numerical Results and Simulations

In this section, numerical and simulation results are presented to confirm the analytical results and investigate the impact of various system parameters in CR spectrum sharing networks. First, the effect of peak transmit power of SU $P_{m,i}$ (in dB) on the average capacity (in nats per second per hertz) is shown for different values of IT values Ψ_i in Figure 2.6. Unlike the conventional systems, the SU average capacity is here saturated after a certain value of peak SU transmit power because of the IT constraint in spectrum sharing systems. In Figure 2.7, the SU mean capacity against the IT constraint is presented. It turns out that the analytical results agree well with the simulation results. The results shown in Figures 2.6 and 2.7 are in the presence of a single PU, i.e., $n \in [1, N]$, and the number of subcarriers in sets F, F_m^S and F_n^S are chosen arbitrarily.[11] A common observation for both Figures 2.6 and 2.7 is that the saturation level of capacity increases as the IT constraint relaxes, and the capacity keeps growing until a saturation point as the transmit power of SU increases as expected. It can also be underlined from Figure 2.6 that the capacity gain due to relaxation in the IT constraint disappears at low SU transmit power. Therefore, in the high transmit power or SINR regime, the impact of IT relaxation differs significantly. Similarly, the same effect can be observed for the results in

[11]The unit AWGN noise variance is used ($\eta = 1$) in all the following figures.

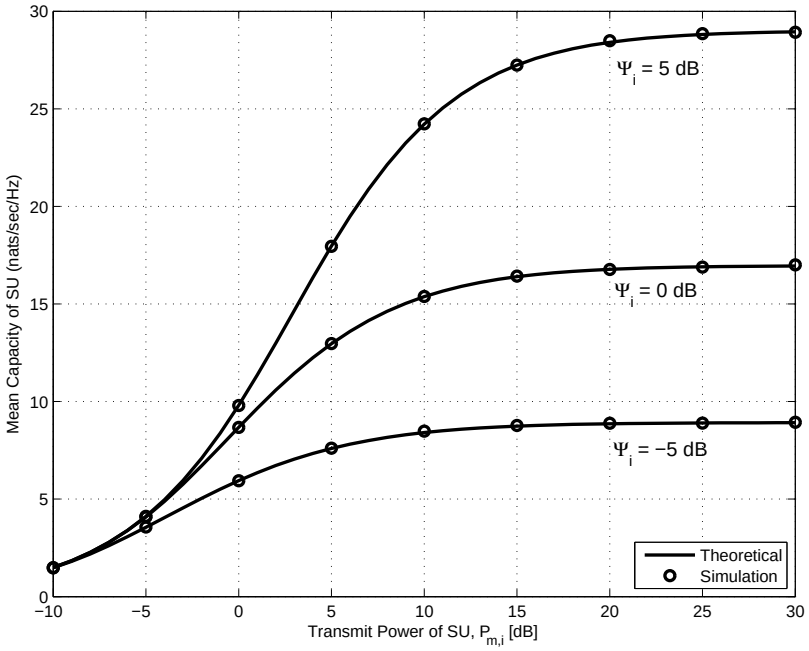

Figure 2.6: SU mean capacity versus the transmit power $P_{m,i}$ with different IT Ψ_i values for $F_m^S = 20$, $F_n^P = 30$, $F = 128$ and $P_{n,i} = 10$ dB.

Figure 2.7.

Consider now the practical scenario when there are multiple PUs available. Therefore, the number of free subcarriers in the available set F is smaller than that of the single PU case. The SU mean capacity against peak transmit power $P_{m,i}$ in the presence of multiple PUs is shown in Figure 2.8. In order to illustrate the effects of multiple PUs, during the simulations, it is assumed that the number of subcarriers and the transmit power of all PUs are the same, $P_{n,i} = 5$dB and $F_n^P = 10$ for $n = 1, \ldots, N$, respectively. Since the number of subcarrier collisions in the presence of multiple PUs follows a multivariate hypergeometric distribution, the multivariate hypergeometric random variates are generated by using the sequential method given in [22, p. 206]. It can be observed that increasing the number of PUs degrades the performance of SU as expected. In addition, as the number of PUs decreases, i.e., the

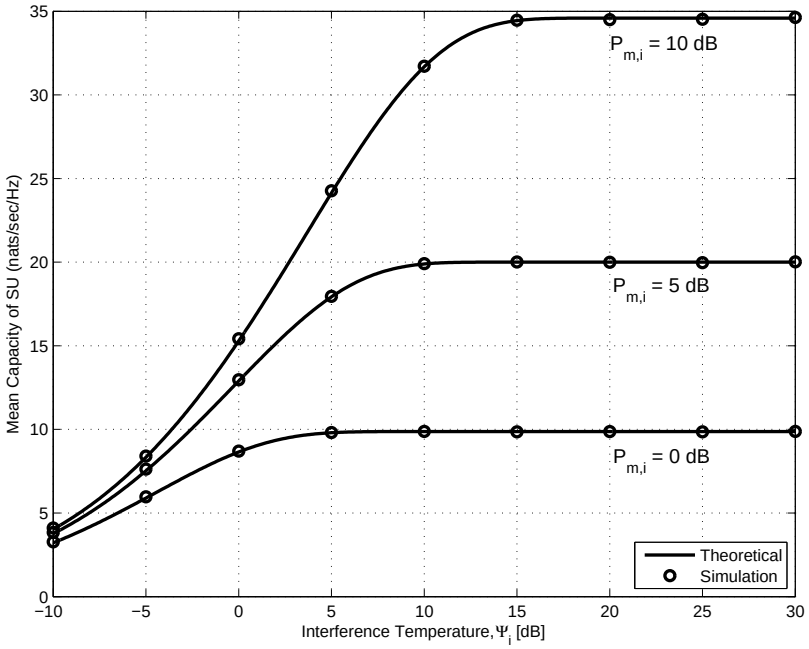

Figure 2.7: SU mean capacity versus the interference temperature Ψ_i with different transmit power $P_{m,i}$ values for $F_m^S = 20$, $F_n^P = 30$, $F = 128$ and $P_{n,i} = 10$ dB.

number of unoccupied subcarriers increases, the average capacity of SUs converges to the upper bound, where all SU's subcarriers are collision-free. On the other hand, the lower bound of the average capacity indicates that all SU's subcarriers are colliding.

Figure 2.9 shows how the SU average capacity scales with the number of subcarriers in sets F and F_n^P, respectively, where the single PU case is assumed. As the number of available subcarriers increases for a fixed number of SU's and PU's subcarriers, the SU mean capacity asymptotically converges to the limit point given in (2.3), where the rate of convergence is logarithmic. It is immediate to see that the SU average capacity scales as $\Theta\left(1 + 1/F\right)$, $\Theta\left(F_m^S\right)$ and $\Theta\left(1 - F_n^P\right)$, as proved in *Corollary* 3.

The performance of the proposed centralized algorithm with and without the opportunistic scheduling is simulated and shown in Figure 2.10. The results for the algorithm with multiuser diversity are in the presence of $M = 10$ and $M = 40$

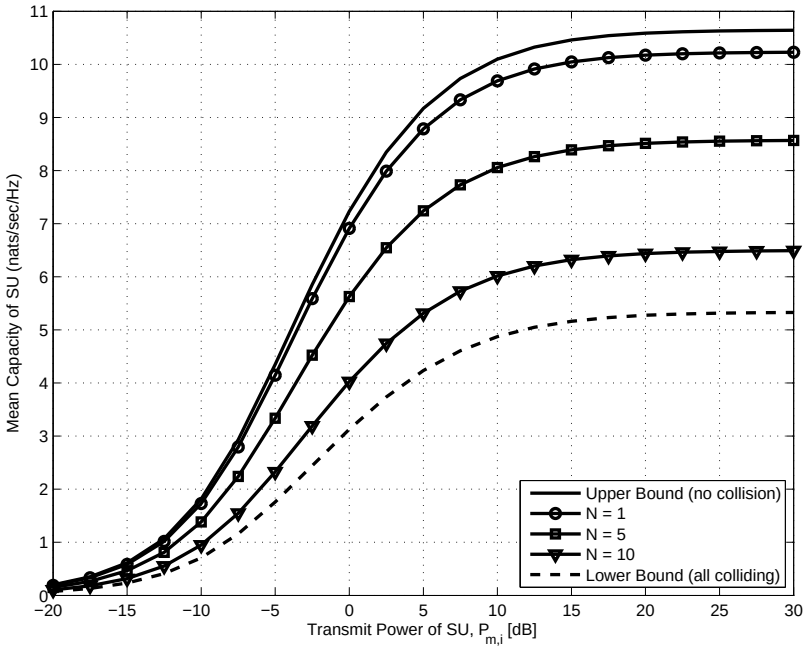

Figure 2.8: SU mean capacity versus the transmit power $P_{m,i}$ with different number of PUs N for $F_m^S = 20$, $F = 128$, $F_n^P = 10$, $P_{n,i} = 5$ dB for $n = 1, \ldots, N$ and $\Psi_i = -5$ dB.

SUs and among them $\hat{M} = 5$ SUs are selected using the opportunistic selection method. Also, $\hat{M} = 5$ SUs are selected when no opportunistic scheduling method is employed. Note also that without opportunistic scheduling, the number of SUs M does not affect the sum capacity of $\hat{M}$ selected SUs. Therefore, this scheme is not plotted for different numbers of SUs (M). One can observe that the effect of multiuser diversity manifests into the fact that an increase in the number of SUs M results in higher capacity in the proposed algorithm. Furthermore, in order to reveal the impact of collisions between SUs subcarriers on the sum capacity of any arbitrarily $\hat{M}$ selected SUs, we simulate the performance of $\hat{M} = 5$ selected SUs in the presence of $M = 10$ and $M = 40$ SUs in the secondary network when no centralized algorithm with opportunistic scheduling is employed. In other words, the orthogonality among the subcarriers of SUs is not maintained, and the multiuser diversity gain is not

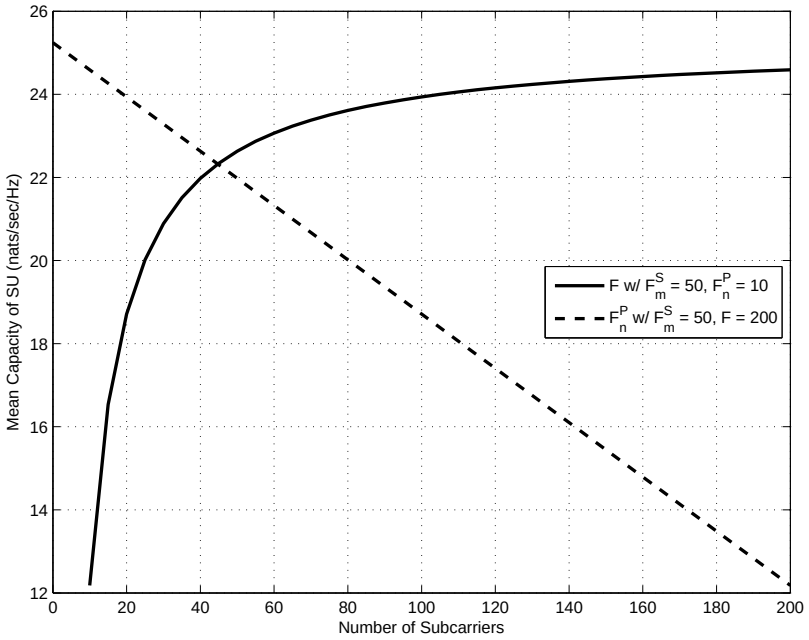

Figure 2.9: SU mean capacity versus the number of subcarriers F and F_n^P, for $P_{n,i} = 5$ dB, $P_{m,i} = 10$ dB and $\Psi_i = -5$ dB.

exploited. Hence, there can be the collisions between the subcarriers of any SU with the rest of the SUs in the secondary network in addition to those that are utilized by PU. This scheme could be considered as the worst case scenario, where the collisions among the SUs' subcarriers severely affect the performance due to high probability of interference level among SUs as shown in Figure 2.10.

2.8 Summary

This chapter studied the performance of OFDM-based CR systems with spectrum sharing feature using a random subcarrier allocation method. The subcarrier collision models for single and multiple PU(s) are shown to assume univariate and multivariate hypergeometric distributions, respectively. The expressions of SU average capacity for both general and Rayleigh channel fading models are presented. It turns out that the closed-form expression for the instantaneous SU capacity in the presence

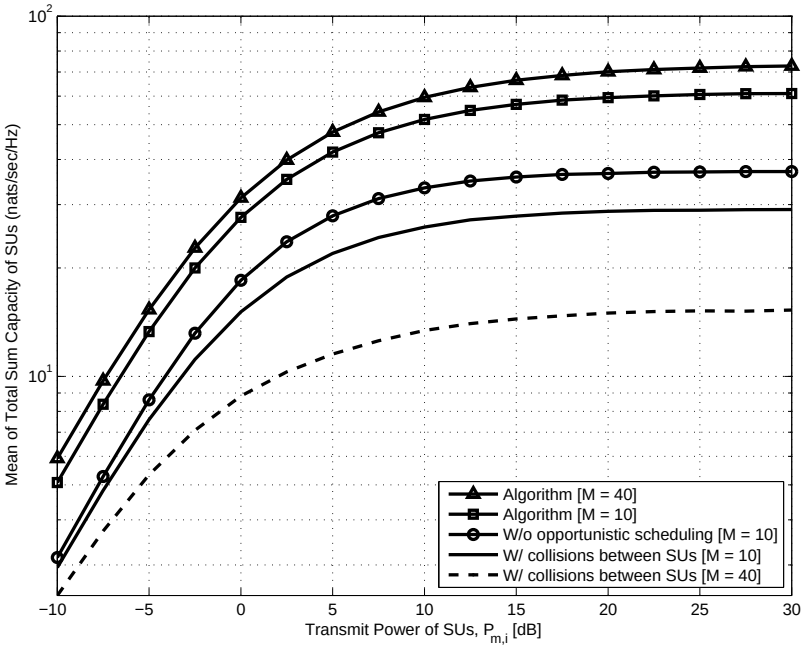

Figure 2.10: Sum capacity of $\hat{M} = 5$ selected SUs versus the transmit powers $P_{m,i}$ for $F_m^S = 10$, $m = 1, \ldots, M$, $F_n^P = 40$, $F = 100$, $P_{n,i} = 10$ dB and $\Psi_i = 0$ dB.

of Rayleigh channel fading is intractable. Therefore, the Gamma approximation of the SU capacity expression is obtained by employing the moment matching method and Moschopoulos PDF representation for a sum of independent but not necessarily Gamma distributed RVs. Through the asymptotic analysis of SU mean capacity, it is found that the capacity scales with the number of subcarriers as $\Theta\left(1 + 1/F\right)$, $\Theta\left(F_m^S\right)$ and $\Theta\left(1 - F_n^P\right)$.

The asymptotic analysis of capacity assuming an opportunistic selection method is investigated by using extreme value theory. When multiple SUs are randomly allocated the subcarriers, the primary issue that causes drastic performance degradation is the collision(s) among their subcarrier sets. In order to prevent such a situation, a centralized algorithm was developed to sequentially assign orthogonal subcarrier sets to SUs based on a random allocation scheme while benefiting from the multiuser

diversity gain for maximum SUs sum rate. Besides, it is found that the extreme value limiting distribution of RVs that follow the Moschopoulos PDF belongs to the domain of attraction of the Gumbel distribution.

3. INTER-CELL SUBCARRIER COLLISIONS DUE TO RANDOM SUBCARRIER ALLOCATION

3.1 Introduction

Advancing one step further, we now turn our attention to a more practical model, the multiple cells case, where inter-cell subcarrier collisions are investigated, assuming that no centralized subcarrier scheduling algorithm is employed. Similarly, this chapter assumes a set-up in which no spectrum sensing is performed as well as the CSI between the PU transmitter and receiver pair is not known. Therefore, the complexity of the proposed random access method with respect to the methods based on spectrum sensing is much lower.

In Chapter 1.4, we proposed a random subcarrier allocation technique and studied its performance in terms of average capacity and multiuser diversity by taking into consideration the effect of collisions between multiple PUs and SUs in a set-up that assumes multiple SUs in a single secondary network (cell). Nonetheless, considering practical systems (multiple secondary networks or cells), there may exist inter-cell subcarrier collisions not only between SUs and PUs but also among the SUs themselves due to the random access scheme. Therefore, in this chapter, two different SU transmitter and receiver pairs belonging to different cells are considered.

The main contributions of this chapter are summarized as follows.

- The performance of target SU in terms of capacity and rate loss due to collisions (interference) between SUs in addition to that of PU are studied.
- The average capacity expressions of target SU's (SU-1) at the ith subcarrier are derived for no interference case, and when there is interference from only

SU-2, only PU, and both SU-2 and PU.

- The number of subcarriers required by PU or SUs can also vary based on either PU or SUs rate requirements. The long term average performance of the system is investigated by using a stochastic model for the required number of subcarriers of PU and SUs, which is assumed to be *fixed* in Chapter 1.4.

- The statistical analysis of the number of subcarrier collisions between the users is also conducted. The PMFs and the average number of subcarrier collisions are derived when there are *fixed* and *random* number of subcarriers required by users.

- Finally, upper bounds for instantaneous and average maximum capacity (rate) loss of SU-1 due to collisions are derived.

3.1.1 Organization

The rest of the chapter is arranged as follows. In Section 3.2, the system and channel models are presented. The statistical analysis of the number of subcarrier collisions is studied in Section 3.3. The SU capacity analysis over an arbitrary and Rayleigh fading channel models are investigated in Section 3.4. The analytical and simulation results are described in Section 3.5. Finally, concluding remarks are given in Section 3.6.

Definition 7 (Total Performance)**.** *The total performance of a SU with F^S subcarriers is defined as the summation of performances for each subcarrier. Let δ_i be the performance metric for the ith subcarrier of the SU such as ergodic or outage capacity, then the total performance is given by*

$$\delta_T = \sum_{i=1}^{F^S} \delta_i.$$

3.2 System and Channel Models

The OFDM-based CR system is illustrated in Figure 3.1, where a PU and SUs are assumed to be present in the primary and secondary networks, respectively, where each SU transmitter and receiver pair belongs to separate cells. The total number of available subcarriers in the primary network is denoted by F, and the number of PU's subcarriers is denoted by F^P. The number of subcarriers utilized by SU-1 and SU-2 are represented by F_1^S and F_2^S, respectively. SUs randomly access the available subcarriers set, F, in the primary network without having access to the PU's channel occupancy information. Subcarrier collisions occur when SUs randomly employ subcarriers, which are in use by PU and/or other SU, and the probabilistic model for the number of subcarrier collisions follows a hypergeometric distribution. Due to the random access (allocation) of subcarriers by SUs in different secondary cells, collisions occur with a certain probability between the subcarriers of SUs and PU. In addition, inter-cell collisions between the subcarriers of SUs might occur in addition to those that are utilized by PU. This set-up could be considered as the worst case scenario, where the collisions among the SUs subcarriers severely affect the performance due to the overall caused interference. One can observe from Figure 3.1 that the occurrence of collisions can be classified into different groups such as collisions between PU and SU-1, PU and SU-2, SU-1 and SU-2, and the worst case situation that assumes collisions among PU, SU-1 and SU-2.

In Figure 3.2, the channel model at the ith subcarrier ($i \in \{1, \ldots, F\}$) is shown. The *channel power gains* from PU-Tx to PU-Rx, SU-Rx-1, and SU-Rx-2 are denoted by g_i, $g_{s1,i}$ and $g_{s2,i}$, respectively. Similarly, $h_{1,i}$, $h_{1p,i}$ and $h_{1s,i}$ represent the channel power gains from SU-Tx-1 to SU-Rx-1, PU-Rx, and SU-Rx-2, respectively, and $h_{2,i}$, $h_{2s,i}$ and $h_{2p,i}$ denote the channel power gains from SU-Tx-2 to SU-Rx-2, SU-Rx-

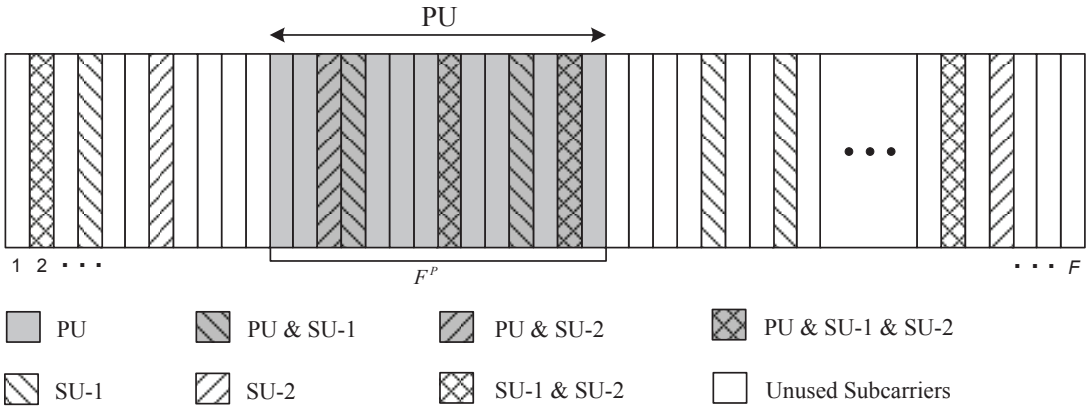

Figure 3.1: OFDM-based CR system for SUs in different secondary networks (cells) with subcarrier collisions with each other and PU due to the random access method.

1, and PU-Rx, respectively. The performance analysis of shaded SU (SU-1) is of interest in this work. To preserve the QoS requirement of PU, the interference power levels caused by the SU-transmitters at the PU-Rx must not be larger than a predefined value for each subcarrier, referred to as the interference temperature (power) constraint. It is assumed that there is no correlation among the subcarriers. Nevertheless, due to the inherent nature of random access method and the high number of available subcarriers available in practice, the probability of selecting (accessing) consecutive subcarriers by SUs will be considerably negligible.

All the channel gains are assumed to be *unit mean* independent and identically distributed (i.i.d.) flat Rayleigh fading channels. The channel *power* gains are hence exponentially distributed with unit mean [24]. In order for SUs to implement the transmit power adaptation and to have a tractable theoretical analysis, it is assumed that perfect information about the interference channels power gains, $h_{1p,i}$ and $h_{2p,i}$, is available at SUs. The SUs can obtain this channel side information, through various means, e.g., from the channel reciprocity condition or from an entity called mediate band or CR network manager between the PU-Rx and SU-Tx [6, 72]. For

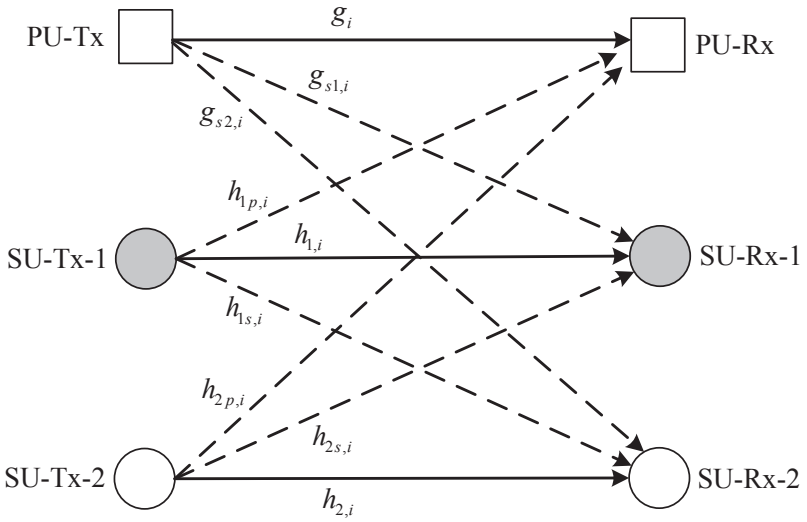

Figure 3.2: Channel model for the ith subcarrier, $i \in \{1, \ldots, F\}$, with SUs- and PU-transmitter and receiver pairs, the performance of shaded SU pairs (SU-1) is of interest.

the sake of analysis simplicity, it is further assumed that the value of interference constraint is the same for all the subcarriers in the system, and the peak transmit power of each user is the same for all its subcarriers, i.e., $P_i = P$, $P_{1,i} = P_1$ and $P_{2,i} = P_2$, where P_i, $P_{1,i}$ and $P_{2,i}$ are the transmit power levels of PU, SU-1 and SU-2. The thermal AWGN is assumed to have circularly symmetric complex Gaussian distribution with zero mean and variance η, i.e., $\mathcal{CN}(0, \eta)$.

3.3 Statistical Analysis of the Number of Subcarrier Collisions

Herein section, the PMFs and the average number of subcarrier collisions for different cases are derived.

3.3.1 Fixed Number of Subcarriers

Throughout this section, the number of subcarriers required by PU and SUs is assumed fixed. In order to properly assess the effect of the random access scheme on the subcarrier collisions, first only a single SU case (secondary cell) is considered.

3.3.1.1 Single Secondary Cell

Here, only a single SU (SU-1) is assumed to be available in the system. Recalling from Chapter 1.4, the following result holds.

Proposition 3. *If SU-1 randomly utilizes (accesses) F_1^S subcarriers from a set of F available subcarriers without replacement, while F^P subcarriers are being utilized by PU, then the PMF of the number of subcarrier collisions, k_{p1}, follows the hypergeometric distribution, $k_{p1} \sim \texttt{HYPG}(F_1^S,\ F^P,\ F)$, and is expressed as:*

$$Pr(K_{p1} = k_{p1}) = p(k_{p1}) = \binom{F^P}{k_{p1}} \binom{F - F^P}{F_1^S - k_{p1}} \Big/ \binom{F}{F_1^S}.$$

The average number of subcarrier collisions is $\mathbb{E}[k_{p1}] = F_1^S F^P / F$, where $\mathbb{E}[\cdot]$ denotes the expectation operator, and the support of k_{p1} is

$$k_{p1} \in \left[\left(F_1^S + F^P - F \right)^+, \ldots, \min\left\{ F_1^S, F^P \right\} \right],$$

Notice from Chapter 1.4 that in the case of N PUs in the primary network, the SU-1 might experience subcarrier collisions with up to N PUs. In such a case, the resulting joint PMF of the number of subcarrier collisions follows a modified *multivariate* hypergeometric distribution.

3.3.1.2 Two Secondary Cells

In this scenario, due to the random access method, there can be inter-cell collisions between the subcarriers of SUs (belonging to the separate cells) in addition to those that collide with PU subcarriers. There are four possible cases of subcarrier collisions for the target SU (say SU-1):

- *Case 1*: collisions between SU-1, PU and SU-2 subcarriers: k_{p12}.

- *Case 2*: collisions *only* between SU-1 and PU subcarriers: $k_{p1}^{o} = k_{p1} - k_{p12}$.
- *Case 3*: collisions *only* between SU-1 and SU-2 subcarriers: $k_{12}^{o} = k_{12} - k_{p12}$.
- *Case 4*: collisions-free subcarriers of SU-1: $k_{f1} = F_1^S - k_{p1}^{o} - k_{12}^{o} - k_{p12}$.

Random variable k_{p1} represents the number of subcarrier collisions between SU-1 and PU in the absence of SU-2. Similarly, k_{12} denotes the number of subcarrier collisions between SU-1 and SU-2 in the absence of PU. It is evident to observe from *Proposition* 3 that the PMF of k_{12} also follows a hypergeometric distribution, $k_{12} \sim \texttt{HYPG}(F_1^S,\ F_2^S,\ F)$. The PMFs and expected values of the aforementioned RVs are presented next.

- *Case 1* (k_{p12}): Let k_{p2} stand for the number of subcarrier collisions between SU-2 and PU in the absence of SU-1: $k_{p2} \sim \texttt{HYPG}(F_2^S,\ F^P,\ F)$. Once the number of subcarrier collisions between SU-2 and PU is given, one can obtain the conditional PMF:

$$p\left(k_{p12} \mid k_{p2}\right) = \binom{k_{p2}}{k_{p12}} \binom{F - k_{p2}}{F_1^S - k_{p12}} \Big/ \binom{F}{F_1^S} = \texttt{HYPG}(F_1^S,\ k_{p2},\ F). \tag{3.1}$$

Using (3.1), the following PMF is obtained:

$$\begin{aligned} p(k_{p12}) &= \sum_{k_{p2}} p\left(k_{p12}, k_{p2}\right) \\ &= \sum_{k_{p2}} p\left(k_{p12} \mid k_{p2}\right) p\left(k_{p2}\right) \\ &= \sum_{k_{p2}=\left(F_2^S + F^P - F\right)^+}^{\min\left\{F_2^S, F^P\right\}} \binom{k_{p2}}{k_{p12}} \binom{F - k_{p2}}{F_1^S - k_{p12}} \\ &\quad \times \binom{F^P}{k_{p2}} \binom{F - F^P}{F_2^S - k_{p2}} \Big/ \left[\binom{F}{F_1^S}\binom{F}{F_2^S}\right]. \end{aligned} \tag{3.2}$$

The average number of subcarrier collisions, $\mathbb{E}[k_{p12}]$, is expressed as follows:

$$\begin{aligned}
\mathbb{E}[k_{p12}] &= \sum_{k_{p12}} k_{p12}\; p(k_{p12}) \\
&\overset{(a)}{=} \sum_{k_{p12}} \sum_{k_{p2}=\left(F_2^S+F^P-F\right)^+}^{\min\left\{F_2^S,F^P\right\}} k_{p12}\binom{k_{p2}}{k_{p12}}\binom{F-k_{p2}}{F_1^S-k_{p12}}\binom{F^P}{k_{p2}} \\
&\quad \binom{F-F^P}{F_2^S-k_{p2}}\Big/\left[\binom{F}{F_1^S}\binom{F}{F_2^S}\right] \\
&= \sum_{k_{p2}} \Bigg\{ \left[\binom{F^P}{k_{p2}}\binom{F-F^P}{F_2^S-k_{p2}}\Big/\binom{F}{F_2^S}\right] \\
&\quad \underbrace{\left[\sum_{k_{p12}} k_{p12}\binom{k_{p2}}{k_{p12}}\binom{F-k_{p2}}{F_1^S-k_{p12}}\Big/\binom{F}{F_1^S}\right]}_{\Delta_1} \Bigg\},
\end{aligned}$$

where $\Delta_1 = \mathbb{E}[k_{p12} \mid k_{p12}] = F_1^S k_{p2}/F$, and in (a) the support of k_{p12} is given by

$$k_{p12} \in \left[\left(F_1^S + \left(F_2^S + F^P - F\right)^+ - F\right)^+ \ldots \min\left\{F_1^S, F_2^S, F^P\right\}\right].$$

Plugging Δ_1 yields

$$\begin{aligned}
\mathbb{E}[k_{p12}] &= \frac{F_1^S}{F} \underbrace{\sum_{k_{p2}} k_{p2}\binom{F^P}{k_{p2}}\binom{F-F^P}{F_2^S-k_{p2}}\Big/\binom{F}{F_2^S}}_{\mathbb{E}[k_{p2}]=\frac{F_2^S F^P}{F}} \\
&= \frac{F_1^S F_2^S F^P}{F^2}.
\end{aligned}$$

In Figure 3.3, the PMF of k_{p12} is plotted for arbitrary values of parameters, F, F^P, F_1^S and F_2^S. As it can be observed, the simulation and exact numerical results in (3.1) match very well.

- *Case 2* (k_{p1}^o): Following the same approach as in *Case 1*, the PMF of k_{p1}^o is

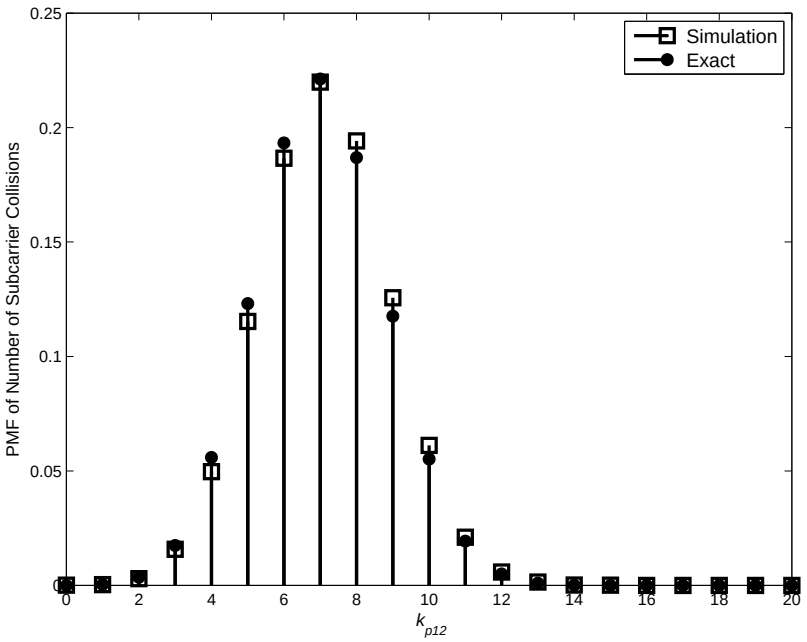

Figure 3.3: PMF of the number of subcarrier collisions between the PU, SU-1 and SU-2 for $F = 50$, $F^P = 35$, $F_1^S = 25$, $F_2^S = 20$.

expressed as:

$$\begin{aligned} p(k_{p1}^o) &= \sum_{k_{p12}} p\left(k_{p1}^o, k_{p12}\right) \\ &= \sum_{k_{p12}} p\left(k_{p1}^o \mid k_{p12}\right) p\left(k_{p12}\right) \\ &= \sum_{k_{p12}} \left[p\left(k_{p1}^o \mid k_{p12}\right) \left[\sum_{k_{p2}} p\left(k_{p12} \mid k_{p2}\right) p\left(k_{p2}\right) \right] \right]. \end{aligned} \tag{3.3}$$

Plugging (3.2) into the equation above yields the desired PMF. The average number of subcarrier collisions between SU-1 and PU, $\mathbb{E}[k_{p12}]$, is given by

$$\begin{aligned}\mathbb{E}[k_{p1}^{o}] &= \mathbb{E}[k_{p1} - k_{p12}] \\ &= \mathbb{E}[k_{p1}] - \mathbb{E}[k_{p12}] \\ &= \frac{F_1^S F^P}{F} - \frac{F_1^S F_2^S F^P}{F^2} \\ &= \frac{F_1^S F^P \left(F - F_2^S\right)}{F^2}.\end{aligned}$$

- *Case 3* (k_{12}^{o}): Similar to the *Case 2*, the PMF of k_{12}^{o} can be obtained by replacing k_{p1}^{o} with k_{12}^{o} in (3.3), and its expression is omitted for brevity. Nonetheless, the expression for the average number of subcarrier collisions between SU-1 and SU-2, $\mathbb{E}[k_{12}^{o}]$, is expressed as

$$\begin{aligned}\mathbb{E}[k_{12}^{o}] &= \mathbb{E}[k_{12} - k_{p12}] \\ &= \frac{F_1^S F_2^S \left(F - F^P\right)}{F^2}.\end{aligned}$$

- *Case 4* (k_{f1}): Lastly, the average number of collisions-free subcarriers for SU-1, $\mathbb{E}[k_{f1}]$, is given by

$$\begin{aligned}\mathbb{E}[k_{f1}] =& \mathbb{E}[F_1^S - k_{p1}^{o} - k_{12}^{o} - k_{p12}] \\ =& F_1^S - \frac{F_1^S F^P \left(F - F_2^S\right)}{F^2} - \frac{F_1^S F_2^S \left(F - F^P\right)}{F^2} - \frac{F_1^S F_2^S F^P}{F^2} \\ =& \frac{F_1^S \left(F - F_2^S\right)\left(F - F^P\right)}{F^2}.\end{aligned}$$

3.3.2 Random Number of Subcarriers

In the preceding section, the number of utilized subcarriers by both PU and SUs are assumed to be fixed. However, considering practical scenarios, the number

of subcarriers required by PU or SUs can vary. Based on either PU or SUs rate requirements, the number of subcarriers utilized by users can be different at any time instant. Next the long term average performance of the system is investigated by using a stochastic model for the required number of subcarriers for PU and SUs. The distribution of the required number of subcarriers can be approximated either by a uniform or binomial distribution [48]. In this chapter, it is assumed that the number of subcarriers utilized by the users follows a binomial distribution. Mathematically, the number of utilized subcarriers by SU-1 is $f_1^s \sim \mathtt{B}(T_{s1}, q_{s1})$, and its PMF is given by

$$\begin{aligned}\Pr(F_1^S = f_1^s) &= p(f_1^s) \\ &= \binom{T_{s1}}{f_1^s} (q_{s1})^{f_1^s} (1 - q_{s1})^{T_{s1} - f_1^s},\end{aligned}$$

where T_{s1} is the number of trials, which can be considered as the maximum number of subcarriers used by SU-1, and $q_{s1} \in [0, 1]$ is the probability of success in each trial. Under these assumptions, the average number of required subcarriers is given by $\mathbb{E}[f_1^s] = T_{s1} q_{s1}$. Similarly, the numbers of subcarriers utilized by PU and SU-2 are assumed to be binomially distributed RVs, i.e., $f^p \sim \mathtt{B}(T_p, q_p)$ and $f_2^s \sim \mathtt{B}(T_{s2}, q_{s2})$, respectively.

To save space, only the essential results in Section 3.3.1, which will be used in the upcoming sections, will be revisited. Let $\hat{k}_{p1}$ denote the number of subcarriers collisions between SU-1 and PU when both of them utilize a random number of subcarriers. Heretofore, the notation $(\hat{\cdot})$ represented the fact that the user's number of subcarriers is a RV, e.g., $\hat{k}_{p1}^o$, $\hat{k}_{12}$, $\hat{k}_{12}^o$, $\hat{k}_{p12}$ and $\hat{k}_{f1}$. When the users utilize random numbers of subcarriers, *Proposition* 3 can be restated in the following form.

Proposition 4. *Let f_1^s and f^p be independent but not necessarily identically dis-*

tributed binomial RVs, representing the utilized number of subcarriers by SU-1 and PU, respectively. If SU-1 randomly accesses f_1^s subcarriers from a set of F available subcarriers without replacement while f^p subcarriers are being used by the PU, then the PMF of the number of subcarrier collisions, $\hat{k}_{p1}$, is given by:

$$\begin{aligned} Pr(\hat{K}_{p1} = \hat{k}_{p1}) =& p(\hat{k}_{p1}) \\ &= \sum_{f_1^s=0}^{T_{s1}} \sum_{f^p=0}^{T_p} \left[\binom{f^p}{\hat{k}_{p1}} \binom{F - f^p}{f_1^s - \hat{k}_{p1}} \binom{T_{s1}}{f_1^s} \binom{T_p}{f^p} \Big/ \binom{F}{f_1^s} \right] \\ &\quad \times (q_{s1})^{f_1^s} (1 - q_{s1})^{T_{s1} - f_1^s} (q_p)^{f^p} (1 - q_p)^{T_p - f^p}, \end{aligned}$$

and the average number of subcarrier collisions is: $\mathbb{E}[\hat{k}_{p1}] = T_{s1} T_p q_{s1} q_p / F$.

Proof. The proof is given in Appendix F. □

Following a similar reasoning, one can readily obtain the expressions for the PMFs and the expected values of $\hat{k}_{p1}^o$, $\hat{k}_{12}$, $\hat{k}_{12}^o$, $\hat{k}_{p12}$ and $\hat{k}_{f1}$. Briefly, the following important results for the expected values of $\hat{k}_{p12}$, $\hat{k}_{p1}^o$, $\hat{k}_{12}^o$ and $\hat{k}_{f1}$, can be expressed, respectively, as:

$$\begin{aligned} \mathbb{E}[\hat{k}_{p12}] &= \frac{T_{s1} T_{s2} T_p q_{s1} q_{s2} q_p}{F^2}, \\ \mathbb{E}[\hat{k}_{p1}^o] &= \frac{T_{s1} T_p q_{s1} q_p \left(F - T_{s2} q_{s2}\right)}{F^2}, \\ \mathbb{E}[\hat{k}_{12}^o] &= \frac{T_{s1} T_{s2} q_{s1} q_{s2} \left(F - T_p q_p\right)}{F^2}, \\ \mathbb{E}[\hat{k}_{f1}] &= \frac{T_{s1} q_{s1} \left(F - T_{s2} q_{s2}\right) \left(F - T_p q_p\right)}{F^2}. \end{aligned} \tag{3.4}$$

3.4 Performance Analysis of Secondary User

In this section, the performance of the target SU (SU-1) is investigated by using the average capacity as performance measure. In addition, the capacity (rate) loss of

SU-1 due to the subcarrier collisions with the subcarriers of PU and SU-2 is studied. The sets of subcarriers are defined as follows. Let $\mathcal{K}_{p1}^{o}$ be the set of collided subcarriers only between the SU-1 and PU, and $k_{p1}^{o} = \left|\mathcal{K}_{p1}^{o}\right|$ (fixed case) or $\hat{k}_{p1}^{o} = \left|\mathcal{K}_{p1}^{o}\right|$ (random case), the cardinality of the set $\mathcal{K}_{p1}^{o}$. Similarly, the same reasoning can be applied for the sets $\mathcal{K}_{12}^{o}$, $\mathcal{K}_{p12}$, $\mathcal{K}_{f1}$, $\mathcal{F}^{P}$, $\mathcal{F}_{1}^{S}$, and $\mathcal{F}_{2}^{S}$ with their cardinalities[1] given, respectively, as $\hat{k}_{12}^{o} = |\mathcal{K}_{12}^{o}|$, $\hat{k}_{p12} = |\mathcal{K}_{p12}|$, $\hat{k}_{f1} = |\mathcal{K}_{f1}|$, $f^{p} = \left|\mathcal{F}^{P}\right|$, $f_{1}^{s} = \left|\mathcal{F}_{1}^{S}\right|$, and $f_{2}^{s} = \left|\mathcal{F}_{2}^{S}\right|$.

3.4.1 Average Capacity of SU

Next the expressions for the instantaneous and average capacity of SU-1 over an arbitrary channel fading model with a random access scheme are presented.

Theorem 5. *Let $S_{p1,i}^{o}$, $S_{12,i}^{o}$ and $S_{p12,i}$ denote the signal-to-interference plus noise ratio (SINR) levels for the ith subcarrier of SU-1 with interference component coming only from PU, only from SU-2 and from both PU and SU-2, respectively. Similarly, let $S_{f1,i}$ stand for the signal-to-noise ratio (SNR) for the ith collision-free subcarrier of the SU-1. Mathematically, the SINRs and SNR are defined as*

$$
\begin{aligned}
S_{p1,i}^{o} &= \frac{h_{1,i}P_{1,i}}{g_{s1,i}P_{i} + \eta}, \\
S_{12,i}^{o} &= \frac{h_{1,i}P_{1,i}}{h_{2s,i}P_{2,i} + \eta}, \\
S_{p12,i} &= \frac{h_{1,i}P_{1,i}}{g_{s1,i}P_{i} + h_{2s,i}P_{2,i} + \eta}, \\
S_{f1,i} &= \frac{h_{1,i}P_{1,i}}{\eta}.
\end{aligned}
$$

Then, the instantaneous capacity of SU-1 with the random access method is expressed as

[1]Hereafter, to ease the notations, the cardinalities of the sets will be mentioned for the *random* number of subcarriers utilized by users. The case of *fixed* number of subcarriers utilization by users can be readily interpreted.

$$
\begin{aligned}
C_{S_1} &= \sum_{i\in\mathcal{K}^o_{p1}} C^o_{p1,i} + \sum_{i\in\mathcal{K}^o_{12}} C^o_{12,i} + \sum_{i\in\mathcal{K}_{p12}} C_{p12,i} + \sum_{i\in\mathcal{K}_{f1}} C_{f1,i} \\
&= \sum_{i\in\mathcal{K}^o_{p1}} \log\left(1+S^o_{p1,i}\right) + \sum_{i\in\mathcal{K}^o_{12}} \log\left(1+S^o_{12,i}\right) \\
&\quad + \sum_{i\in\mathcal{K}_{p12}} \log\left(1+S_{p12,i}\right) + \sum_{i\in\mathcal{K}_{f1}} \log\left(1+S_{f1,i}\right),
\end{aligned} \tag{3.5}
$$

and the mean value of C_{S_1} *is given by*

$$
\begin{aligned}
\mathbb{E}[C_{S_1}] =& \frac{T_{s1}q_{s1}}{F^2}\left\{(F-T_{s2}q_{s2})\left[T_pq_p\mathbb{E}[C^o_{p1,i}] + (F-T_pq_p)\,\mathbb{E}[C_{f1,i}]\right]\right. \\
&\left. + T_{s2}q_{s2}\left[(F-T_pq_p)\,\mathbb{E}[C^o_{12,i}] + T_pq_p\mathbb{E}[C_{p12,i}]\right]\right\},
\end{aligned} \tag{3.6}
$$

where the expected values of capacities at the i*th subcarrier for the four different cases,* $C^o_{p1,i}$*,* $C^o_{12,i}$*,* $C_{p12,i}$ *and* $C_{f1,i}$ *over the Rayleigh channel fading model are investigated in Section 3.4.3.*

Proof. The proof is given in Appendix G. □

3.4.2 Capacity Loss Due to Collisions

The upper bounds for the SU-1 instantaneous and average capacity loss due to subcarrier collisions are given by the following result.

Corollary 6. *The maximum capacity (rate) loss of SU-1 due to subcarrier collisions is upper-bounded by* $\frac{1}{\eta}\left[\sum_{i\in\mathcal{K}_{p1}} g_{s1,i}P_i + \sum_{i\in\mathcal{K}_{12}} h_{2s,i}P_{2,i}\right]$*. Mathematically,*

$$
\Delta C_{S_1} = C^f_{S_1} - C_{S_1} \le \frac{1}{\eta}\left[\sum_{i\in\mathcal{K}_{p1}} g_{s1,i}P_i \; + \sum_{i\in\mathcal{K}_{12}} h_{2s,i}P_{2,i}\right],
$$

where $C^f_{S_1}$ *is the capacity of SU-1 when all of its subcarriers are collision-free, and*

is defined as $C_{S_1}^f = \sum_{i=1}^{F_1^S} \log\left(1 + h_{1,i}P_{1,i}/\eta\right)$. *The upper bound for the maximum average capacity loss is given by*

$$\mathbb{E}[\Delta C_{S_1}] \leq \frac{T_{s2}q_{s2}\left(T_p q_p P_i + T_{s1}q_{s1}P_{2,i}\right)}{\eta F}.$$

Proof. The proof is given in Appendix H. □

3.4.3 Capacity over Rayleigh Channel Fading Model

In this section, the average capacity expressions at the ith subcarrier for the four different collision cases, given in Section 3.3, are studied. There have been various methods proposed to protect the operation of PU by maintaining the QoS requirements above some predefined threshold, and in this regard peak or average interference power constraints are two well known methods [72]. To investigate the performance of the proposed random access scheme, the well known peak interference power constraint at each ith subcarrier is adapted similar to the Chapter 1.4. It is assumed that the peak transmit powers of SUs are the same for a tractable analysis $P_1 = P_2 = P_s$. Therefore, the transmit power of the SU-1 is adapted to protect PU, and is given by[2]

$$P_s^T = \begin{cases} P_s\ , & \beta P_s \leq \Psi \\ \frac{\Psi}{\beta}, & \beta P_s > \Psi \end{cases} = \min\left\{P_s, \frac{\Psi}{\beta}\right\},$$

where $\beta = h_{1p} + h_{2p}$, and Ψ is the interference power constraint. It is worth to note that due to the random access scheme, the transmit power is adopted (regulated)

[2]Heretofore, since the analysis is for the ith subcarrier, the subscript i in the parameters is dropped for the ease of notation, e.g., $P_{1,i} \to P_1$, $h_{1p,i} \to h_{1p}$, $S_{f1,i} \to S_{f1}$, $C_{f1,i} \to C_{f1}$, etc.

considering the worst case scenario, as if there are collisions between both SUs and PU (interference from both SUs at PU-Rx, i.e., $h_{1p}P_s + h_{2p}P_s$). This condition assures the QoS requirement of PU. In addition, instead of considering the worst case scenario, it could be further assumed that the interference constraint of PU, Ψ, is low enough to protect the operation of PU even when there is interference from both SUs, or the interference constraint is set as Ψ/N_c, where N_c is the number of secondary networks (cells). In such case, the approach to derive expressions of average capacities would be relatively more tractable and similar to the approach given in Chapter 1.4.

Notice also that considering the Rayleigh channel fading model, all the channel power gains are exponentially distributed with unit mean, e.g., $h_{1p},\ h_{2p},\ h_1,\ g_s \sim \texttt{Exp}(1)$. Therefore, the RV β follows Erlang distribution with shape and rate parameters of 2 and 1, respectively, i.e., $\beta \sim \texttt{Erlang}(2,1)$, $f_\beta(x) = xe^{-x}, x \geq 0$.

Once the transmit power of the SU-1 is regulated, the received power of SU-1 at the SU-Rx can be defined as $\alpha = h_1 P_s^T$. Exploiting properties of order statistics [50], and by following a similar approach to [62], the cumulative distribution function (CDF) of α can be obtained:

$$\begin{aligned} F_\alpha(x) &= 1 - \Pr\left(h_1 > \frac{x}{P_s}\right)\Pr\left(\beta < \frac{\Psi}{P_s}\right) - \int_{\Psi/P_s}^{\infty} \Pr\left(h_1 > \frac{xy}{\Psi}\right) f_\beta(y)\mathrm{d}y \\ &= 1 - e^{-\frac{x}{P_s}}\left[1 - \left(\frac{\Psi + P_s}{P_s}\right)e^{-\frac{\Psi}{P_s}}\right] - \frac{\Psi^2\left(x + P_s + \Psi\right)}{P_s\left(x+\Psi\right)^2}e^{-\frac{x+\Psi}{P_s}}. \end{aligned} \tag{3.7}$$

Also, the probability density function (PDF) of α can be readily expressed as

$$f_\alpha(x) = \frac{e^{-\frac{x}{P_s}}}{P_s} - \frac{e^{-\frac{x+\Psi}{P_s}}}{P_s^2}\left[\Psi + P_s - \frac{\Psi^2\left(\left(x+\Psi\right)^2 + 2\left(x+\Psi\right)P_s + 2P_s^2\right)}{\left(x+\Psi\right)^3}\right]. \tag{3.8}$$

Once the PDF and CDF of α are obtained, the average capacity expressions are derived as follows.

3.4.3.1 Ergodic Capacity with no Interference

The CDF of SNR, $S_{f1} = \alpha/\eta$, can be expressed by using the transformation of RVs: $F_{S_{f1}}(x) = F_{\alpha}(\eta x)$. Using $F_{S_{f1}}(x)$, and the partial integration method [62], the average capacity in the collision-free case is given by

$$\begin{aligned}
\mathbb{E}[C_{f1}] =& \int_0^{\infty} \log(1+x)\, f_{S_{f1}}(x)\mathrm{d}x \\
=& \int_0^{\infty} \frac{1 - F_{S_{f1}}(x)}{1+x}\mathrm{d}x \\
=& e^{\frac{\eta}{P_s}} \left(1 - \frac{e^{-\frac{\Psi}{P_s}}(P_s+\Psi)}{P_s}\right) E_1\left(\frac{\eta}{P_s}\right) + \frac{\Psi e^{-\frac{\Psi}{P_s}}}{P_s(\Psi-\eta)^2} \\
& \times \left[P_s\left(\eta - \Psi - \Psi e^{\frac{\Psi}{P_s}} E_1\left(\frac{\Psi}{P_s}\right)\right) + \Psi e^{\frac{\eta}{P_s}}(P_s + \Psi - \eta) E_1\left(\frac{\eta}{P_s}\right)\right],
\end{aligned}$$

where the exponential integral is defined as [2, Eq. 5.1.1] $E_1(a) = \int_a^{\infty} t^{-1} e^{-t}\mathrm{d}t$.

3.4.3.2 Ergodic Capacity with Interference only from PU

The CDF of $S_{p1}^{o} = \alpha/(g_{s1}P + \eta)$ can be obtained by using (3.7) and expressed as

$$\begin{aligned}
F_{S_{p1}^{o}}(x) =& \Pr\left(\frac{\alpha}{g_{s1}P + \eta} < x\right) \\
=& \int_0^{\infty} F_{\alpha}\left(x(yP+\eta)\right) f_{g_s}(y)\mathrm{d}y \\
=& 1 + e^{-\frac{\Psi + x\eta}{P_s}} \left[\frac{P_s + \Psi - P_s e^{\frac{\Psi}{P_s}}}{P_s + xP} + \frac{\Psi^2}{x^2P^2}\right. \\
& \left. \times \left(e^{\frac{(P_s+xP)(\Psi+x\eta)}{xPP_s}} E_1\left(\frac{(P_s+xP)(\Psi+x\eta)}{xPP_s}\right) - \frac{xP}{\Psi + x\eta}\right)\right],
\end{aligned}$$

where $f_{g_s}(x) = e^{-x}$. The average capacity is hence given by

$$\begin{aligned}\mathbb{E}[C_{p1}^{o}] =& \int_{0}^{\infty} \frac{1 - F_{S_{p1}}(x)}{1+x} \mathrm{d}x \\ =& \frac{e^{-\frac{\Psi}{P_s}}}{P - P_s} \left(P_s - e^{\frac{\Psi}{P_s}} P_s + \Psi\right) \left(e^{\frac{\eta}{P_s}} E_1\left(\frac{\eta}{P_s}\right) - e^{\frac{\eta}{P}} E_1\left(\frac{\eta}{P}\right)\right) + \frac{\Psi^2}{P^2} \\ & \times \int_{0}^{\infty} \frac{e^{-\frac{\Psi + x\eta}{P_s}}}{(1+x)x^2} \left[\frac{xP}{\Psi + x\eta} - e^{\frac{(P_s + xP)(\Psi + x\eta)}{xPP_s}} E_1\left(\frac{(P_s + xP)(\Psi + x\eta)}{xPP_s}\right)\right] \mathrm{d}x,\end{aligned}$$

where the integration will be evaluated numerically.

3.4.3.3 Ergodic Capacity with Interference only from SU-2

Let $\theta = h_{2s} P_s^T$ be the received power of SU-2 at SU-Rx. It very important to observe that due to the interference power constraint of PU, SU-2 also adapts its transmit power, and θ is hence identically distributed as α. Following a similar approach, the CDF of S_{12}^{o} can be expressed as $F_{S_{12}^{o}}(x) = \int_0^\infty F_\alpha\left(x\left(y + \eta\right)\right) f_\theta(y) \mathrm{d}y$. Once the CDF is obtained, the average capacity can be derived. However, due to the complicated and long expressions of the involved PDF and CDF, the analysis unfortunately leads to intractable results. Even if we obtain the expressions, it will hardly provide any insights because of the very long and complicated expressions. Therefore, the resulting integrals can be readily estimated by employing the Gauss-Chebyshev quadrature (GCQ) formula. For instance, the average capacity of C_{12}^{o} can be expressed as

$$\begin{aligned}\mathbb{E}[C_{12}^{o}] &= \int_{0}^{\infty} \frac{1 - F_{S_{12}^{o}}(x)}{1+x} \mathrm{d}x \\ &\simeq \sum_{n=1}^{N_t} \omega_n \frac{1 - F_{S_{12}^{o}}(s_n)}{1 + s_n},\end{aligned}$$

where the weights (w_j) and abscissas (s_j) are defined in [70, Eqs. (22) and (23)], respectively. Further, the truncation index in the sum, N_t, could be chosen to make the approximation error negligibly small.

3.4.3.4 Ergodic Capacity with Interference from both PU and SU-2

Let ρ be the sum of interferences from PU and SU-2 at SU-Rx: $\rho = \lambda + \theta$, where $\lambda = g_s P$. The PDF of ρ can be obtained by convolving the PDFs of RVs as $f_\rho(x) = f_\lambda(x) * f_\theta(x) = \int_0^\infty f_\lambda(x-y)\, f_\theta(y)\, \mathrm{d}y$. Following an approach similar to the ones presented in the previous sections, the average capacity expression, $\mathbb{E}[C_{p12}]$, can be obtained. It is worth to notice that for the ease of numerical evaluation, the capacity can be expressed by means of triple integrals as

$$\mathbb{E}[C_{p12}] = \int_0^\infty \int_0^\infty \int_0^\infty \frac{e^{-z}e^{-y} - F_\alpha\left(x\left(y+z+\eta\right)\right) f_\theta(y) f_\lambda(z)}{1+x} \mathrm{d}z\ \mathrm{d}y\ \mathrm{d}x,$$

where $f_\lambda(x) = e^{-x/P}/P$, and $f_\theta(x) = f_\alpha(x)$, given in (3.8), and the exponential terms are added to take all the terms in the same integrals. Also, a similar expression can be obtained for $\mathbb{E}[C_{12}^o]$, in which a double integration will be necessary.

3.5 Numerical Results and Simulations

In this section, the numerical and simulation results are presented to confirm the analytical results and investigate the impact of various system parameters on the performance of CR networks. Further, equal transmit powers of SUs are assumed to verify the simulation results with the numerical ones derived in Section 3.4.3, and the unit noise variance, $\eta = 1$, is used in all the following figures. In Figures 3.4 and 3.5, the average capacities (in nats per second per hertz) of the ith subcarrier, investigated in Section 3.4.3, are shown versus the peak transmit power of SU, P_s, and interference power constraint of PU, Ψ, respectively. The simulation results match perfectly the

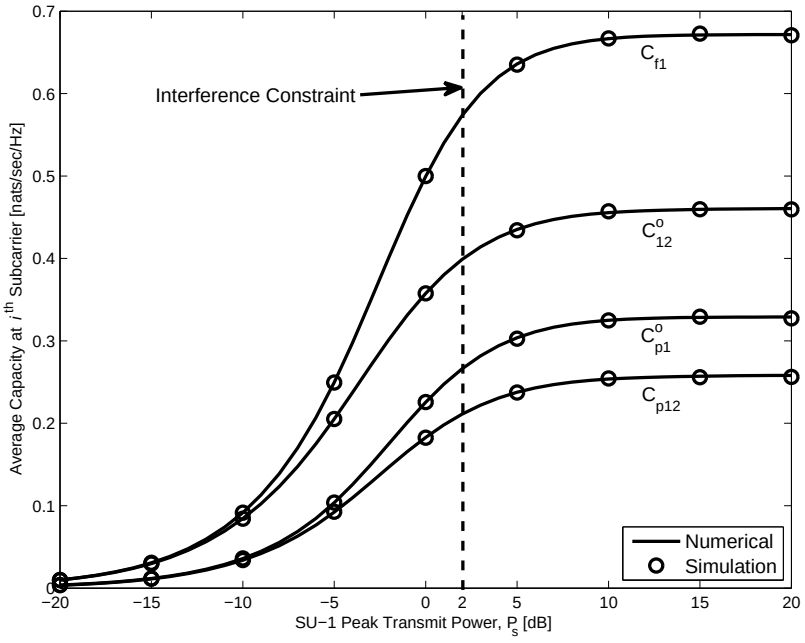

Figure 3.4: Average capacity at the ith subcarrier versus peak transmit power, P_s, in case of collision-free (no-interference) and interference from only PU, only SU-2 and both PU and SU-2 with $P = 5$ dB and $\Psi = 2$ dB.

analytical results. Due to the interference power constraint of PU, average capacities are saturated after a certain value of SUs' peak transmit powers. The channel power gains are assumed to be exponentially distributed with unit mean. Therefore, the saturation of the capacities starts at around the point, shown by vertical dashed line, when the SUs' transmit powers and interference constraint are equal, i.e., $\Psi = P_s$. Comparing the average capacities given in Figures 3.4 and 3.5, the best and the worst case performances belong to the collision-free case and collisions with both SU-2 and PU, respectively, as expected. The average capacity in case of interference (collision) only from PU is lower than the average capacity in case of interference only from SU-2. This result is due to the fact that the SUs' transmit powers are equal and the low interference constraint. Therefore, SU-2 transmit power is also adapted, and the effect of interference on SU-1 capacity coming from SU-2 is lower than that of PU.

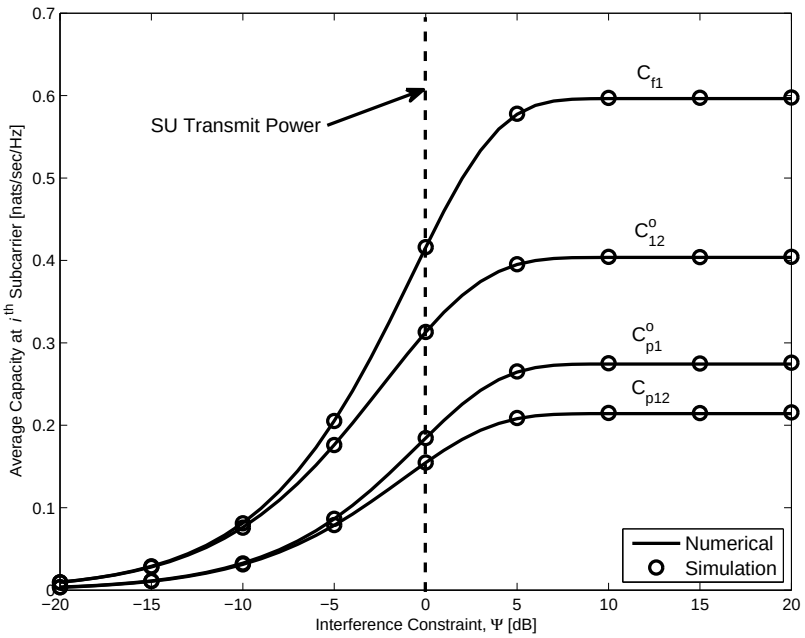

Figure 3.5: Average capacity at the ith subcarrier versus interference power constraint, Ψ, in case of collision-free (no-interference) and interference from only PU, only SU-2 and both PU and SU-2 with $P = 5$ dB and $P_s = 0$ dB.

Figure 3.6 presents the total average capacity of SU-1, given in (3.6), versus the interference constraint for different SUs' transmit powers. The simulations are performed assuming *random* subcarrier requirements for users, where $q_p = q_{s1} = q_{s2} = 0.5$. A similar saturation effect, observed in Figures 3.4 and 3.5, is present in Figure 3.6 as well, where two saturation points are available due to the different values for transmit powers of SUs, $P_s = 0$dB and $P_s = 10$dB.

The average capacity loss due to subcarrier collisions is investigated in Figure 3.7. The percentage of average capacity loss, $\mathbb{E}[\Delta C_{S_1}]/\mathbb{E}[C^f_{S_1}]$, versus the ratio of available subcarriers to the utilized subcarriers, $R_a = F/T_{s1}$, $F = 40, \ldots, 200$ and $T_{s1} = 40$, is shown for different values of PU's transmit power. It is immediate to observe that an increase in the number of available subcarriers in the primary network, leads to a larger number of collision-free subcarriers for SU-1. Therefore, SU-1 average

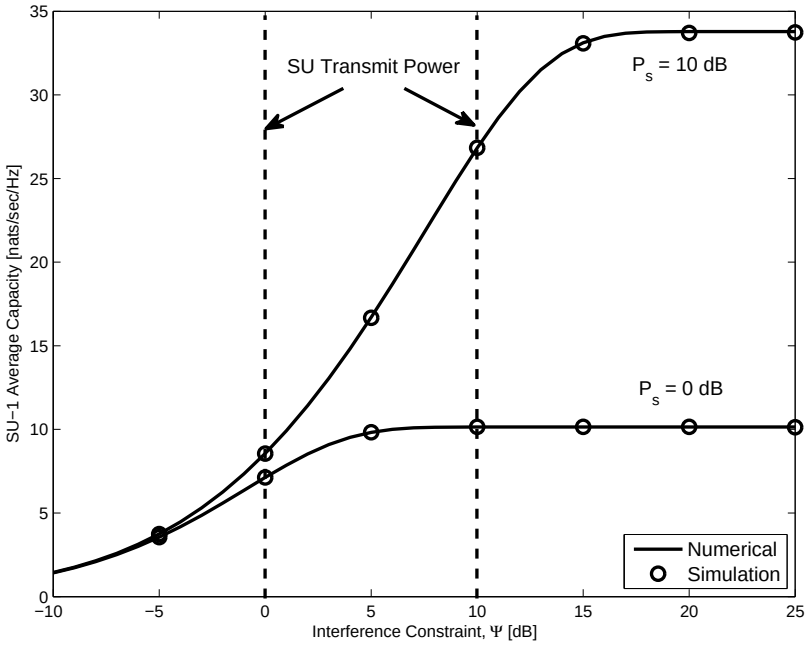

Figure 3.6: SU-1 average capacity versus interference power constraint, Ψ, for different SU's transmit power with $T_p = T_{s1} = 40$, $T_{s2} = 30$, $F = 100$, and $P = 5$ dB.

capacity loss decreases as the number of available subcarriers increases. Notice also that an increase in PU transmit power results in higher interference at SU-1, and hence higher capacity loss on the average.

3.6 Summary

In this chapter, the random subcarrier access scheme is considered for an OFDM-based CR system with spectrum sharing feature and two different secondary networks (cells). It is assumed that no spectrum sensing is performed, i.e., the information for the subcarrier occupation (utilization) by PU is not available at the SUs. It is shown that the PMFs of the number of subcarrier collisions between any two arbitrary users follows a hypergeometric distribution. It is further shown that due to the randomness of the access scheme and the absence of cooperation between the SUs, there can be inter-cell collisions between the SUs' subcarriers with a certain probability.

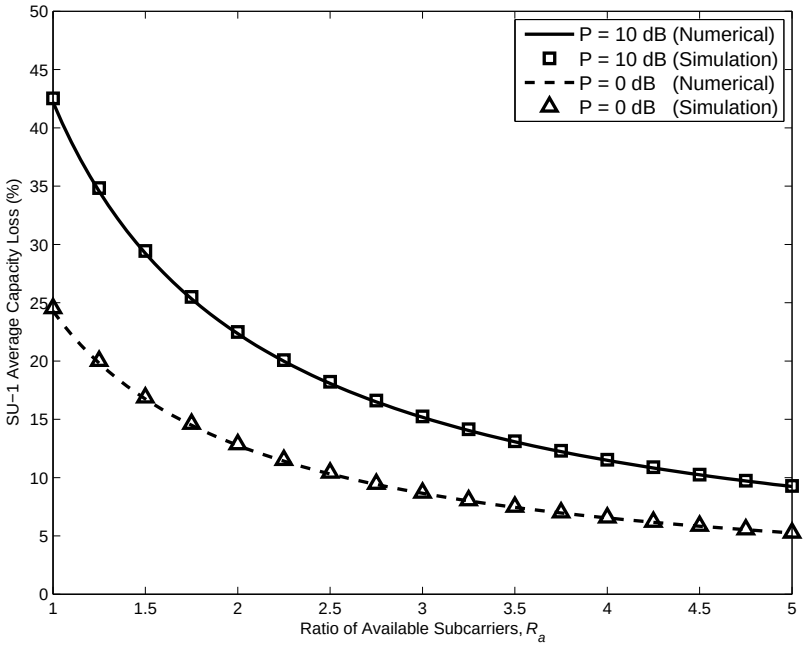

Figure 3.7: SU-1 average capacity loss versus the ratio of available subcarriers to utilized subcarriers, R_a, for different PU's transmit power with $T_p = T_{s1} = 40$, $T_{s2} = 30$, $\Psi = 2$ dB, and $P_s = 20$ dB.

The expressions for the PMFs and the average of number of subcarrier collisions, considering both fixed and random (to obtain the long term average) number of subcarriers utilized by PU and SUs, are derived. The performance of the random access scheme is analyzed by using the average capacity as performance measure. To maintain the QoS of the PU, the well known interference power constraint is applied to the SUs' transmit powers at their subcarriers. The expressions for the maximum instantaneous and average capacity (rate) loss due to subcarrier collisions for the target SU are derived.

4. COGNITIVE RADIO SPECTRUM SHARING SYSTEMS OVER HYPER FADING CHANNELS*

4.1 Introduction

The previous works provided the motivation to develop a theoretical fading model that can be used to perform a unified analysis for cognitive radio spectrum sharing systems. Due to the highly dynamic nature of propagation environments, several single-fading models are employed in the literature for the analysis of CR spectrum sharing systems. However, considering practical scenarios, it would be more efficient and convenient to use a generic fading model, which can be degenerated onto widely used single-fading models with the appropriate selection of parameters. In addition, when the environment conditions and primary network constraints allow, SUs can opportunistically allocate spectrum regions with different frequencies and bandwidths. Since the small-scale fading is frequency dependent, the resulting channel fading model can be dynamic.

In this chapter, the proposed generic fading model, termed hyper Nakagami-m fading, representing several widely encountered propagation scenarios such as line-of-sight (LOS)/non-line-of-sight (NLOS) environments and fixed/mobile transmissions, is considered. Additionally, instantaneous and average power capacity calculations can also be properly carried out with the proposed generic model. In the light of

*Reprinted with permissions from "Capacity limits of spectrum-sharing systems over hyper-fading channels" by Sabit Ekin, Ferkan Yilmaz, Hasari Celebi, Khalid A. Qaraqe, Mohamed-Slim Alouini, and Erchin Serpedin, Wireless Communications and Mobile Computing, Volume 12, Issue 16, Page(s):1471–1480, Nov. 2012, Copyright 2012 by WILEY, and "Achievable capacity of a spectrum sharing system over hyper fading channels," by Sabit Ekin, Ferkan Yilmaz, Hasari Celebi, Khalid A. Qaraqe, Mohamed-Slim Alouini, and Erchin Serpedin IEEE Global Telecommunications Conference (GLOBECOM), Page(s):1–6, Dec. 2009, Copyright 2012 by IEEE.

the analysis presented for the proposed method, the capacity of SU in a spectrum sharing system is studied under the interference temperature constraint.

The main contributions of this chapter are as follows.

- A theoretical channel fading model called hyper fading model that is suitable for the dynamic nature of CR channel is proposed.
- Closed-form expressions of the PDF and CDF of the SNR for SUs in spectrum sharing systems are derived.
- The achievable capacity gains in spectrum sharing systems in high and low power regions are obtained.
- The effects of different fading figures, average fading powers, interference temperatures, peak powers of secondary transmitters, and numbers of SUs on the achievable capacity are investigated.
- The analytical and simulation results show that the fading figure of the channel between SUs and primary base-station, which describes the diversity of the channel, does not contribute significantly to the system performance gain.

4.1.1 Organization

The rest of the chapter is organized as follows. In Section 4.2, the system model is presented. This is followed by the providing statistical background on the proposed hyper fading model in Section 4.3. In Section 4.4, capacity of spectrum sharing systems is derived for both high and low power regions. In Section 4.5, the analytical and numerical results are presented. Finally, the summary is provided in Section 4.6.

4.2 System Model

A symmetric fading channel is considered where SU transmitter-PU receiver (interference channel) and SU transmitter-SU receiver (desired channel) channel gains are assumed to be independent and identically distributed exponential random variables with unit mean in independent Rayleigh fading channels. However, in practice, these channels can be dynamic, as a result, the fading conditions and link powers can be time-varying. Therefore, in this work, we assume that both channels are independent and non-identically distributed hyper Nakagami-m fading random variables that might represent any type of fading environments.

The system model is shown in Fig. 4.1, where φ_i and ψ_i are the interference and desired channel gains, respectively, and N_s stands for the number of secondary transmitters. In spectrum sharing systems, the interference power levels caused by the SU-transmitters at the primary receivers must not to be larger than some predefined value Q, referred to as the interference temperature. It is assumed that the perfect information of interference channels, φ_i, is available at SU-transmitters. The SU-transmitters can obtain this information, which is also termed as CSI, through various ways such as direct feedback from PU-receiver [23] or from a mediate band manager between the PU-receiver and SU-transmitters [6, 51]. In addition, the opportunistic SU selection strategy is employed herein [6], where SU receiver selects the SU with the maximum SNR value.

Note also that the interference from PUs is not considered in this analysis and the detailed analysis of the operation and protocol between the PU-receiver and SU-transmitters has been already studied in [6, 23, 51]. The interference from PUs can be considered as an additive disturbance which can be modeled as a colored noise source in PBS. Recalling that basic transmitter-receiver chain such disturbances as

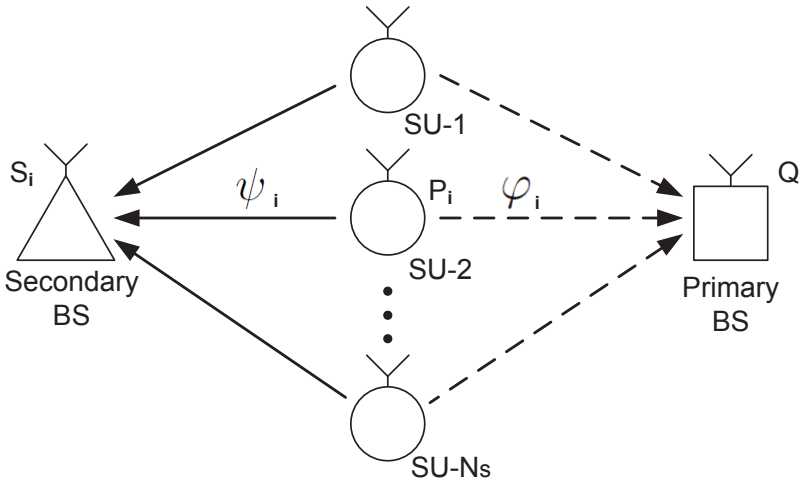

Figure 4.1: System model for CR spectrum sharing systems.

noise and interference are assumed to be added into the signal after the transmit signal is convolved with the channel impulse response. Since the focus of this study is to propose a model for fading statistics of cognitive radio channels, such additive disturbances would not change the analysis of fading statistics. However, as future work, it would be very interesting to observe how the proposed model performs in the presence of interference plus noise from the system capacity perspective. For the rest of the chapter, we will refer to the primary receiver as the primary base-station (PBS) and to the secondary receiver as the secondary base-station (SBS).

4.3 Statistical Background

Radio wave propagation in wireless cognitive channels is a complex phenomenon characterized by three nearly independent phenomena, which are the path-loss variance with distance, shadowing (or long-term fading), and multipath (or short-term) fading. Except path-loss variance, which is only distance dependent, such various effects as fading, reflection, refraction, scattering and shadowing are related to the other two phenomena. Therefore, the majority of the studies in the literature are

considerably devoted to characterizing these effects through the medium of statistical models, which are based on measurements performed for a specific channel environment. Furthermore, these three nearly independent phenomena change according to the communication environment, carrier-frequency and bandwidth. There are numerous channel fading models have been proposed in the literature to statistically model these phenomena with envelope distributions, regarding pretest evaluation of wireless communications systems in general, and of fading mitigation techniques in particular. Briefly, several statistical distributions have been proposed for channel fading modeling under short-term and long-term fading conditions due to the existence of a great variety of fading environments. For instance, short-term fading models include the well-known Rayleigh, Weibull, Rice, and Nakagami-m [41, 49, 55, 58, 75] distributions, while long-term fading models are modeled by the well-known log-normal distribution [27, 65].

In cognitive radio communications, the fading conditions are subject to change according to the environment ξ, in each of which the fading conditions are indexed by the carrier frequency f_c, the bandwidth B and the position X such that $\xi \sim \xi(f_c, B, X)$. The fading can be expressed as follows.

4.3.1 Definition: Hyper-Nakagami-m Fading Distribution

Consider a random variable R which follows the hyper-Nakagami-m fading envelope distribution with a PDF given by

$$f_R(r) = \sum_{k=1}^{N} \frac{2\xi_k}{\Gamma(m_k)} \left(\frac{m_k}{\Omega_k}\right)^{m_k} r^{2m_k-1} \exp\left(-\frac{m_k}{\Omega_k} r^2\right),$$

where, for $1 \leq k \leq N$, the parameters $m_k \geq 0.5$, $\Omega_k > 0$ and $0 \leq \xi_k \leq 1$ are the fading figure, the average power, and the accruing factor of the kth fading environment,

respectively. The accruing factors due to N possible fading environments satisfy the condition:

$$\sum_{k=1}^{N} \xi_k = 1 \ .$$

If the users are subject to the Hyper-Nakagami-m fading, then the distribution of the instantaneous SNR, $\gamma \triangleq R^2/N_0$ in AWGN channels can be directly expressed in terms of average SNR, $\overline{\gamma} \triangleq E\{R^2\}/N_0$ with $E\{\cdot\}$ denoting the expectation operator and N_0 representing the power of AWGN noise. The SNR variable γ is assumed to be hyper-Gamma distributed.

4.3.2 Definition: Hyper-Gamma Fading Power Distribution

The expression of hyper-Gamma distribution of RV γ is given by

$$f_\gamma(r) = \sum_{k=1}^{N} \frac{\xi_k}{\Gamma(m_k)} \left(\frac{m_k}{\overline{\gamma}_k}\right)^{m_k} r^{m_k - 1} \exp\left(-\frac{m_k}{\overline{\gamma}_k} r\right),$$

where $\overline{\gamma}_k > 0$ is the average SNR value.

It is well known that in a communication system the obstructions between the transmitter and the receiver make the system to undergo different types of channel fading such as Rayleigh, Nakagami-m. Moreover, basic effects such as the speed and the motion direction of the user cause the communication channel fading conditions to change even for very short periods of time. In spite of the aforementioned dynamic nature of fading channels, single fading models are mainly used for the analysis of CR systems. However, it is more realistic to use mixture models, which are the weighted combination of different fading distributions [1]. Such a dynamic fading phenomenon is more pronounced in CR channels since the utilized f_c and B can change in addition to the changes in the environment. Therefore, mixture fading models are more

suitable for the analysis of CR channels. As a result, in our system, we use the Hyper-Nakagami-m fading model, in which the CR communication system might undergo a different number of channel fading models such as Rayleigh, Gaussian or Nakagami-3. Let us consider a case where the CR system undergoes four different fading channels ($N = 4$). Assume that the CR system experiences first one-sided Gaussian fading ($m_1 = 0.5$) with accruing factor of $\xi_1 = 0.1361$, then Rayleigh fading ($m_2 = 1$) with accruing factor of $\xi_2 = 0.3319$, and then Nakagami-m fading ($m_3 = 2$) with accruing factor of $\xi_3 = 0.38$, and finally Nakagami-m fading ($m_4 = 3$) with accruing factor of $\xi_4 = 0.152$. Note that based on the simulations, we found that the accruing factors for Rayleigh (i.e., $m = 1$) and for Nakagami-m (i.e., $m = 2$) are higher than the values corresponding to other fading environments such as the one-sided Gaussian fading (i.e., $m = 0.5$). The above case is simulated in Fig. 4.2, which shows the PDF of power for different channel fading models ξ_k with $N = 4$ different environments. It is assumed that the average power for each type of fading is unity. Furthermore, it is well known that the one-sided Gaussian fading and Rayleigh fading are special cases of the Nakagami-m fading.

4.4 Capacity of Spectrum Sharing System

In this system, there are two assumptions for the SU-transmitter power. First, it needs to be within its allowable maximum power constraints. Second, it is not allowed to be higher than the predefined interference temperature value Q, in order not to cause any interference on PU-receiver. When the interference power level P caused by SU-transmitter at the PU-receiver achieves a value larger than Q, an adaptive scheme is used to adjust its value. Therefore, the transmit power of the ith

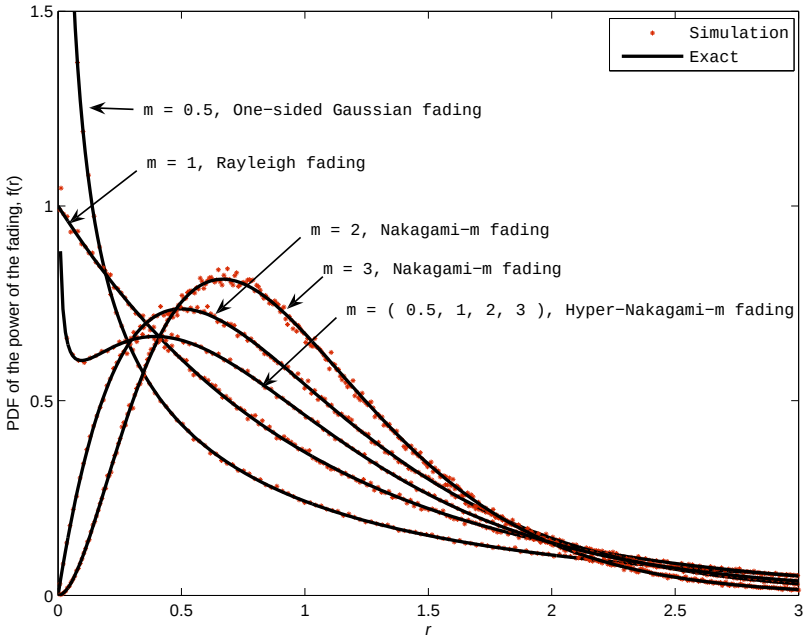

Figure 4.2: Probability density functions of the power of the fading for different values of fading figure m in Nakagami-m fading and Hyper-Nakagami-m fading channels.

secondary user is given by

$$P_i = \begin{cases} P, & \varphi_i \leq \frac{Q}{P} \\ \frac{Q}{\varphi_i}, & \text{otherwise} \end{cases},$$

where φ_i is a hyper-Gamma RV, which represents the distribution for the fading power of the channel between the ith SU and the PBS, and P and Q are the peak power of the SUs and the allowable interference temperature level at the PBS, respectively. Then, the adjusted power P_i is used for sending data from the ith SU to a target SBS. Thus, the received SNR at the target SBS is given by

$$S_i = \begin{cases} \psi_i P, & \varphi_i \leq \frac{Q}{P} \\ \frac{\psi_i}{\varphi_i} Q, & \text{otherwise} \end{cases}, \tag{4.1}$$

where both φ_i and ψ_i are modeled as mutually independent and non identically distributed two hyper-Gamma fading power distributions whose PDFs are given, respectively, by

$$f_{\varphi,\gamma}(r) = \sum_{l=1}^{N} \frac{\xi_{\varphi,l}}{\Gamma(m_{\varphi,l})} \left(\frac{m_{\varphi,l}}{\overline{\gamma}_{\varphi,l}}\right)^{m_{\varphi,l}} r^{m_{\varphi,l}-1} \mathrm{e}^{-\frac{m_{\varphi,l}}{\overline{\gamma}_{\varphi,l}} r} \quad , \tag{4.2}$$

$$f_{\psi,\gamma}(r) = \sum_{k=1}^{N} \frac{\xi_{\psi,k}}{\Gamma(m_{\psi,k})} \left(\frac{m_{\psi,k}}{\overline{\gamma}_{\psi,k}}\right)^{m_{\psi,k}} r^{m_{\psi,k}-1} \mathrm{e}^{-\frac{m_{\psi,k}}{\overline{\gamma}_{\psi,k}} r} \ .$$

The conditional PDF of the received SNR at the target SBS, $f_{S_i}(r|\varphi_i)$ is given by

$$f_{S_i}(r|\varphi_i) = \begin{cases} \sum_{k=1}^{N} \frac{\xi_{\psi,k} r^{m_{\psi,k}-1}}{\Gamma\left(m_{\psi,k}\right)} \left(\frac{m_{\psi,k}}{\overline{\gamma}_{\psi,k} P}\right)^{m_{\psi,k}} \mathrm{e}^{-\frac{m_{\psi,k}}{\overline{\gamma}_{\psi,k} P} r}, & \varphi_i \leq \frac{Q}{P} \\ \sum_{k=1}^{N} \frac{\xi_{\psi,k} r^{m_{\psi,k}-1}}{\Gamma\left(m_{\psi,k}\right)} \left(\frac{m_{\psi,k}}{\overline{\gamma}_{\psi,k}} \frac{\varphi_i}{Q}\right)^{m_{\psi,k}} \mathrm{e}^{-\frac{m_{\psi,k}}{\overline{\gamma}_{\psi,k}} \frac{\varphi_i}{Q} r}, & \varphi_i > \frac{Q}{P} \end{cases} \tag{4.3}$$

Then, the PDF of the received SNR at the target SBS can be obtained as

$$f_{S_i}(r) = \int_0^{\infty} f_{S_i}(r|\varphi_i) \, f_{\varphi_i}(\varphi) \, d\varphi \ . \tag{4.4}$$

Considering the limits of summation in both (4.2) and (4.3) along with the integration interval of (4.4), $f_{S_i}(r)$ is obtained by manipulating the cross terms and given by in

a more simplified form as

$$
\begin{aligned}
f_{S_i}(r) = & \sum_{k=1}^{N}\sum_{l=1}^{N} \frac{\xi_{\psi,k}\xi_{\varphi,l}}{\Gamma(m_{\psi,k})\,\Gamma(m_{\varphi,l})} \left(\frac{m_{\psi,k}}{\overline{\gamma}_{\psi,k}}\frac{1}{P}\right)^{m_{\psi,k}} r^{m_{\psi,k}-1} \\
& \times \left[\exp\left(-\frac{m_{\psi,k}}{\overline{\gamma}_{\psi,k}}\frac{1}{P}r\right)\left\{\Gamma(m_{\varphi,l}) - \Gamma\left(m_{\varphi,l}, \frac{m_{\varphi,l}}{\overline{\gamma}_{\varphi,l}}\frac{Q}{P}\right)\right\}\right. \\
& \left. + \frac{\Gamma\left(m_{\psi,k}+m_{\varphi,l}, \frac{m_{\varphi,l}}{\overline{\gamma}_{\varphi,l}}\frac{Q}{P} + \frac{m_{\psi,k}}{\overline{\gamma}_{\psi,k}}\frac{r}{P}\right)}{\left(\frac{m_{\varphi,l}}{\overline{\gamma}_{\varphi,l}}\frac{Q}{P}\right)^{m_{\psi,k}}\left(1+\frac{m_{\psi,k}\overline{\gamma}_{\varphi,l}}{\overline{\gamma}_{\psi,k}m_{\varphi,l}}\frac{r}{Q}\right)^{m_{\psi,k}+m_{\varphi,l}}}\right],
\end{aligned} \tag{4.5}
$$

where $\Gamma(x,y) = \int_y^\infty t^{x-1}e^{-t}dt$ is the incomplete gamma function. Then, the CDF of S_i is obtained by using

$$
F_{S_i}(r) \triangleq \int_0^r f_{S_i}(r)\,dr. \tag{4.6}
$$

By plugging (4.5) into (4.6) and carrying out the integral, the CDF $F_{S_i}(r)$ is given by

$$
\begin{aligned}
F_{S_i}(r) = & \sum_{k=1}^{N}\sum_{l=1}^{N} \frac{\xi_{\psi,k}\xi_{\varphi,l}}{\Gamma(m_{\psi,k})\,\Gamma(m_{\varphi,l})} \left[\left\{\Gamma(m_{\psi,k}) - \Gamma\left(m_{\psi,k}, \frac{m_{\psi,k}}{\overline{\gamma}_{\psi,k}}\frac{r}{P}\right)\right\}\right. \\
& \left. \times \left\{\Gamma(m_{\varphi,l}) - \Gamma\left(m_{\varphi,l}, \frac{m_{\varphi,l}}{\overline{\gamma}_{\varphi,l}}\frac{Q}{P}\right)\right\} + \left(\frac{m_{\psi,k}\overline{\gamma}_{\varphi,l}}{\overline{\gamma}_{\psi,k}m_{\varphi,l}Q}\right)^{m_{\psi,k}} \int_0^\infty \Xi(u)\,du\right],
\end{aligned}
$$

where the integration is evaluated by the Gauss-Laguerre quadrature rule [2, Eq. (25.4.45)] and $\Xi(u)$ is given by

$$
\Xi(u) = \frac{u^{m_{\psi,k}-1}\Gamma\left(m_{\psi,k}+m_{\varphi,l}, \frac{m_{\varphi,l}}{\overline{\gamma}_{\varphi,l}}\frac{Q}{P} + \frac{m_{\psi,k}}{\overline{\gamma}_{\psi,k}}\frac{u}{P}\right)}{\left(1+\frac{m_{\psi,k}\overline{\gamma}_{\varphi,l}}{\overline{\gamma}_{\psi,k}m_{\varphi,l}}\frac{u}{Q}\right)^{m_{\psi,k}+m_{\varphi,l}}}.
$$

Consequently, the SBS selects an SU transmitter with the best channel quality

among the N_s (number of SUs) SNR values of SU transmitters. The received SNR of the selected SU S_{max} is obtained as

$$S_{max} = \max_{1 \leq i \leq N_s} S_i \tag{4.7}$$

Assuming that every user is equally faded, then the PDF of S_{max} is given by [6]

$$f_{S_{max}}(r) = N_s f_{S_i}(r) F_{S_i}(r)^{N_s - 1} \ , \tag{4.8}$$

and overall average achievable capacity is obtained by

$$\begin{aligned} C &= \mathbb{E}\left[\log_2(1 + S_{max})\right] \\ &= \int_0^\infty \log_2(1 + S_{max}) f_{S_{max}}(r)\, dr \ . \end{aligned} \tag{4.9}$$

Since outage probability is a common performance metric, here we consider the outage probability of S_{max} for different scenarios in terms of the following:

$$f_{S_{max},out}(r_{th}) = \int_0^{r_{th}} f_{S_{max}}(r)\, dr \ .$$

which is the CDF of the maximum received SNR evaluated at the outage threshold r_{th} [dB]. The results for outage probability with respect to number of SUs are given in Fig. 4.3. As expected, the probability of outage saturates as r_{th} increases which implies that the received signal power is weakening. For a specific outage threshold value, increasing the number of SUs results a decrease in the probability of outage, which stems from the effects of multiuser diversity.

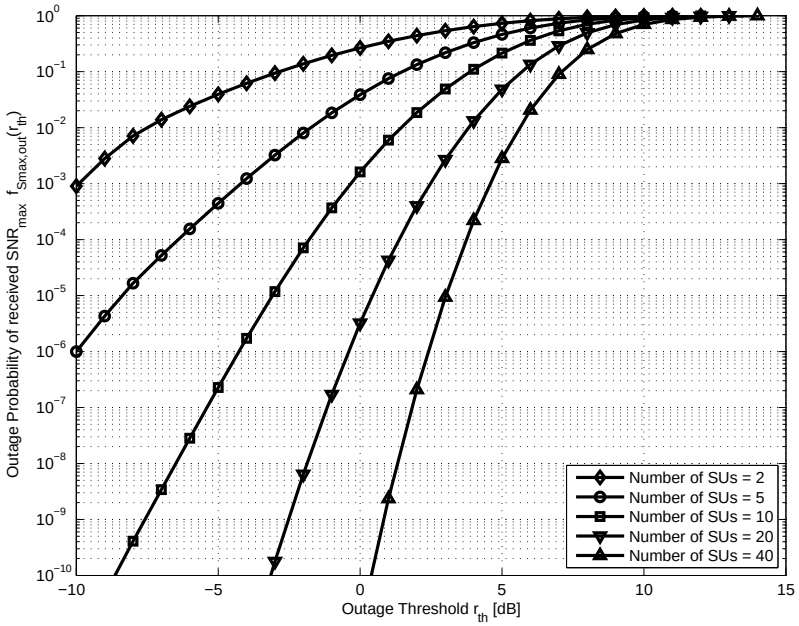

Figure 4.3: Comparison of outage probability of maximum received SNR for different number of SUs (N_s) versus outage threshold in logarithmic scale, when $P = 5$ dB and $Q = 0$ dB.

4.4.1 Low Power Region Analysis

If $P \ll Q$ then the effect of interference temperature level Q disappears. Therefore, the conditional PDF of the received SNR at the target SBS, $f_{S_i}(r|\varphi_i)$ is given by

$$f_{S_i}(r|\varphi_i) = \sum_{k=1}^{N} \frac{\xi_{\psi,k} r^{m_{\psi,k}-1}}{\Gamma(m_{\psi,k})} \left(\frac{m_{\psi,k}}{\overline{\gamma}_{\psi,k} P}\right)^{m_{\psi,k}} \mathrm{e}^{-\frac{m_{\psi,k}}{\overline{\gamma}_{\psi,k} P} r} \ ,$$

Then, the PDF of the received SNR at the target SBS is approximated as

$$f_{S_i}(r) = \sum_{k=1}^{N} \frac{\xi_{\psi,k} r^{m_{\psi,k}-1}}{\Gamma(m_{\psi,k})} \left(\frac{m_{\psi,k}}{\overline{\gamma}_{\psi,k} P}\right)^{m_{\psi,k}} \mathrm{e}^{-\frac{m_{\psi,k}}{\overline{\gamma}_{\psi,k} P} r} \ ,$$

and using (4.4), the corresponding CDF is obtained as

$$F_{S_i}(r) = \sum_{k=1}^{N} \xi_{\psi,k} \left\{ 1 - \frac{1}{\Gamma(m_{\psi,k})} \Gamma\left(m_{\psi,k}, \frac{m_{\psi,k}}{\overline{\gamma}_{\psi,k}} \frac{r}{P} \right) \right\} .$$

The received SNR of the selected secondary user S_{max} is obtained using (4.7). Assuming that every user is equally faded, then the PDF of S_{max} and overall average achievable capacity is obtained using (4.8) and (4.9), respectively.

4.4.2 High Power Region Analysis

If $P \gg Q$, then the conditional PDF of the received SNR at the target SBS, $f_{S_i}(r|\varphi_i)$ is given by

$$f_{S_i}(r|\varphi_i) = \sum_{k=1}^{N} \frac{\xi_{\psi,k}}{\Gamma(m_{\psi,k})} \left(\frac{m_{\psi,k}}{\overline{\gamma}_{\psi,k}} \frac{\varphi_i}{Q} \right)^{m_{\psi,k}} r^{m_{\psi,k}-1} \mathrm{e}^{-\frac{m_{\psi,k}}{\overline{\gamma}_{\psi,k}} \frac{\varphi_i}{Q} r},$$

Then, using (4.4), the PDF of the received SNR at the target SBS is obtained as

$$\begin{aligned} f_{S_i}(r) = & \sum_{k=1}^{N} \sum_{l=1}^{N} \frac{\xi_{\psi,k} \xi_{\varphi,l}}{\Gamma(m_{\psi,k}) \Gamma(m_{\varphi,l})} \left(\frac{m_{\psi,k} \overline{\gamma}_{\varphi,l}}{\overline{\gamma}_{\psi,k} m_{\varphi,l}} \frac{1}{Q} \right)^{m_{\psi,k}} \\ & \times \; r^{m_{\psi,k}-1} \frac{\Gamma\left(m_{\psi,k} + m_{\varphi,l}, \frac{m_{\psi,k}}{\overline{\gamma}_{\psi,k}} \frac{r}{P} \right)}{\left(1 + \frac{m_{\psi,k} \overline{\gamma}_{\varphi,l}}{\overline{\gamma}_{\psi,k} m_{\varphi,l}} \frac{r}{Q} \right)^{m_{\psi,k}+m_{\varphi,l}}} , \end{aligned}$$

Then, using (4.6), the CDF of S_i is obtained as

$$\begin{aligned} F_{S_i}(r) = & \sum_{k=1}^{N} \sum_{l=1}^{N} \frac{\xi_{\psi,k} \xi_{\varphi,l}}{\Gamma(m_{\psi,k}) \Gamma(m_{\varphi,l})} \left(\frac{m_{\psi,k} \overline{\gamma}_{\varphi,l}}{\overline{\gamma}_{\psi,k} m_{\varphi,l}} \frac{1}{Q} \right)^{m_{\psi,k}} \\ & \times \int_0^{\infty} u^{m_{\psi,k}-1} \frac{\Gamma\left(m_{\psi,k} + m_{\varphi,l}, \frac{m_{\psi,k}}{\overline{\gamma}_{\psi,k}} \frac{u}{P} \right)}{\left(1 + \frac{m_{\psi,k} \overline{\gamma}_{\varphi,l}}{\overline{\gamma}_{\psi,k} m_{\varphi,l}} \frac{u}{Q} \right)^{m_{\psi,k}+m_{\varphi,l}}} du . \end{aligned}$$

where the integration can be easily evaluated by Gauss-Laguerre quadrature rule [2].

Consequently, the SBS selects a SU using (4.7). Assuming that every user is equally faded, then the PDF of S_{max} and overall average achievable capacity are obtained using (4.8) and (4.9), respectively.

4.5 Numerical Results and Simulations

The effect of peak power of secondary transmitters on the average capacity is investigated under different values for the number of environments N and interference temperature values Q in Fig. 4.4. These simulations assume the same environment accruing factors ξ, the fading figure values m and average fading power between the SUs and the SBS as given in Fig. 4.2. In addition, the comparison of the hyper-Nakagami-m fading channel model with the Rayleigh fading channel is performed. It is shown that the average capacity increases as the peak power of the secondary transmitters increases for both Rayleigh and Nakagami-m fading as expected. However, unlike the non-spectrum sharing systems the average capacity is here saturated after a certain value of peak power because of the spectrum sharing system opportunistic user selection algorithm [6]. It is seen from the figures that the analytical results agree well with the simulation results.

In Fig. 4.5, the effect of interference temperature on the average capacity is investigated in detail under different values of the number of environments N and peak power of secondary transmitters P, with the same environment accruing factors ξ, the fading figure values m and the average fading power between the SUs and the SBS as given for Fig. 4.2. The comparison of the hyper-Nakagami-m fading channel model with the Rayleigh fading channel is studied as well. Average capacity keeps growing as the interference temperature increases, and this relationship can be easily seen from (4.1) and (4.5) that the selected peak power of SU increases with interference temperature.

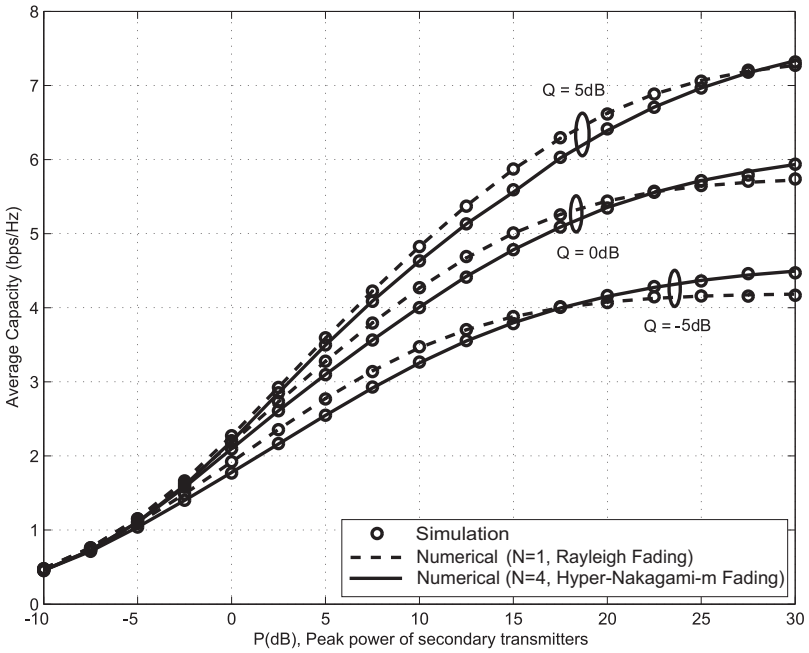

Figure 4.4: Average capacity vs peak power of secondary transmitters P for different Q and N values when $N_s = 30$.

In Figs. 4.4 and 4.5, the number of SUs (N_s) is chosen as 30. Moreover, it can also be inferred from Figs. 4.4 and 4.5 that the capacity over the hyper-Nakagami-m channel achieves higher values than in the Rayleigh fading channel after some certain values of P and Q (see Figs. 4.4 and 4.5). This observation can be justified by (4.5), which shows that as P increases, the high power region ($P \gg Q$) becomes present. In this region, as P increases the incomplete gamma function part of (4.5) goes to zero when $r < P$. In other words, it can be deduced that the SNR at the SUs becomes negatively skewed, and the average power increases. Note that an increase in average power means that there is a decrease in outage probability and finally an increase in capacity. Nevertheless, when $P < Q$ the PDF of SNR will be different than zero for $r < P$, and the average power decreases. Note also that decrease in average power means that there is an increase in outage probability and finally a

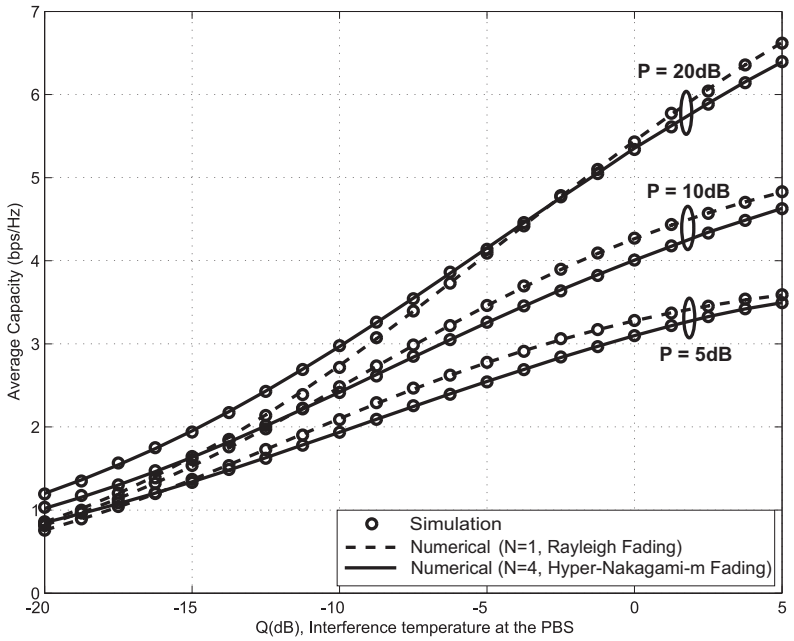

Figure 4.5: Average capacity vs interference temperature Q, at the PBS for different P and N values when $N_s = 30$.

decrease in capacity.

Figs. 4.6 and 4.7 show the average capacity versus the fading figure of the channel between the SUs and the PBS (m_φ) and the fading figure of the channel between the SUs and the SBS (m_ψ), respectively, with $P = 15$ dB, $Q = 0$ dB and Nakagami-m fading channel ($N = 1$). The effect of number of SUs (N_s) is also investigated for the values $N_s = 5, 20$ and 40. As N_s increases the capacity increases as well, which can be observed from (4.8). In Fig. 4.6, with the constant values of m_ψ (i.e., $\mathrm{m}_\psi = 1$ and 2) the average capacity decreases as the value of the m_φ increases, which can be inferred from (4.5) that the received SNR at the target SBS is reduced. More interestingly, it is observed that there is only slight difference on average capacity while m_ψ increases for constant the values of m_φ in Fig. 4.7. The capacity saturates after certain values of m_ψ. From this result, it can be concluded that, since the

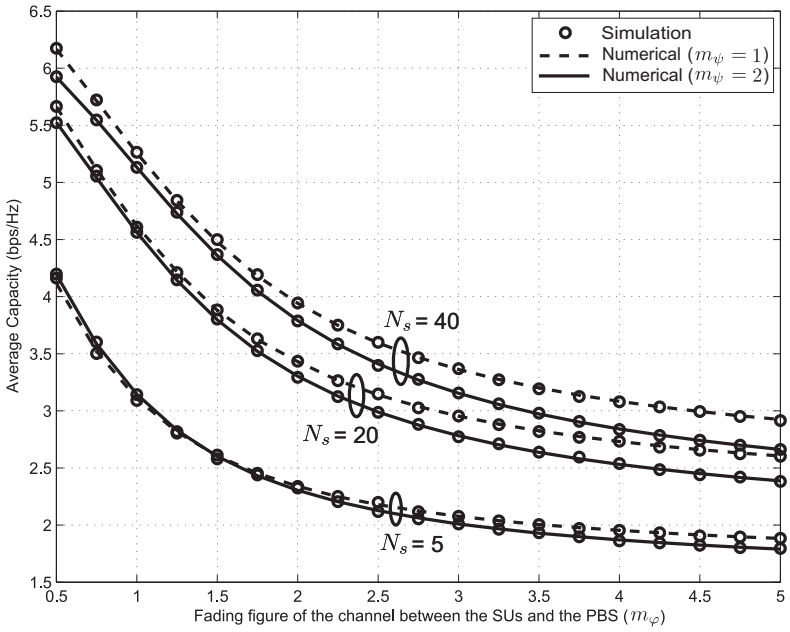

Figure 4.6: Average capacity vs fading figure of the channel between the SUs and the PBS m_φ for different N_s values and fading figure of the channel between the SUs and the SBS m_ψ (1 and 2) when $P = 15$ dB and $Q = 0$ dB.

fading figure describes the diversity of the channel, diversity techniques at the SBS do not contribute significantly to the system performance gain. This is one of the important results observed in this work.

Figs. 4.8 and 4.9 show the average capacity versus the average fading power between the SUs and the SBS ($\overline{\gamma}_\psi$) and the average fading power between the SUs and the PBS ($\overline{\gamma}_\varphi$), respectively, for different N_s values with $P = 15$ dB, $Q = 0$ dB, and hyper-Nakagami-m fading channel with $N = 4$. The same environment accruing factors ξ, the fading figure values m and the average fading power between the SUs and the SBS are used as in Fig. 4.2. The same effect of N_s is observed in Figs. 4.8 and 4.9 as expected, since the capacity increases as N_s increases. In Fig. 4.8, as the $\overline{\gamma}_\psi$ increases while keeping the $\overline{\gamma}_\varphi$ with two constant values (i.e., $\overline{\gamma}_\varphi = 1$ and 2) the average capacity increases as well. However, for high values of $\overline{\gamma}_\psi$ this increase

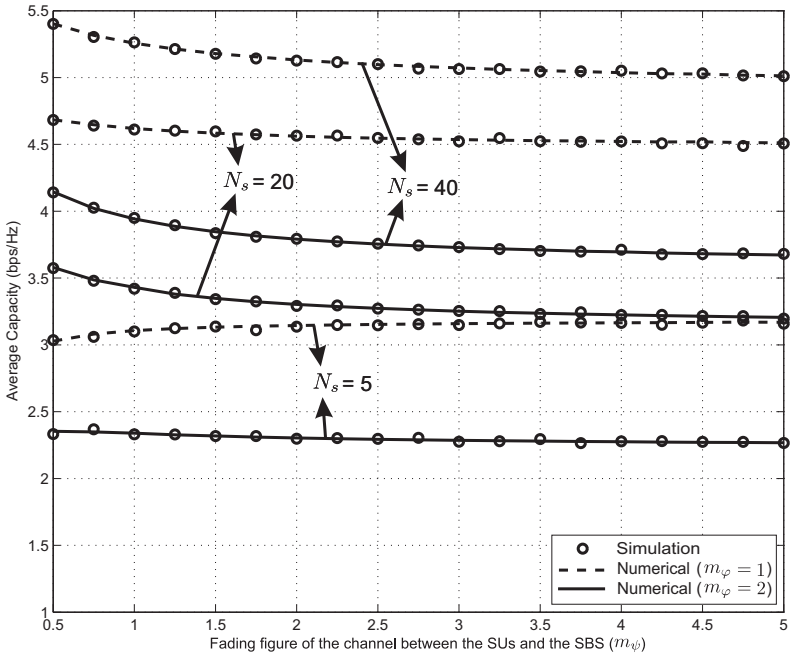

Figure 4.7: Average capacity vs fading figure of the channel between the SUs and the SBS m_ψ for different N_s values and fading figure of the channel between the SUs and the PBS m_φ (1 and 2) when $P = 15$ dB and $Q = 0$ dB.

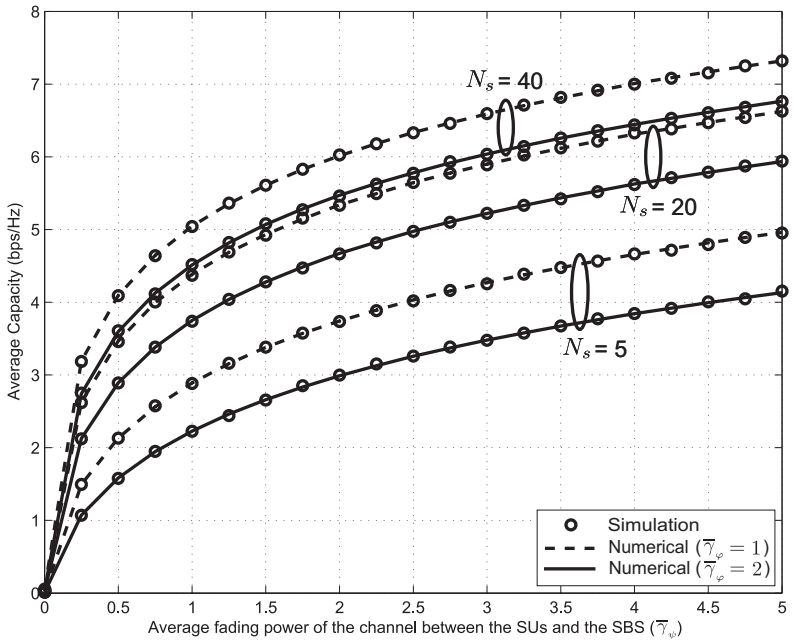

Figure 4.8: Average capacity vs average fading power between the SUs and the SBS $\overline{\gamma}_\psi$ for different N_s values and average fading power between the SUs and the PBS $\overline{\gamma}_\varphi$ (1 and 2) when $P = 15$ dB and $Q = 0$ dB and $N = 4$.

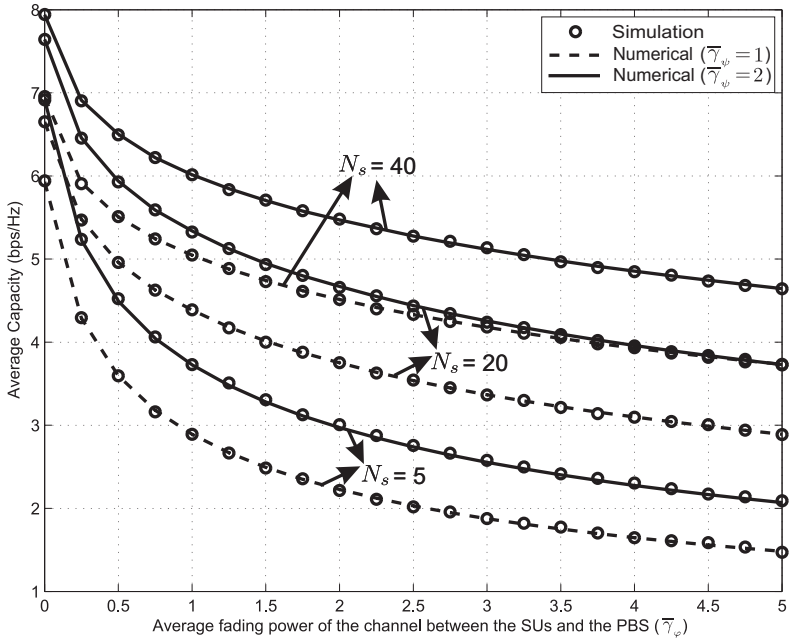

Figure 4.9: Average capacity vs average fading power between the SUs and the PBS $\overline{\gamma}_\varphi$ for different N_s values and average fading power between the SUs and the SBS $\overline{\gamma}_\psi$ (1 and 2) when $P = 15$ dB and $Q = 0$ dB and $N = 4$.

reduces. In addition, the effect of $\overline{\gamma}_{\varphi}$ on average capacity is also investigated in Fig. 4.9 for the two constant values of $\overline{\gamma}_{\psi}$ (i.e., $\overline{\gamma}_{\psi} = 1$ and 2). It is seen from Fig. 4.9 that the capacity decreases as $\overline{\gamma}_{\varphi}$ increases for constant values of $\overline{\gamma}_{\psi}$. These results can be easily inferred from (4.5) in the sense that an increase in $\overline{\gamma}_{\varphi}$ decreases the capacity while an increase in $\overline{\gamma}_{\psi}$ increases the capacity.

4.6 Summary

In this chapter, a theoretical fading model that fits to the dynamic nature of spectrum sharing systems is proposed. The PDF and CDF of the SNR of the SU transmitters at SU receiver along with the PDF of the SU with the highest SNR are derived in closed-forms. The achievable capacity of SU in a spectrum sharing system is derived for both high and low power regions. The analytical and simulation results are presented to study the effects of fading symmetry and asymmetry in terms of the fading figure and the average power, the number of SUs, and the interference temperature on the capacity of SU in such systems. In spectrum sharing systems, it is observed that the fading figure of the channel between the SUs and the PBS m_{φ} which describes the diversity of the channel does not affect the achievable capacity of the channel significantly. The results show that the proposed model is a promising model that can represent a wide variety of fading models for CR systems.

5. CONCLUSIONS AND FUTURE DIRECTIONS

In this dissertation, an OFDM-based CR network with spectrum sharing feature was investigated under the assumption of random subcarrier allocation (random access) and no availability of spectrum sensing information at the secondary (cognitive) network. The assumption of absence of sensing information is due to the challenges and implementation issues in the spectrum sensing mechanism, which make such spectrum sensing information unreliable and misleading.

First, the set-up of multiple users (SUs and PUs) in a single cell was considered. The performance analysis was carried out in terms of different aspects. In particular, the expressions for the SU average capacity and the related upper and lower bounds, the PDF and CDF of instantaneous SU capacity were derived, and the asymptotic analysis of multiuser diversity gain and the proposed centralized random subcarrier scheduling algorithm were studied. Furthermore, the centralized subcarrier allocation algorithm assumed random and sequential access mechanisms to assure that the assigned SUs' subcarrier sets are orthogonal to each other similar to the PUs' subcarriers in the primary network.

Next, the random access scheme when the SUs belong to different cells was investigated, where inter-cell subcarrier collisions occur between the SUs' subcarriers. In other words, there can be subcarrier collisions between not only subcarriers of SUs and PUs but also among SUs' subcarriers. The PMFs and the expected values of the number of subcarrier collisions between the SUs' and PU's subcarriers were derived under the assumption of fixed and random number of subcarriers requirements for each user.

Finally, we proposed a theoretical fading model that fits the dynamic nature

of CR systems, termed hyper-fading, and which is considered in a point-to-point communication scenario with single PU receiver and multiple SUs (transmitter), and where an opportunistic scheduling is employed to benefit from multiuser diversity gain.

Some of the potential future research directions that are worthy of further investigation are:

- Since bit error rate (BER) is a common performance measure, one can further investigate the performance limits of the proposed random access scheme in terms of BER.

- The random access scheme can be compared with the scenario when there is spectrum sensing information available at the secondary network, i.e., PUs' spectrum occupancy information is available at the SUs. This will provide deeper insights about the performance of the proposed random access scheme.

- In the proposed centralized random and sequential subcarrier allocation algorithm, the equal number of subcarrier requirements for both SUs and PUs is assumed. The algorithm can be further improved by considering more practical cases, where the users (SUs and PUs) can request different numbers of subcarriers based on their rate requirements.

REFERENCES

[1] A. Abdi, W. C. Lau, M.-S. Alouini, and M. Kaveh. A new simple model for land mobile satellite channels: first-and second-order statistics. *IEEE Transactions on Wireless Communications*, 2(3):519–528, 2003.

[2] M. Abramowitz and I. A. Stegun. *Handbook of Mathematical Functions with Formulas, Graphs, and Mathematical Tables*. Dover publications, 1964.

[3] I. F. Akyildiz, W. Y. Lee, M. C. Vuran, and S. Mohanty. NeXt generation/dynamic spectrum access/cognitive radio wireless networks: a survey. *Computer Networks*, 50(13):2127–2159, 2006.

[4] S. Al-Ahmadi and H. Yanikomeroglu. On the approximation of the generalized-k distribution by a gamma distribution for modeling composite fading channels. *IEEE Transactions on Wireless Communications*, 9(2):706–713, 2010.

[5] M.-S. Alouini, A. Abdi, and M. Kaveh. Sum of gamma variates and performance of wireless communication systems over nakagami-fading channels. *IEEE Transactions on Vehicular Technology*, 50(6):1471–1480, 2001.

[6] T. W. Ban, W. Choi, B. C. Jung, and D. K. Sung. Multi-user diversity in a spectrum sharing system. *IEEE Transactions on Wireless Communications*, 8(1):102–106, 2009.

[7] R. Bosisio and U. Spagnolini. Interference coordination vs. interference randomization in multicell 3gpp lte system. In *IEEE Wireless Communications and Networking Conference (WCNC)*, pages 824–829, 2008.

[8] R. R. Chen, K. H. Teo, and B. Farhang-Boroujeny. Random access protocols for collaborative spectrum sensing in multi-band cognitive radio networks. *IEEE Journal of Selected Topics in Signal Processing*, 5(1):124–136, 2011.

[9] C. A. Coelho. The generalized integer gamma distribution: a basis for distributions in multivariate statistics. *Journal of Multivariate Analysis*, 64(1):86–102, 1998.

[10] H. A. David and H. N. Nagaraja. *Order Statistics*. Wiley Online Library, 2003.

[11] M. Dohler and M. Arndt. Inverse incomplete gamma function and its application. *Electronics Letters*, 42(1):35–6, 2006.

[12] D. Duan, L. Yang, and J. C. Principe. Cooperative diversity of spectrum sensing for cognitive radio systems. *IEEE Transactions on Signal Processing*, 58(6):3218–3227, 2010.

[13] S. Ekin, M. M. Abdallah, K. A. Qaraqe, and E. Serpedin. On ofdm-based cognitive radio spectrum sharing systems with random access. In *IEEE Wireless Advanced*, June 2012.

[14] S. Ekin, M. M. Abdallah, K. A. Qaraqe, and E. Serpedin. Random subcarrier allocation in ofdm-based cognitive radio networks. *IEEE Transactions on Signal Processing*, 60(9):4758–4774, Sept. 2012.

[15] S. Ekin, M. M. Abdallah, K. A. Qaraqe, and E. Serpedin. A study on inter-cell subcarrier collisions due to random access in ofdm-based cognitive radio networks. *IEEE Transactions on Communications*, 2012. (under review).

[16] S. Ekin, F. Yilmaz, H. Celebi, K. A. Qaraqe, M.-S. Alouini, and E. Serpedin. Achievable capacity of a spectrum sharing system over hyper fading channels. In

IEEE Global Telecommunications Conference (GLOBECOM), pages 1–6, Dec. 2009.

[17] S. Ekin, F. Yilmaz, H. Celebi, K. A. Qaraqe, M.-S. Alouini, and E. Serpedin. Capacity limits of spectrum-sharing systems over hyper-fading channels. *Wireless Communications and Mobile Computing*, 12(16):1471–1480, Nov. 2012.

[18] S. E. Elayoubi, O. Ben Haddada, and B. Fourestie. Performance evaluation of frequency planning schemes in ofdma-based networks. *IEEE Transactions on Wireless Communications*, 7(5):1623–1633, 2008.

[19] Federal Communications Commission (FCC). Facilitating opportunities for flexible, efficient, and reliable spectrum use employing cognitive radio technologies. Technical Report ET Docket No. 03-108, Mar. 2005.

[20] M. Gastpar. On capacity under received-signal constraints. In *Proceedings of the 42nd Annual Allerton Conference on Communication, Control and Computing*, 2004.

[21] M. Gastpar. On capacity under receiver and spatial spectrum-sharing constraints. *IEEE Transactions on Information Theory*, 53(2):471–487, Feb. 2007.

[22] J. E. Gentle. *Random Number Generation and Monte Carlo Methods*. Springer Verlag, 2003.

[23] A. Ghasemi and E. S. Sousa. Fundamental limits of spectrum-sharing in fading environments. *IEEE Transactions on Wireless Communications*, 6(2):649–658, 2007.

[24] A. Goldsmith. *Wireless Communications*. Cambridge Univ. Pr., 2005.

[25] I. S. Gradshteuin, I. M. Ryzhik, and A. Jeffrey. *Table of Integrals, Series, and Products*. Academic Pr., 2007.

[26] K. Hamdi, W. Zhang, and K. Letaief. Opportunistic spectrum sharing in cognitive mimo wireless networks. *IEEE Transactions on Wireless Communications*, 8(8):4098–4109, 2009.

[27] F. Hansen and F. I. Meno. Mobile fading-Rayleigh and lognormal superimposed. *IEEE Transactions on Vehicular Technology*, 26(4):332–335, 1977.

[28] S. Haykin. Cognitive radio: brain-empowered wireless communications. *IEEE Journal on Selected Areas in Communications*, 23(2):201–220, 2005.

[29] J. P. Hong and W. Choi. Throughput characteristics by multiuser diversity in a cognitive radio system. *IEEE Transactions on Signal Processing*, (99):1–1, 2011.

[30] C. S. Hwang and J. M. Cioffi. Achieving Multi-user Diversity Gain using User-Identity Feedback. *IEEE Transactions on Wireless Communications*, 7(8):2911–2916, 2008.

[31] S. A. Jafar and S. Srinivasa. Capacity limits of cognitive radio with distributed and dynamic spectral activity. *IEEE Journal on selected Areas in Communications*, 25(3):529–537, 2007.

[32] Y. U. Jang. Performance analysis of cognitive radio networks based on sensing and secondary-to-primary interference. *IEEE Transactions on Signal Processing*, (99):1–1, 2011.

[33] J. Ji, W. Chen, H. Wan, and Y. Liu. Capacity analysis of multicast network in spectrum sharing systems. In *IEEE International Conference on Communications (ICC)*, 2010.

[34] K. Josiam and D. Rajan. Multiuser diversity in wireless networks: A diversity-multiplexing perspective. In *41st Annual Conference on Information Sciences and Systems (CISS)*, 2007.

[35] A. Jovicic and P. Viswanath. Cognitive radio: An information-theoretic perspective. In *IEEE International Symposium on Information Theory (ISIT)*, 2006.

[36] X. Kang, Y. C. Liang, A. Nallanathan, H. K. Garg, and R. Zhang. Optimal power allocation for fading channels in cognitive radio networks: Ergodic capacity and outage capacity. *IEEE Transactions on Wireless Communications*, 8(2):940–950, 2009.

[37] G. K. Karagiannidis, N. C. Sagias, and T. A. Tsiftsis. Closed-form statistics for the sum of squared nakagami-m variates and its applications. *IEEE Transactions on Communications*, 54(8):1353–1359, 2006.

[38] S. H. Kim, B. C. Jung, and D. K. Sung. Effect of other-cell interference on multiuser diversity in cellular networks. In *IEEE ISCIT*, 2007.

[39] D. E. Knuth. Big omicron and big omega and big theta. *ACM Sigact News*, 8(2):18–24, 1976.

[40] D. Li. Performance analysis of uplink cognitive cellular networks with opportunistic scheduling. *IEEE Communications Letters*, 14(9):827–829, 2010.

[41] J. Lieblein. On moments of order statistics from the Weibull distribution. *The Annals of Mathematical Statistics*, 26(2):330–333, June 1955.

[42] A. M. Mathai. Storage capacity of a dam with gamma type inputs. *Annals of the Institute of Statistical Mathematics*, 34(1):591–597, 1982.

[43] M. A. McHenry, D. McCloske, D. Roberson, and J. T. MacDonald. Spectrum occupancy measurements in chicago, illinois. Technical report, Shared Spectrum Company and IIT Wireless Interference Lab Illinois Institute of Technology, Nov. 2005.

[44] J. Mitola III and G. Q. Maguire Jr. Cognitive radio: making software radios more personal. *IEEE Personal Communications*, 6(4):13–18, 1999.

[45] P. G. Moschopoulos. The distribution of the sum of independent gamma random variables. *Annals of the Institute of Statistical Mathematics*, 37(1):541–544, 1985.

[46] L. Musavian and S. Aissa. Ergodic and outage capacities of spectrum-sharing systems in fading channels. In *IEEE Global Telecommunications Conference (GLOBECOM)*, 2007.

[47] L. Musavian and S. Aïssa. Fundamental capacity limits of cognitive radio in fading environments with imperfect channel information. *IEEE Transactions on Communications*, 57(11):3472–3480, 2009.

[48] C. N. Georghiades N. Rahiminan, H. Celebi and K. A. Qaraqe. A probabilistic model of spectrum availability for ofdma based cognitive radio systems. *to appear in IEEE Communication Letters*, 2012.

[49] M. Nakagami. The m-distribution: A general formula of intensity distribution of rapid fading. *Statistical Methods in Radio Wave Propagation*, pages 3–36, 1960.

[50] A. Papoulis and S. U. Pillai. *Probability, Random Variables and Stochastic Processes*. McGraw Hill, 2002.

[51] J. M. Peha. Approaches to spectrum sharing. *IEEE Communications Magazine*, 43(2):10–12, 2005.

[52] K. A. Qaraqe, S. Ekin, T. Agarwal, and E. Serpedin. Performance analysis of cognitive radio multiple-access channels over dynamic fading environments. *Wireless Personal Communications*, pages 1–15, 2011.

[53] Z. Rezki and M.-S. Alouini. Ergodic capacity of cognitive radio under imperfect channel-state information. *IEEE Transactions on Vehicular Technology*, 61(5):2108–2119, 2012.

[54] J. A. Rice. *Mathematical Statistics and Data Analysis*. Thomson Learning, 2006.

[55] N. C. Sagias, G. K. Karagiannidis, D. A. Zogas, P. T. Mathiopoulos, and G. S. Tombras. Performance analysis of dual selection diversity in correlated Weibull fading channels. *IEEE Transactions on Communications*, 52(7):1063–1067, 2004.

[56] U. Salim and D. Slock. Multi-user diversity gain for oblivious and informed users in downlink channels. In *IEEE Wireless Communications and Networking Conference (WCNC)*, pages 1–6, Apr. 2002.

[57] C. H. Sim. Point processes with correlated gamma interarrival times. *Statistics & probability letters*, 15(2):135–141, 1992.

[58] M. K. Simon and M.-S. Alouini. *Digital Communication over Fading Channels*. New York:Wiley-Interscience, 2nd edition, 2004.

[59] M. D. Springer. *The Algebra of Random Variables*. Wiley New York, 1979.

[60] H. A. Suraweera, J. Gao, P. J. Smith, M. Shafi, and M. Faulkner. Channel Capacity Limits of Cognitive Radio in Asymmetric Fading Environments. In *IEEE International Conference on Communications (ICC)*, pages 4048–4053, 2008.

[61] H. A. Suraweera, P. J. Smith, and J. Armstrong. Outage probability of cooperative relay networks in nakagami-m fading channels. *IEEE Communications Letters*, 10(12):834–836, 2006.

[62] H. A. Suraweera, P. J. Smith, and M. Shafi. Capacity limits and performance analysis of cognitive radio with imperfect channel knowledge. *IEEE Transactions on Vehicular Technology*, 59(4):1811–1822, 2010.

[63] Z. Tian and G. B. Giannakis. Compressed sensing for wideband cognitive radios. In *IEEE International Conference on Acoustics, Speech and Signal Processing (ICASSP)*, 2007.

[64] D. N. C. Tse and P. Viswanath. *Fundamentals of Wireless Communication*. Cambridge Univ Pr., 2005.

[65] G. L. Turin, F. D. Clapp, T. L. Johnston, S. B. Fine, and D. Lavry. A statistical model of urban multipath propagation. *IEEE Transactions on Vehicular Technology*, 21(1):1–9, 1972.

[66] A. H. Van Tuyl. Acceleration of convergence of a family of logarithmically convergent sequences. *Mathematics of Computation*, 63:229–229, 1994.

[67] P. Viswanath, D. N. C. Tse, and R. Laroia. Opportunistic beamforming using dumb antennas. *IEEE Transactions on Information Theory*, 48(6):1277–1294, 2002.

[68] J. Wagner, Y. Liang, and R. Zhang. On the balance of multiuser diversity and spatial multiplexing gain in random beamforming. *IEEE Transactions on Wireless Communications*, 7(7):2512–2525, 2008.

[69] L. Wasserman. *All of Statistics: a Concise Course in Statistical Inference*. Springer Verlag, 2004.

[70] F. Yilmaz and M.-S. Alouini. An mgf-based capacity analysis of equal gain combining over fading channels. In *IEEE 21st International Symposium on Personal Indoor and Mobile Radio Communications (PIMRC)*, 2010.

[71] T. Yucek and H. Arslan. A survey of spectrum sensing algorithms for cognitive radio applications. *IEEE Communications Surveys & Tutorials*, 11(1):116–130, 2009.

[72] R. Zhang. On peak versus average interference power constraints for protecting primary users in cognitive radio networks. *IEEE Transactions on Wireless Communications*, 8(4):2112–2120, 2009.

[73] R. Zhang, S. Cui, and Y. C. Liang. On ergodic sum capacity of fading cognitive multiple-access and broadcast channels. *IEEE Transactions on Information Theory*, 55(11):5161–5178, 2009.

[74] R. Zhang and Y. C. Liang. Investigation on multiuser diversity in spectrum sharing based cognitive radio networks. *IEEE Communications Letters*, 14(2):133–135, 2010.

[75] D. Zwillinger and S. Kokoska. *CRC Standard Probability and Statistics Tables and Formulae*. CRC Press, 31th edition, 2002.

APPENDIX A

PROOF OF THEOREM 1

According to *Definition* 5, to evaluate the average of sum capacity of the SU with subcarrier collisions, we have to average *a random sum of RVs* with the set of i.i.d. RVs $C_{m,i}^{I,n}$ and $C_{m,i}^{NI}$ as follows:

$$\begin{aligned}
\mathbb{E}\left[C_m^1\right] &= \mathbb{E}\left[\sum_{i=1}^{k_{nm}} C_{m,i}^{I,n} + \sum_{i=1}^{k_{fm}} C_{m,i}^{NI}\right] \\
&= \mathbb{E}\left[\mathbb{E}\left[\sum_{i=1}^{k_{nm}} C_{m,i}^{I,n}\middle| K_{nm} = k_{nm}\right]\right] + \mathbb{E}\left[\mathbb{E}\left[\sum_{i=1}^{k_{fm}} C_{m,i}^{NI}\middle| K_{fm} = k_{fm}\right]\right] \\
&= \mathbb{E}\left[\sum_{i=1}^{k_{nm}} \mathbb{E}\left[C_{m,i}^{I,n}\right]\right] + \mathbb{E}\left[\sum_{i=1}^{k_{fm}} \mathbb{E}\left[C_{m,i}^{NI}\right]\right] \\
&= \mathbb{E}\left[k_{nm}\mathbb{E}\left[C_{m,i}^{I,n}\right]\right] + \mathbb{E}\left[k_{fm}\mathbb{E}\left[C_{m,i}^{NI}\right]\right],
\end{aligned}$$

where *the rule of iterated expectations* [69, p. 55, Theorem 3.24] also known as *tower rule*, $\mathbb{E}[X] = \mathbb{E}[\mathbb{E}[X|Y]]$, is applied, and the conditional expectations with respect to $k_{nm} \sim \texttt{HYPG}(F_m^S,\ F_n^P,\ F)$ and $k_{fm} \sim \texttt{HYPG}(F_m^S,\ F - F_n^P,\ F)$ are used.

Furthermore, k_{nm} and $C_{m,i}^{I,n}$ are independent, and so are k_{fm} and $C_{m,i}^{NI}$. Then, we have

$$\mathbb{E}\left[C_m^1\right] = \mathbb{E}\left[k_{nm}\right]\mathbb{E}\left[C_{m,i}^{I,n}\right] + \mathbb{E}\left[k_{fm}\right]\mathbb{E}\left[C_{m,i}^{NI}\right].$$

It is also worth to note the relation between the two sums in the first equality that they are independent conditioned with the given k_{nm} and k_{fm} (since $k_{fm} = F_m^S - k_{nm}$).

Taking into account the means of k_{nm} for $n \in [1, N]$ and k_{fm}, it follows that

$$\mathbb{E}\left[k_{nm}\right] = \frac{F_m^S F_n^P}{F},$$

and

$$\mathbb{E}\left[k_{fm}\right] = \frac{F_m^S (F - F_n^P)}{F},$$

which yield the desired result.

APPENDIX B

PROOF OF COROLLARY 1

Following the same approach as in Appendix A, the average capacity in presence of N PUs can be obtained by using (2.12) and the properties of multivariate hypergeometric distribution given in (2.1) with the means of k_{nm} and k_{fm} expressed as

$$\mathbb{E}\left[k_{nm}\right] = \frac{F_m^S F_n^P}{F},\ n = 1, \ldots, N,$$

and

$$\mathbb{E}\left[k_{fm}\right] = \frac{F_m^S}{F}\left(F - \sum_{n=1}^{N} F_n^P\right)$$

.

APPENDIX C

PROOF OF COROLLARY 4

Let $\chi_1 = F_n^P \left(\mathbb{E}\left[C_{m,i}^{I,n}\right] - \mathbb{E}\left[C_{m,i}^{NI}\right] \right)$ and $\chi_2 = \mathbb{E}\left[C_{m,i}^{NI}\right]$, then we have

$$C_{m,F}^{avg} = \mathbb{E}\left[C_m^1\right] = \frac{F_m^S}{F}\chi_1 + F_m^S\chi_2$$

.

Using *Definition* 2, one can show that

$$\lim_{F\to\infty} \frac{\left|\Delta C_{m,F+1}^{avg}\right|}{\left|\Delta C_{m,F}^{avg}\right|} = \lim_{F\to\infty} \frac{\left|\frac{F_m^S}{F+2}\chi_1 + F_m^S\chi_2 - \frac{F_m^S}{F+1}\chi_1 - F_m^S\chi_2\right|}{\left|\frac{F_m^S}{F+1}\chi_1 + F_m^S\chi_2 - \frac{F_m^S}{F}\chi_1 - F_m^S\chi_2\right|} = 1,$$

and

$$\lim_{F\to\infty} \frac{\left|C_{m,F+1}^{avg} - F_m^S\chi_2\right|}{\left|C_{m,F}^{avg} - F_m^S\chi_2\right|} = \lim_{F\to\infty} \frac{\left|\frac{F_m^S}{F+1}\chi_1 + F_m^S\chi_2 - F_m^S\chi_2\right|}{\left|\frac{F_m^S}{F}\chi_1 + F_m^S\chi_2 - F_m^S\chi_2\right|} = 1.$$

Hence, $C_{m,F}^{avg}$ is *logarithmically* convergent to $F_m^S\mathbb{E}\left[C_{m,i}^{NI}\right]$ as $F \to \infty$.

APPENDIX D

EVALUATION OF LIMIT IN EQUATION (2.27)

In the evaluation steps (below), since $f_{C_m^1}(x) \to 0$ and $F_{C_m^1}(x) \to 1$ as $x \to \infty$, first, L'Hopital's rule is applied, and then due to the uniform convergence and the positive terms, the interchange of *limit* and *infinite sum* is viable. Lastly, because the resulting expression is of polynomial type, only the highest-order terms are considered.

$$
\begin{aligned}
\lim_{x\to\infty} \frac{1-F_{C_m^1}(x)}{f_{C_m^1}(x)} &= \lim_{x\to\infty} \frac{1-\mathcal{Q}\sum_{k=0}^{\infty}\delta_k \mathcal{P}\left(\Delta+k, \frac{x}{\hat{\beta}_{\min}}\right)}{\mathcal{Q}\sum_{k=0}^{\infty}\delta_k \frac{x^{(\Delta+k-1)}e^{-x/\hat{\beta}_{\min}}}{\hat{\beta}_{\min}^{\Delta+k}\ \Gamma(\Delta+k)}U(x)} \\
&= \lim_{x\to\infty} \frac{1-\mathcal{Q}\sum_{k=0}^{\infty}\delta_k \left[1-\frac{\Gamma\left(\Delta+k, \frac{x}{\hat{\beta}_{\min}}\right)}{\Gamma(\Delta+k)}\right]}{\mathcal{Q}\sum_{k=0}^{\infty}\frac{\delta_k x^{\Delta+k-1}e^{-x/\hat{\beta}_{\min}}}{\hat{\beta}_{\min}^{\Delta+k}\ \Gamma(\Delta+k)}U(x)} \\
&= \lim_{x\to\infty} \left[\lim_{l_k\to\infty} \frac{-\mathcal{Q}\sum_{k=0}^{l_k}\delta_k \frac{x^{\Delta+k-1}e^{-x/\hat{\beta}_{\min}}}{\hat{\beta}_{\min}^{\Delta+k}\ \Gamma(\Delta+k)}}{\mathcal{Q}\sum_{k=0}^{l_k}\frac{\delta_k\ e^{-x/\hat{\beta}_{\min}}}{\hat{\beta}_{\min}^{\Delta+k}\ \Gamma(\Delta+k)}\left[(\Delta+k-1)x^{\Delta+k-2}-\frac{x^{\Delta+k-1}}{\hat{\beta}_{\min}}\right]}\right] \\
&= \lim_{x\to\infty} \left[\lim_{l_k\to\infty} \frac{-\frac{\delta_{l_k}x^{\Delta+l_k-1}}{\hat{\beta}_{\min}^{\Delta+l_k}\ \Gamma(\Delta+l_k)}}{\frac{\delta_{l_k}}{\hat{\beta}_{\min}^{\Delta+l_k}\ \Gamma(\Delta+l_k)}\left[(\Delta+l_k-1)x^{\Delta+l_k-2}-\frac{x^{\Delta+l_k-1}}{\hat{\beta}_{\min}}\right]}\right] \\
&= \lim_{x\to\infty}\lim_{l_k\to\infty} \frac{-x^{\Delta+l_k-1}}{(\Delta+l_k-1)x^{\Delta+l_k-2}-\frac{x^{\Delta+l_k-1}}{\hat{\beta}_{\min}}} \\
&= \hat{\beta}_{\min} > 0.
\end{aligned}
$$

APPENDIX E

PROOF OF PROPOSITION 2

Recall from (2.1) that the PMF of first SU is given by

$$p(\mathbf{k}_1) = \left[\binom{F_f}{k_{f1}} \prod_{n=1}^{N} \binom{F_n^P}{k_{n1}} \right] \Big/ \binom{F}{F_1^S}.$$

Assuming the orthogonality between subcarriers, given $\mathbf{k}_1$, the conditional PMF of second SU is a multivariate hypergeometric distribution, described by

$$p(\mathbf{k}_2 \big| \mathbf{k}_1) = \left[\binom{F_f - k_{f1}}{k_{f2}} \prod_{n=1}^{N} \binom{F_n^P - k_{n1}}{k_{n2}} \right] \Big/ \binom{F - \mathbf{1}^{\mathrm{T}}\mathbf{k}_1}{F_2^S},$$

where $\mathbf{1}^{\mathrm{T}} = [1, 1, \ldots, 1]^{\mathrm{T}} \in \mathbb{Z}^{N+1}$ and $\mathbf{1}^{\mathrm{T}}\mathbf{k}_1 = \sum_{n=1}^{N} k_{n1} + k_{f1} = F_1^S$. Similarly, for the third SU the conditional PMF for the number of subcarrier collisions is

$$p\left(\mathbf{k}_3 \big| \mathbf{k}_1, \mathbf{k}_2\right) = \left[\binom{F_f - k_{f1} - k_{f2}}{k_{f3}} \prod_{n=1}^{N} \binom{F_n^P - k_{n1} - k_{n2}}{k_{n3}} \right] \Big/ \binom{F - \mathbf{1}^{\mathrm{T}}(\mathbf{k}_1 + \mathbf{k}_2)}{F_3^S}.$$

In general, for the mth SU the conditional PMF is

$$p\left(\mathbf{k}_m \big| \mathbf{k}_1, \mathbf{k}_2, \ldots, \mathbf{k}_{m-1}\right) = \left[\binom{F_f - \sum_{j=1}^{m-1} k_{fj}}{k_{fm}} \prod_{n=1}^{N} \binom{F_n^P - \sum_{j=1}^{m-1} k_{nj}}{k_{nm}} \right] \Big/ \binom{F - \mathbf{1}^{\mathrm{T}} \left(\sum_{j=1}^{m-1} \mathbf{k}_j \right)}{F_m^S}.$$

Using the chain rule and factorization of PMFs, the joint PMF for SUs is expressed as

$$p\left(\mathbf{k}_1, \mathbf{k}_2, \ldots, \mathbf{k}_m\right) = \prod_{r=2}^{m} p\left(\mathbf{k}_r | \mathbf{k}_{r-1}, \mathbf{k}_{r-2}, \ldots, \mathbf{k}_1\right) \; p\left(\mathbf{k}_1\right).$$

Finally, the marginal PMF of the mth SU with multiple N PUs can be obtained. Based on the evaluations above, it is straightforward to obtain the expected value of k_{nm}. Therefore, it is omitted for brevity.

APPENDIX F

PROOF OF PROPOSITION 4

Given f_1^s and f^p, the PMF of $\hat{k}_{p1}$ is expressed as

$$p(\hat{k}_{p1} \mid f_1^s, f^p) = \frac{p(\hat{k}_{p1}, f_1^s, f^p)}{p(f_1^s, f^p)} \overset{(a)}{\Rightarrow} p(\hat{k}_{p1}, f_1^s, f^p) = p(\hat{k}_{p1} \mid f_1^s, f^p)\ p(f_1^s)\ p(f^p),$$

where (a) results from the fact that f_1^s and f^p are independent, and the conditional PMF is given by $p(\hat{k}_{p1}|f_1^s, f^p) = \texttt{HYPG}(f_1^s, f^p, F)$. Once the joint PMF is given, the marginal PMF of $\hat{k}_{p1}$ is straightforwardly obtained. Mathematically, $p(\hat{k}_{p1}) = \sum_{f_1^s=0}^{T_{s1}} \sum_{f^p=0}^{T_p} p(\hat{k}_{p1} \mid f_1^s, f^p)\ p(f_1^s)\ p(f^p)$ yields the desired result. It is immediate to obtain the expression for the expectation of $\hat{k}_{p1}$

$$\begin{aligned}
\mathbb{E}[\hat{k}_{p1}] &= \sum_{\hat{k}_{p1}} \hat{k}_{p1}\ p(\hat{k}_{p1}) \\
&= \sum_{\hat{k}_{p1}} \sum_{f_1^s} \sum_{f^p} \hat{k}_{p1}\ p(\hat{k}_{p1} \mid f_1^s, f^p)\ p(f_1^s)\ p(f^p) \\
&= \sum_{f_1^s} \sum_{f^p} p(f_1^s)\ p(f^p) \underbrace{\left[\sum_{\hat{k}_{p1}} \hat{k}_{p1}\ p(\hat{k}_{p1} \mid f_1^s, f^p) \right]}_{\mathbb{E}[k_{p1}|f_1^s, f^p] = f_1^s f^p / F} \\
&= \frac{1}{F} \sum_{f_1^s} f_1^s\ p(f_1^s) \sum_{f^p} f^p\ p(f^p) \\
&= \frac{\mathbb{E}[f_1^s]\ \mathbb{E}[f^p]}{F}.
\end{aligned}$$

Plugging the expected values of f_1^s and f^p yields the desired result.

APPENDIX G

PROOF OF THEOREM 5

Using the *Definition* 7, and knowing the fact that the subcarrier collisions fall into four different sets, the expression for the instantaneous capacity of SU-1 with random access method can be readily defined. According to (3.5), to evaluate the average capacity of the SU-1 with subcarrier collisions, one needs to average a random sum of RVs with the set of i.i.d. RVs $C^o_{p1,i}$, $C^o_{12,i}$, $C_{p12,i}$ and $C_{f1,i}$. Since the number of subcarriers collisions in the sets ($\hat{k}_{p1}$, $\hat{k}^o_{12}$, $\hat{k}_{p12}$ and $\hat{k}_{f1}$) are not independent of each other, the rule of iterated expectations [69], $\mathbb{E}[X] = \mathbb{E}\left[\mathbb{E}[X|Y]\right]$, can be applied as follows.

$$
\begin{aligned}
\mathbb{E}[C_{S_1}] &= \mathbb{E}\left[\sum_{i=0}^{\hat{k}^o_{p1}} C^o_{p1,i} + \sum_{i=0}^{\hat{k}^o_{12}} C^o_{12,i} + \sum_{i=0}^{\hat{k}_{p12}} C_{p12,i} + \sum_{i=0}^{\hat{k}_{f1}} C_{f1,i}\right] \\
&\overset{(a)}{=} \mathbb{E}\left[\mathbb{E}\left[\sum_{i=0}^{\hat{k}^o_{p1}} C^o_{p1,i}\middle|\hat{k}^o_{p1}\right]\right] + \mathbb{E}\left[\mathbb{E}\left[\sum_{i=0}^{\hat{k}^o_{12}} C^o_{12,i}\middle|\hat{k}^o_{12}\right]\right] \\
&\quad + \mathbb{E}\left[\mathbb{E}\left[\sum_{i=0}^{\hat{k}_{p12}} C_{p12,i}\middle|\hat{k}_{p12}\right]\right] + \mathbb{E}\left[\mathbb{E}\left[\sum_{i=0}^{\hat{k}_{f1}} C_{f1,i}\middle|\hat{k}_{f1}\right]\right] \\
&= \mathbb{E}\left[\sum_{i=0}^{\hat{k}^o_{p1}} \mathbb{E}\left[C^o_{p1,i}\right]\right] + \mathbb{E}\left[\sum_{i=0}^{\hat{k}^o_{12}} \mathbb{E}\left[C^o_{12,i}\right]\right] + \mathbb{E}\left[\sum_{i=0}^{\hat{k}_{p12}} \mathbb{E}\left[C_{p12,i}\right]\right] \\
&\quad + \mathbb{E}\left[\sum_{i=0}^{\hat{k}_{f1}} \mathbb{E}\left[C_{f1,i}\right]\right] \\
&\overset{(b)}{=} \mathbb{E}\left[\hat{k}^o_{p1}\right]\mathbb{E}\left[C^o_{p1,i}\right] + \mathbb{E}\left[\hat{k}^o_{12}\right]\mathbb{E}\left[C^o_{12,i}\right] + \mathbb{E}\left[\hat{k}_{p12}\right]\mathbb{E}\left[C_{p12,i}\right] + \mathbb{E}\left[\hat{k}_{f1}\right]\mathbb{E}\left[C_{f1,i}\right],
\end{aligned}
$$

where (a) stems from the fact that conditioning with respect to the number of subcarriers, the sums are independent, and (b) is due to the independence between the number of subcarrier collisions and capacity, e.g., $\hat{k}^o_{p1}$ and $C^o_{p1,i}$ are independent. Finally, one can obtain the desired SU-1 average capacity expression by plugging the expected values of the number of subcarriers for the four cases given in (3.4) with some mathematical manipulations.

APPENDIX H

PROOF OF COROLLARY 6

Using (3.5), one has

$$
\begin{aligned}
C_{S_1} &= \sum_{i\in\mathcal{K}_{p1}^o} \log\left(1+\frac{h_{1,i}P_{1,i}}{g_{s1,i}P_i+\sigma^2}\right) + \sum_{i\in\mathcal{K}_{12}^o} \log\left(1+\frac{h_{1,i}P_{1,i}}{h_{2s,i}P_{2,i}+\sigma^2}\right) + \\
&\quad \sum_{i\in\mathcal{K}_{p12}} \log\left(1+\frac{h_{1,i}P_{1,i}}{g_{s1,i}P_i+h_{2s,i}P_{2,i}+\sigma^2}\right) + \sum_{i\in\mathcal{K}_{f1}} \log\left(1+\frac{h_{1,i}P_{1,i}}{\sigma^2}\right) \\
&\geq \sum_{i\in\left\{\mathcal{K}_{p1}^o\cup\mathcal{K}_{12}^o\cup\mathcal{K}_{p12}\cup\mathcal{K}_{f1}\right\}} \log\left(1+\frac{h_{1,i}P_{1,i}}{\sigma^2}\right) - \left[\sum_{i\in\mathcal{K}_{p1}^o} \log\left(1+\frac{g_{s1,i}P_i}{\sigma^2}\right) + \right. \\
&\quad \left. \sum_{i\in\mathcal{K}_{12}^o} \log\left(1+\frac{h_{2s,i}P_{2,i}}{\sigma^2}\right) + \sum_{i\in\mathcal{K}_{p12}} \log\left(1+\frac{g_{s1,i}P_i+h_{2s,i}P_{2,i}}{\sigma^2}\right)\right] \\
&\overset{(a)}{\geq} \sum_{i\in\left\{\mathcal{K}_{p1}^o\cup\mathcal{K}_{12}^o\cup\mathcal{K}_{p12}\cup\mathcal{K}_{f1}\right\}} \log\left(1+\frac{h_{1,i}P_{1,i}}{\sigma^2}\right) - \left[\sum_{i\in\mathcal{K}_{p1}^o} \frac{g_{s1,i}P_i}{\sigma^2} + \sum_{i\in\mathcal{K}_{12}^o} \frac{h_{2s,i}P_{2,i}}{\sigma^2} + \right. \\
&\quad \left. \sum_{i\in\mathcal{K}_{p12}} \frac{g_{s1,i}P_i+h_{2s,i}P_{2,i}}{\sigma^2}\right] \\
&= \sum_{i\in\left\{\mathcal{K}_{p1}^o\cup\mathcal{K}_{12}^o\cup\mathcal{K}_{p12}\cup\mathcal{K}_{f1}\right\}} \log\left(1+\frac{h_{1,i}P_{1,i}}{\sigma^2}\right) \\
&\quad - \frac{1}{\sigma^2}\left[\sum_{i\in\left\{\mathcal{K}_{p1}^o\cup\mathcal{K}_{p12}\right\}} g_{s1,i}P_i + \sum_{i\in\left\{\mathcal{K}_{12}^o\cup\mathcal{K}_{p12}\right\}} h_{2s,i}P_{2,i}\right] \\
&\overset{(b)}{=} \sum_{i=1}^{F_1^S} \log\left(1+\frac{h_{1,i}P_{1,i}}{\sigma^2}\right) - \frac{1}{\sigma^2}\left[\sum_{i\in\mathcal{K}_{p1}} g_{s1,i}P_i + \sum_{i\in\mathcal{K}_{12}} h_{2s,i}P_{2,i}\right],
\end{aligned}
$$

where (a) is due to $\log(1+x)\leq x, \forall x\geq 0$, (b) is due to $\mathcal{F}_1^S=\mathcal{K}_{p1}^o\cup\mathcal{K}_{12}^o\cup\mathcal{K}_{p12}\cup\mathcal{K}_{f1}$, $\mathcal{K}_{p1}=\mathcal{K}_{p1}^o\cup\mathcal{K}_{p12}$ and $\mathcal{K}_{12}=\mathcal{K}_{12}^o\cup\mathcal{K}_{p12}$. Furthermore, the bound for the average

capacity loss can be obtained by considering the fact that $g_{s1,i}P_i \sim Exp(1/P_i)$ and $h_{2s,i}P_{2,i} \sim Exp(1/P_{2,i})$, and their average values are hence given, respectively, by $\mathbb{E}[g_{s1,i}P_i] = P_i$ and $\mathbb{E}[h_{2s,i}P_{2,i}] = P_{2,i}$. Also, the means of $\hat{k}_{p1}$ and $\hat{k}_{12}$ are given by $T_pT_{s2}q_pq_{s2}/F$ and $T_{s1}T_{s1}q_{s2}q_{s2}/F$, respectively. Following an approach similar to the proof of *Theorem* 5 yields the desired result.